The Dissertation Committee for Lynn Sun Felts Mirigian Certifies that this is the approved version of the following Dissertation:

PROCOLLAGEN BIOSYNTHESIS AND OSTEOBLAST MALFUNCTION IN THE G610C MOUSE MODEL OF OSTEOGENESIS IMPERFECTA

Committee:

Sergey Leikin, Ph.D., Mentor

José Bastral, Ph.D., Mentor

Darren Boehning, Ph.D., Chair

Kyung Choi, Ph.D.

Dan Sackett, Ph.D.

David Niesel, Ph.D., Dean, Graduate School of Biomedical Sciences

PROCOLLAGEN BIOSYNTHESIS AND OSTEOBLAST MALFUNCTION IN THE G610C MOUSE MODEL OF OSTEOGENESIS IMPERFECTA

by

Lynn Sun Felts Mirigian, B.S.

Dissertation

Presented to the Faculty of the Graduate School of

The University of Texas Medical Branch

in Partial Fulfillment

of the Requirements

for the Degree of

Doctor of Philosophy

The University of Texas Medical Branch

February, 2015

To Matthew James Mirigian

Acknowledgements

I had the exceptionally good fortune to have two wonderful mentors guiding me through graduate school, Dr. Sergey Leikin and Dr. José Barral, I would like thank my mentor Dr. Sergey Leikin for spending countless hours teaching me to do good science and encouraging me when I did not believe it was possible that I would ever make progress, either intellectually or at the bench. I looked forward to coming in to the lab each day because his curiosity and positive, inspiring nature makes science and research fun. I would also like to thank my mentor Dr. José Barral for making me excited about biochemistry through his truly excellent teaching and helping me in every way possible through this partnership between UTMB and NIH. My fondest memory at UTMB is thinking I had “arrived” the first time I got to sit with him and Dr. Boehning in his office to talk about protein folding and leaving the meeting completely awestruck by their intelligence and graciousness in teaching me. I also would like to thank the members of my committee, to whom I am greatly indebted. Dr. Dan Sackett, for sharing his in depth knowledge of everything from fundamentals of cell biology to new techniques with me on a daily basis, for constantly letting me borrow reagents and equipment, and for his wisdom on every other random question I asked him over the past 5.5 years. There were many. Dr. Darren Boehning, for always being available to share UTMB-related and scientific wisdom with honesty and encouragement. The NIH/UTMB partnership would not have been possible without him, and I am truly grateful. Dr. Kyung Choi, for her depth of knowledge in shaping my thesis project by asking important questions that I had not considered, and for giving her time to provide me with much needed career guidance.

There are many other people to acknowledge both from UTMB and NIH. At UTMB, Dr. Coppenhaver for graciously making all the NIH/UTMB agreement paperwork happen year after year, and Dr. Joan Nichols for continuing the process after Dr. Coppenhaver's retirement. I would also like to thank Dr. Tracy Toliver-Kinsky for believing that I had potential as a scientist when I was applying to grad school, and for her continued kindness in making my transition to graduate school smooth. At NIH, all the members in the lab, past and present. Dr. Elena Makareeva for patiently teaching me fine technical details and assisting with experiments (especially differentiation and mineralization), for helpful scientific discussion, and for her friendship, allowing me to see day in and day out that it is possible to be a wonderful mother, wife, and scientist. Dr. Edward Mertz for performing Raman measurements, and Nydea, Aaron, and Dr. Shakib Omari for helpful scientific discussion. Apart from the lab, Dr. Larry Fisher and Dr. Ruth Etzensperger for guidance on biochemistry and animal techniques.

Finally, I am so incredibly indebted to my friends and family for being my support system. Listing all of the ways Matt and my parents have supported me would require more pages than this thesis. Their love and constant encouragement means the world to me, but more importantly they taught me I could have a relationship with my eternal savior Jesus. The Mirigians, both Steve and dad, for checking in on me and giving advice when needed. There are too many to acknowledge in my Restoration Church family, but to include a few Page and Joey Craft, Liz and Luke Strimer, Ruthie Etzensperger, Amy and Daniel Burgener and Brandi Golden. Thank you Ashley Kierath, Ashley Bohman, and Dawn Bennett-Ingold for the many hours of listening to me and simply being my friend through this process.

All thanks be to God, the creator of everything. It's been an incredible gift to learn about His creation.

PROCOLLAGEN BIOSYNTHESIS AND OSTEOBLAST MALFUNCTION IN THE G610C MOUSE MODEL OF OSTEOGENESIS IMPERFECTA

Publication No._____

Lynn Sun Felts Mirigian, Ph.D.

The University of Texas Medical Branch and National Institutes of Health, 2015

Primary Supervisor: Sergey Leikin

UTMB Supervisor: José Barral

Osteogenesis imperfecta (OI) is a hereditary disease that disrupts bone formation and function resulting in skeletal deformities and fragile bones. OI is diagnosed based on clinical and radiological examination, with patient symptoms ranging in severity from relatively mild (increased incidence of fractures) to severe (low impact fractures, severe skeletal deformities) to lethal (respiratory insufficiency soon after birth). To date, mutations in over a dozen genes that cause OI have been identified, of which ~90% are autosomal dominant and ~10% are autosomal recessive. In 5-10% of clinical cases the mutations remain unknown. Mutations in type I collagen, the triple helical protein that makes up the fibrous organic scaffold (matrix) of bone, are responsible for over 80% of OI cases. Interestingly, OI severity in patients with the same collagen mutation is highly variable, suggesting it may be possible to find a treatment that does not require gene repair. Furthermore, as OI pathology shares features with other

disorders such as common osteoporosis, studying this rare genetic disorder may unmask common molecular mechanisms and result in novel approaches to treatment of both disorders. Nevertheless, even the most basic mechanisms of OI pathophysiology are still poorly understood.

The goal of the present study was to lay the foundation for understanding how malfunction of bone producing cells contributes to OI pathology with the aim of finding treatments that do not involve presently unrealistic gene repair. Specifically, we focused on characterizing how the most common OI mutations in collagen affect: (1) collagen synthesis in bone producing cells, (2) bone cell differentiation and function, and (3) bone formation *in vivo.* To answer these questions, we chose to use a recently developed mouse model of moderately severe OI that mimics the genetic defect and phenotype variability found in the largest known group of OI patients with the same mutation.

Table of Contents

List of Tables

List of Figures

List of Illustrations

List of Abbreviations

α1(I) - procollagen α1 chain of type I collagen

α2(I) - procollagen α2 chain of type I collagen

αCP - α-complex protein

ADAMTS2- a disintegrin and metalloproteinase with thrombospondin motifs 2

Aha - azidohomoalanine

APC - Adenomatous polyposis coli protein

Arg- arginine

ATF4 - activating transcription factor 4 protein

ATF6 - activating transcription factor 6 protein

Atg - autophagy related protein

ATP - adenosine triphosphate

βTrCP - beta-transducing repeat containing E3 ubiquitin protein ligase

BIP- binding immunoglobulin protein

BMP - bone morphogenetic protein

BMSC - bone marrow stromal cell

Ca2+ - calcium

C/EBPβ - CCAAT/enhancer binding protein β

CFU - colony forming unit

CRTAP - cartilage associated protein

cTAGE5 - cutaneous T-cell lymphoma-associated antigen protein 5

Cypb - cyclophilin B

Cys - cysteine

Cy5 - N-hydroxysuccinimide ester

DIBO- AF555 - dibenzocyclooctyne derivative of AlexaFluor 555

Dkk - dikkopf protein

DSC - differential scanning calorimetry

eIF2α - eukaryotic initiation factor 2 protein

ER - endoplasmic reticulum

ERAD - ER associated degradation

ERGIC - ER-Golgi intermediate compartment

FKBP65 - 65-kDa FK506-binding protein

GLT - glycosyl transferase

Gly or G - glycine

GRP94 - heat shock protein 90kDa β member 1

GSK3β - Glycogen synthase kinase 3 β

HSP - heat shock protein

Hyp - hydroxyproline

IRE1 - endoplasmic reticulum to nucleus signaling 1

IS - internal standard conjugated to AlexaFluor 488

LH2 - lysyl hydroxylase 2

LRP5 - low-density lipoprotein receptor-related protein 5

LRP6 - low-density lipoprotein receptor-related protein 6

Lys - lysine

MEFs - mouse embryonic fibroblasts

MMP1 - matrix metalloprotease 1

MSC - mesenchymal stromal cell

NFκB - nuclear factor κB

OASIS - cAMP-responsive element-binding protein 3-like protein 1

OI - Osteogenesis imperfecta

PEDF - pigment epithelial derived factor protein

PERK - doublestranded RNA-activated protein kinase-like ER kinase

PDI - protein disulfide isomerase

pOBs - primary parietal calvaria osteoblasts

PPARγ - Peroxisome proliferator-activated receptor protein gamma

Pro or P - proline

p180 - p180 ribosome receptor protein

P3H1 - prolyl 3-hydroxylase

P4H1 - prolyl 4-hydroxylase

Rankl - receptor activator of nuclear factor kappa-B ligand

ROS - reactive oxygen species

Runx2 - runt related transcription factor 2 protein

Sost - sclerostin protein

TAK1 - transforming growth factor β protein kinase 1

Tango1 - transport and Golgi organization 1 protein

TGFβ - transforming growth factor β protein

TricB - transmembrane protein 38B

UPR - unfolded protein response

UTR - untranslated region

Wnt - wingless protein

XBP1 - x-box binding protein 1

4-Hyp - 4-hydroxyproline

SECTION 1: INTRODUCTION

Chapter 1: Bone

STRUCTURE AND FUNCTION

Bone is strong yet lightweight, rigid yet not brittle. It is made of an organic scaffold (matrix), the main component of which is type I collagen fibers. Hydroxyapatite mineral crystals fill voids inside and between the fibers. The resulting alloy of elastic collagen fibers and rigid mineral provides a balance between stiffness to resist bending upon application of a force and flexibility to absorb the force without shattering (1). The amount of mineralization primarily determines the stiffness: flexibility ratio is dictated by bone cells as well as other factors. Increased mineralization results in increased stiffness but reduced flexibility. Different bones can have different levels of mineralization depending on their function. For instance, inner ear bones need increased sensitivity to vibration, requiring increased stiffness and higher mineralization compared to the femur, which needs some flexibility to absorb the forces exerted on it while standing (1). The size, shape and composition of hydroxyapatite crystals varies as well and is affected by multiple factors, including the environment, diet, etc. (2). Most bones have a dense outer, cortical layer and a porous inner, trabecular layer, which maximize strength while reducing weight (Illustration 1). The bone marrow, which fills the voids in the trabecular layer, serves as a reservoir of bone producing cells as well as the source of blood cells.

In addition to type I collagen, the organic matrix of bone contains many other proteins, carbohydrates, lipids, and water. Type I collagen comprises ~85% of the protein content of bone, and most water in bone is found in collagen fibers

(2). Among the most important non-collagen bone proteins are proteoglycans that contain at least one glycosaminoglycan (mostly chondroitin or heparin sulfate) chain (2). Proteoglycans regulate collagen fibrillogenesis, structural organization of the matrix and binding of important ligands. Other non-collagen proteins include alkaline phosphatase that maintains phosphate and pyrophosphate homeostasis, matricellular proteins that affect bone cell function, proteins that mediate cell attachment to bone, and a variety of growth factors and regulatory proteins that bind to bone matrix and hydroxyapatite (2). Roughly 2% of the dry weight of bone is attributed to lipids, which have an unknown, but important function to bone physiology (2,3).

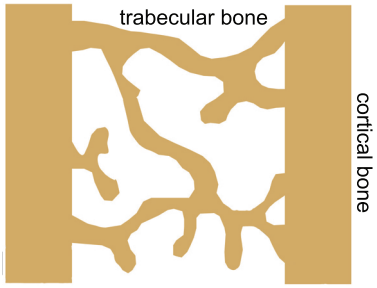

Illustration 1. Bone structure

Cortical bone is dense, compact, and provides most of the structural support. Trabecular bone is contained within the cavity of cortical bone and is surrounded by bone marrow. Trabecular bone makes up ~20% of the cavity, the rest being filled with bone marrow. Relative fractions of both types of bone vary depending on the diameter of the bone at a particular region and the intended function. Reprinted from Trends in Cell Biology, 21/3, Makareeva, E., Aviles, N., Leikin, S. Chaperoning osteogenesis: new protein-folding disease paradigms, 168-176 Copyright (2011), with permission from Elsevier.

Bone is not just a part of the skeleton but also (a) a vast Ca^{2+} reserve that the rest of the body may draw upon when needed, (b) a niche for hematopoiesis and a variety of stem cells that reside in the bone marrow cavity and require signaling from bone cells, and (c) an endocrine organ that produces hormones and responds to signals from other organs in the body.

FORMATION, MODELING, AND REMODELING

During development, bone nucleation and formation occurs either via endochondral or intramembranous ossification depending on the type of bone and origin of bone cells. Briefly, endochondral ossification starts from formation of mineralized cartilage to a template for deposition of bone by osteoblasts, which are specialized bone-producing cells. The cartilage is subsequently removed by bone-matrix absorbing osteoclasts during modeling and remodeling (4). Intramembranous ossification is *de novo* bone formation through creation of an ossification center containing osteoblast precursors without a cartilage matrix template (5). After bone has formed, there are no distinguishable differences between the material formed by endochondral or intramembranous ossification.

Once initial ossification is complete, bone formation occurs through modeling or remodeling processes (Illustration 2). Bone modeling is the deposition of new material at the existing bone, usually at the periosteal (outer) surface of the cortical layer (Illustration 2a). It is typically accompanied by resorption at the other side of the cortical layer. The balance between periosteal bone deposition and endosteal (inner surface) bone resorption determines changes in the thickness of the cortical layer. However, mineralized matrix may also be deposited at endosteal and resorbed at periosteal surface when required for changing the bone geometry. Bone modeling may also modify the thickness

of trabecular bone and the size and strength of bone attachment points of tendons and ligaments. The sites as well as rate of formation and resorption of bone are regulated through complex interactions between osteoblasts, osteoclasts and osteocytes. Osteocytes are mechanosensing cells inside the bone, which are produced by differentiation of osteoblasts that become embedded inside bone matrix during its deposition (Illustration 2b). The bone modeling process is affected by a variety of hereditary and environmental factors, allowing for optimization of bone size, shape, strength, and weight during growth (1).

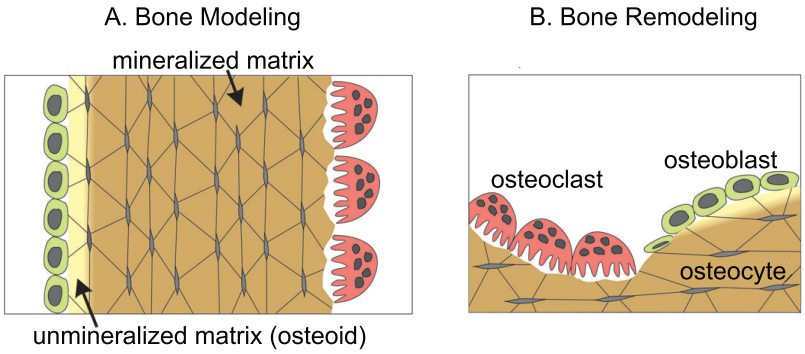

Illustration 2. Bone modeling and remodeling.

(A.) Bone modeling occurs doing bone formation. Osteoblasts at the periosteum deposit unmineralized matrix called osteoid while osteoclasts absorb mineralized bone at the endosteal surface. The osteoid becomes hardened, mineralized matrix, embedding some osteoblasts in the process. These osteoblasts differentiate into osteocytes, which signal to other cells through long caniculi processes. (B.) Bone remodeling occurs at sites of bone damage. Osteocytes sense damage to the matrix and send signals to bone absorbing osteoclasts, which degrade the matrix. Osteoblasts come in and deposit new osteoid in a highly coordinated manner to form organized bone. These figures are simplified to highlight only bone formation and remodeling via bone cells, and do not contain blood vessels, marrow, etc. Reprinted from Trends in Cell Biology, 21/3, Makareeva, E., Aviles, N., Leikin, S. Chaperoning osteogenesis: new protein-folding disease paradigms, 168-176 Copyright (2011), with permission from Elsevier.

Remodeling replaces existing bone with new material, which enables bones to achieve maximum functional capability during and after development. Remodeling is usually activated by microscopic cracks in the bone. Osteocytes recognize these microfractures and signal to osteoclasts and osteoblast to replace the old and damaged material. Osteoclasts digest and break down the area. In a tightly coordinated fashion, osteoblasts refill the resorbed area with newly synthesized collagen matrix, which is mineralized to become new bone. (Illustration 2b). During normal remodeling, the matrix deposited is well organized due to the cell-cell adhesions of coordinating osteoblasts to produce ordered bone. Dysregulation of signaling between bone cells disrupts the balance between bone resorption and deposition during remodeling and may lead to accumulation of microfractures, bone loss, or excessive bone formation.

Chapter 2: Collagen Biosynthesis

Since type I collagen is the most prevalent building block of the bone matrix, its homeostasis plays the key role in bone health and pathology. Disruptions in collagen biosynthesis lead to abnormal bone formation, skeletal deformities and bone fragility.

Type I collagen belongs to a large family of collagens distinguished by at least one triple helix domain with an obligatory glycine (Gly or G) in every third position. Roughly 30% of the amino acids in the other two positions of the repeating Gly-X-Y triplets are proline (Pro or P). It is the most abundant protein in vertebrates, forming the foundation of extracellular matrix in skin, bone, and other tissues, yet it is synthesized primarily by only a few specialized cells including osteoblasts in bone, odontoblasts in teeth, and fibroblasts in skin, tendons and other soft connective tissues (6).

Type I collagen (referred to as collagen hereafter) is a ~300 nm long heterotrimer of two α1 chains and one α2 chain, each being approximately 1000 amino acid residues long (Illustration 3). It is synthesized and folded as a procollagen precursor, in which the long collagen triple helix is bounded by propeptides at the –COOH (C) and -NH_2 (N) terminal ends. Once procollagen is secreted by the cell the propeptides are cleaved off by specialized enzymes, and the remaining collagen triple helix is assembled into fibrils. The fibrils are bundled together into thicker fibers, which form the structural scaffold of extracellular matrix in a variety of tissues.

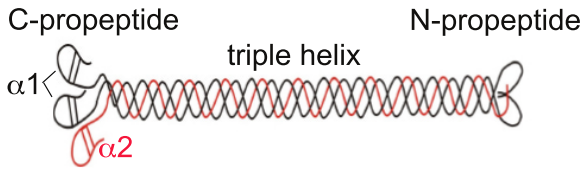

Illustration 3. Procollagen structure.

Type I procollagen consists of two α1 chains and one α2 chain. Procollagen contains a C-propeptide with a globular hydrophobic core, a long, relatively inflexible triple helix region, and a small N-propeptide that contains both a small triple helix and a globular region. Propeptides are enzymatically cleaved off to yield mature collagen in the extracellular space.

BIOSYNTHESIS OVERVIEW

Transcription and Translation

The α1 chain gene of procollagen, Col1a1 is located on chromosome 11 in mouse (chromosome 17 in human), and the α2 chain gene, Col1a2 is located on chromosome 6 in mouse (chromosome 7 in human). Both genes are similar, containing 51 and 52 exons in Col1a1 and Col1a2, respectively. The first 6 exons encode the N-propeptide and a flexible N-telopeptide link, which connects the propeptide to the triple helix; the next 41 exons in Col1a1 and 42 exons in Col1a2 encode the triple helix; and the last 4 exons encode the C-telopeptide link and C-propeptide (7).

Cytokines, hormones, growth factors, cell stress, and vitamins regulate procollagen mRNA transcription. Col1a1 and Col1a2 transcription is coordinated by similar transcription factors (7). Procollagen mRNA stability is regulated predominantly by the untranslated regions (UTR) (8-10). In particular, a cytosine rich region in the 3' UTR (untranslated region) of Col1a1 recruits the RNA binding protein αCP (α-complex protein), which prevents mRNA degradation (11). To the

best of our knowledge, the regulation of Col1a2 mRNA stability has not been characterized.

The translation efficiency of procollagen mRNA is enhanced by the ribosome adaptor protein p180 (p180 ribosome receptor protein), which is important for cells like osteoblasts that synthesize large amounts of procollagen (12). Mature procollagen α1 and α2 mRNA are co-translated through polysomes and the resulting chains are translocated into the rough endoplasmic reticulum (ER or rER). Maintaining the optimal ratio of α1 to α2 translation potentially requires a conserved stem loop region within the 5' UTR of both chains, especially during times of abundant procollagen synthesis (13). At the translation rate of approximately 3.5 amino acids/second, the synthesis of each chain takes approximately 7 minutes (14).

Folding

Unlike most other proteins, procollagen folding begins only after the chains are completely translated and translocated into the ER. The first step is association and folding of two α1 and one α2 chains at the globular C-propeptide region, which requires both interchain and intrachain disulfide bond formation (Illustration 4) (15-18). A conserved set of 15 amino acids within the middle of the C-propeptide is believed to be at least partially responsible for the chain recognition and proper heterotrimeric composition of type I collagen (19).

Completion of the C-propeptide domain folding sets up the three polypeptide chains in the proper position and register to begin folding of the triple helix (20). The helix folds in a zipper-like fashion from C- toward the N-propeptide. The folding requires all prolines to be in the trans conformation; their isomerization by peptidyl-prolyl cis-trans isomerases is essential for faster triple

helix folding (21). In the triple helix, the –H “side chain” of Gly faces inside, allowing room for the Gly-NH to form a hydrogen bond with a backbone carbonyl of a second polypeptide chain. The side chains of the X and Y amino acids of Gly-X-Y triplets face outside and are exposed to the surrounding solution. Because the inside of the triple helix cannot accommodate any side chains except for the Gly hydrogen, replacement of obligatory Gly disrupts the triple helix folding and structure, particularly when the substituting amino acid has a bulky or charged side chain (22). The N-propeptide folds last. It contains a second, small triple helical region, the functional role of which is unknown.

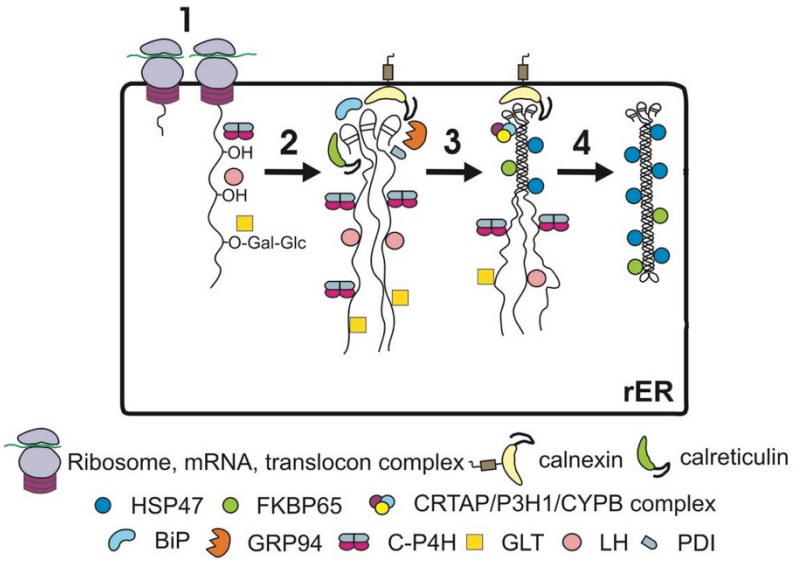

Illustration 4. Procollagen folding

Described in detail in text. GLT- glycosyl transferase. LH- lysyl hydroxylase. C-P4H- prolyl-4-hydroxylase. Reprinted from Trends in Cell Biology, 21/3, Makareeva, E., Aviles, N., Leikin, S. Chaperoning osteogenesis: new protein-folding disease paradigms, 168-176 Copyright (2011), with permission from Elsevier.

The mechanism of procollagen folding is unlike most other proteins studied (23). The native state of most polypeptide chains is more thermodynamically favorable than the random coil conformation assumed upon

synthesis, regardless of whether the native state is ordered or disordered (24). The folding is driven by energetic benefit of the native conformation (25). For smaller proteins, the free energy landscape may have few or just one low energy conformation. The native state may then be the most energetically favorable one and the folding may not require chaperones. Such proteins are thermodynamically stable. For larger proteins, the free energy landscape may contain multiple low energy conformations, some of which may be more thermodynamically favorable and therefore more stable than the native state. The native conformation of the latter proteins is metastable, meaning that the protein may eventually assume a more stable non-native conformation, e.g. within amyloid fibrils. To prevent nonproductive formation of low energy states that are "traps" rather than folding intermediates, cells utilize specialized chaperone proteins, which lower the probability of reaching such conformations and are discussed later in this chapter.

Procollagen is unique in that its final, folded native conformation has higher free energy than the initial unfolded chains at body temperature (23). For instance, the enthalpy benefit upon folding of human type I procollagen exceeds the entropy loss caused by ordering of the chains only below 34-35 ^{o}C but not at the normal body temperature. Above this temperature, procollagen slowly denatures. At normal body temperature, human procollagen denatures within about a day and murine procollagen denatures within several hours (26). After secretion, propeptide cleavage and incorporation into fibrils, the collagen molecule is stabilized by interactions with its neighbors, and it does not denature below 50-60 ^{o}C (27). The molecules not incorporated into fibrils do denature, become susceptible to degradation by general enzymes and can be removed from tissues or circulation. The resistance of the triple helix to all enzymes, except for specialized collagenases (28,29), would make such cleanup much

more difficult, which may be one of the reasons why collagen molecules evolved to be thermodynamically unstable (23).

Inside the ER, where procollagen is folded, the native conformation has to be made thermodynamically favorable by some interactions with the ER environment; otherwise this conformation would be very improbable. Binding of ER chaperones reduces the free energy of the polypeptide chain in the conformation to which the chaperones bind. Since general ER chaperones preferentially bind to unfolded or partially unfolded polypeptide chains, their binding would make the native conformation of procollagen chains even more thermodynamically unfavorable (23). Instead, collagen-producing cells utilize a collagen-specific ER heat-shock protein HSP47, as discussed in more detail later in this chapter. HSP47 preferentially binds to the natively folded triple helix, reduces its free energy and makes the folding of procollagen into its native conformation thermodynamically possible and favorable (23,30).

Post-translational Modifications

During procollagen chain translation and folding, the unfolded regions of each chain undergo several posttranslational modifications (Illustration 4). Within the Gly-X-Y motif, almost all Y position prolines become hydroxylated to 4-hydroxyproline (4-Hyp) by P4H1 (prolyl 4-hydroxylase) (31). At specific locations, a few X position prolines become hydroxylated to 3-hydroxyproline by P3H1 (prolyl 3-hydroxylase) (32). Prolyl hydroxylases require the cofactor ascorbic acid to catalyze the hydroxylation (33). Hydroxylation of Y-prolines increases the stability of the triple helix and it is required for normal procollagen folding (34). 4-hydroxyproline stabilizes the triple helix due to complex mechanisms involving networks of water bridges and stereoelectronic effects that favor triple helix

conformation (35). For instance, to form stable triple helices, proline favors the C^{γ}-*endo* pyrrolidine pucker, which is favorable in the X position of the G-X-Y triplet, but hydroxyproline favors the C^{γ}-e*xo* pyrrolidine pucker, which is favorable in the Y position of the G-X-Y triplet (35). The role of X-proline hydroxylation is still being debated (36). Some lysine (Lys or L) residues at the X and Y positions are also known to be hydroxylated by lysyl hydroxylases (LH), and subsequently glycosylated by galactosyl and glycosyl transferases (GLT) (37). All these posttranslational modifications take place only within unfolded regions of procollagen chains.

Trafficking and Secretion

Procollagen follows the conventional secretory pathway from ER to Golgi, secretory vesicles, and extracellular space. However, many aspects of its intracellular trafficking are still poorly understood. In particular, exit from the ER requires packaging into COPII-coated vesicles that direct proteins toward their destination. Procollagen is ~300 nm in length, which is significantly larger than the diameter of such vesicles. Recent studies have suggested that procollagen trafficking may require Tango1 (transport and Golgi organization 1 protein) and cTAGE5 (cutaneous T-cell lymphoma associated antigen protein 5) to increase the size of the vesicles for accommodating procollagen, but many aspects of this process are still unclear (38,39).

Unlike other proteins for which the release of ER chaperones signal that they are ready to be exported from the ER, procollagen is cotransported to the ERGIC (intermediate ER-Golgi compartment) together with HSP47 and probably with a peptidyl-prolyl isomerase cyclophilin B (Cypb) (40). *In vitro* studies evidence structures of laterally “aggregated” procollagen molecules observed at

a pH similar to the Golgi apparatus, thus, it has been hypothesized that these may also be found in the Golgi of cells, which are then packaged into secretory vesicles and released into the extracellular space (41). It has also been proposed that propeptide cleavage may begin in the Golgi apparatus and continue through the secretory pathway, but the majority of procollagen molecules are secreted with intact propeptides (42,43).

Extracellular Processing and Fibrillogenesis

After secretion into extracellular space, the N- and C- propeptides are cleaved off by ADAMTS2 (a disintegrin and metalloproteinase with thrombospondin motifs 2) and BMP1 (bone morphogenetic protein 1), respectively, which initiates the process collagen fibril formation (Illustration 5) (44,45). While propeptide cleavage can occur inside the cell, the C-propeptide may be necessary to mediate the transport out of the ER and to prevent detrimental fibrillogenesis inside the cell (42). The cleaved propeptides have been proposed to have secondary functions that mediate an increase (C-propeptide) or decrease (N-propeptides) in procollagen synthesis, although these mechanisms are not well described (46).

After C-propeptide cleavage, collagen molecules become capable of assembly into fibrils, in which the molecules associate with one another in a quarter-stagger orientation (Illustration 5). The low thermal stability of individual collagen molecules allows for local triple helix unfolding, which promotes association of the molecules and fibril nucleation, which is followed by rapid fibril growth (26,30,43,47,48). Subsequent fibril maturation involves crosslinking of aldehyde derivatives formed by deamination of hydroxylysines with lysine and hydroxylysine residues on adjacent molecules (7). *In vivo,* type I collagen

coassembles into fibrils with a small fraction of type V collagen molecules and its fibrillogenesis is tightly regulated by cells with the help of a variety of other proteins and proteoglycans (49).

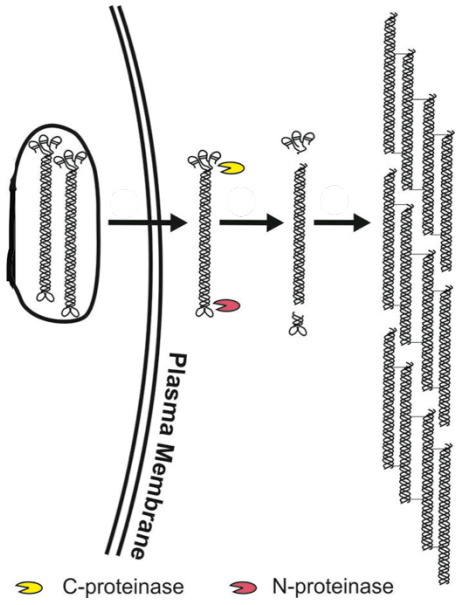

Illustration 5. Extracellular processing and collagen fibrillogenesis.

Procollagen is secreted from the cell via secretory vesicles. The C and N propeptides are typically cleaved once secreted into the extracellular space by specific C- and N- proteases that cleave at the telopeptide domain connecting the propeptides to the triple helix. Collagen molecules assemble with a ¼ stagger called a D-period and form intermolecular crosslinks to become fibrils. Reprinted from Trends in Cell Biology, 21/3, Makareeva, E., Aviles, N., Leikin, S. Chaperoning osteogenesis: new protein-folding disease paradigms, 168-176 Copyright (2011), with permission from Elsevier.

CONTROL OF PROCOLLAGEN FOLDING IN THE ER

Since the focus of the present study is to understand how procollagen misfolding contributes to bone pathology by affecting osteoblast function, the regulation of procollagen folding in the ER deserves separate, more detailed

discussion. As discussed above, thermodynamic instability of natively folded procollagen at normal body temperature presents a unique challenge for folding. This process is regulated by general ER chaperones and isomerases as well as by ER proteins and protein complexes that appear to be collagen-specific, summarized in Table 1. Furthermore, distinct combinations of ER proteins seem to be involved in folding of different procollagen domains.

Protein Disulfide Isomerase (PDI) and ERp57

While the triple helix of type I collagen has no cysteine (Cys) residues, procollagen propeptide folding involves formation of multiple Cys-Cys disulfide bonds. The environment of the ER promotes disulfide bond formation (50). PDI protects free sulfide groups from premature and promiscuous disulfide bond formation as well as catalyzes proper intrachain and interchain disulfide bond formation in the propeptides (20). ERp57 is a member of the same family, which might play a similar role in procollagen folding. In order for the PDI family members to function, its active site must itself be in the reduced state, which requires the presence of glutathione in the ER (51)

Notably, PDI has a dual role in procollagen folding, acting also as the β subunit of the tetrameric $\alpha_2\beta_2$ collagen prolyl 4-hydroxylase (52,53). This collagen-specific ER enzyme catalyzes hydroxylation of Y-proline residues into 4-hydroproline, making procollagen folding less thermodynamically unfavorable.

Calnexin and Calreticulin

After procollagen is cotranslated into the ER, N-linked glycosylation occurs on the C-propeptide domains of the α1 and α2 chains (54). A branched

oligosaccharide is then added, which is trimmed by glucosidases until a single glucose remains, which facilitates binding to transmembrane and ER lumen lectin chaperones, calnexin and calreticulin, respectively (55). This binding facilitates disulfide bond formation within the C-propeptide through ERp57, which are associated with calnexin\calreticulin. C-propeptide binding to calnexin also explains earlier observations of procollagen being attached to the ER membrane during triple helix folding (56). Because of relatively weak interactions, calnexin/calreticulin can dissociate from the folding protein, which allows the remaining glucose to be cleaved (57). If the protein is folded by the time this occurs, it can leave the ER. If the protein is not folded, a new, branched oligosaccharide will be added and the process repeats.

In addition to their chaperone functions, calnexin and calreticulin are also calcium or Ca^{2+} binding proteins involved in ER Ca^{2+} homeostasis through interaction with calcium channels, for example (58). Their involvement in Ca^{2+} regulation may also be important for procollagen folding, as discussed later in several chapters.

General Heat Shock Proteins

Folding of the C-propeptide, which has a globular native conformation, follows the conventional protein folding pathway. It is assisted by several general ER heat shock proteins (HSP) including HSP70 and HSP90 family members BIP (binding immunoglobulin protein), and GRP94 (heat shock protein 90kDa β member 1), respectively. These chaperones utilize ATP (adenosine triphosphate) to bind and release exposed hydrophobic surfaces on polypeptide chains. Such binding prevents nonproductive association between hydrophobic moieties and aggregation of polypeptide chains en route to the natively folded conformation

(59). Once the native conformation is attained, the hydrophobic regions are buried in the protein core and these chaperones are no longer able to bind to the polypeptide chain. Their binding/release cycles protect against misfolding of the C-propeptide hydrophobic core and to a lesser extent against the N-propeptide misfolding (60).

It is believed that the triple helix folding does not involve BIP or GRP94 binding. For instance, the BIP binding site is a stretch of 7 amino acids with multiple hydrophobic residues and without prolines or charged residues (61). The triple helical regions of procollagen α1(I) and α2(I) chains do not contain sites expected to strongly bind BIP. In fact, such binding would be counterproductive for the helix folding, since it would reduce the free energy of unfolded chains without affecting the free energy of the native helix. This would make the helix folding even more thermodynamically unfavorable than it were to begin with (23).

Collagen-Specific Heat Shock Protein 47 (HSP47)

Folding of the triple helix requires binding of HSP47, which is an ER resident protein that is expressed only in collagen-synthesizing cells in correlation with collagen expression (62). While HSP47 belongs to the serpin superfamily of serine protease inhibitors, its primary role is to assist procollagen folding and it does not have protease inhibitor functions (62)

HSP47 preferentially binds to Gly-X-Arg (arginine) triplets in natively folded procollagen triple helix via electrostatic interactions at neutral pH in the ER environment (63-66). The interaction between each HSP47 molecule and collagen triple helix is relatively weak, as evidenced by dissociation constants in the range of 1-100 μM (64) but the helix contains ~30 proposed binding sites (67). As procollagen triple helix folding propagates toward the N-terminus,

HSP47 binding stabilizes the folded region by reducing its free energy, allowing further helix propagation. At concentrations typical for HSPs in the ER, enough HSP47 molecules are expected to bind, making the native procollagen conformation thermodynamically favorable and folding feasible in the physiological range of temperatures (30,66). HSP47 is released from procollagen only in ERGIC/cis-Golgi where lower pH disrupts the electrostatic binding, after which HSP47 is recycled back to the ER through a KDEL ER-signal peptide (62).

Other proposed HSP47 functions include preventing aggregation of folded procollagen in the ER (68) and quality control of procollagen folding (69). However, it is unclear how HSP47 may perform the latter function. Unlike other HSP chaperones that prevent the export of bound unfolded and misfolded proteins from the ER, HSP47 is exported from the ER together with folded procollagen. HSP47 does not appear to be required for the export either, since cells lacking HSP47 secrete partially unfolded collagen (70).

65-kDa FK506-Binding Protein (FKBP65)

Another protein proposed to make procollagen folding more thermodynamically favorable by stabilizing the triple helix is FKBP65 (71,72). In addition, FKBP65 is a peptidylprolyl cis-trans isomerase, but as procollagen refolding experiments measured its isomerase activity as 10 times lower than other ER cis-trans isomerases in the cyclophilin family, it is likely not the primary procollagen peptidyl cis-trans isomerase in the ER (73). FKBP65 also regulates posttranslational modifications of procollagen. It has been shown to be a necessary component of a complex with lysyl hydroxylase 2, which ensures proper lysyl hydroxylation of procollagen telopeptides (74). FKBP65 also may be involved in calcium regulation (75).

Cyclophilin B (Cypb)/Prolyl-3-Hydroxylase 1 (P3H1)/Cartilage Associated Protein (CRTAP) Complex

The prolyl cis-trans isomerase that appears to be most crucial for procollagen folding is Cypb, since Cypb deficiency or inhibition delays procollagen folding (76). Like FKBP65, Cypb is involved in regulation of procollagen posttranslational modification, but it appears to affect the function of lysyl hydroxylase 1 rather than lysyl hydroxylase 2 (76,77). Furthermore, Cypb forms a complex with P3H1 and CRTAP. This complex helps to retain Cypb in the ER, since P3H1 is an ER-resident protein with a KDEL ER-retention signal, and it has additional functions in procollagen folding.

The Cypb/P3H1/CRTAP complex binds to both folded and unfolded procollagen chains (78). It has been proposed to bind at the junction between the folded triple helix and unfolded chains, assisting in the propagation of the helix from the C- toward N-terminal end (79), although this speculative idea has not been experimentally validated so far. A well-established function of the complex is 3-hydroxylation of X-proline 986 in the triple helix (80-82) by P3H1, which might be important in extracellular fibril formation and organization (36). Interaction between CRTAP and P3H1 is required for stabilizing each of the two proteins in the ER. When one of them is not expressed, the other is not observed in the ER (83). In contrast, Cypb is present in the ER without the complex and the lack of Cypb expression leads to only a moderate reduction in the ER level of CRTAP and P3H1 (84,85).

Transmembrane Protein 38B (TricB)

Among the most surprising recent observations is that TricB deficiency results in abnormal thermal stability of a fraction of secreted procollagen, suggesting procollagen misfolding (86). TricB is an ER membrane monovalent ion channel proposed to be important for rapid calcium release from the ER (87,88). By affecting Ca^{2+} flux, TricB deficiency may indirectly affect procollagen folding through altering the function of calnexin, calreticulin and FKBP65 and other Ca^{2+}-binding proteins in the ER. It may also affect procollagen folding by disrupting the overall ER homeostasis. Yet, the most interesting possibility is that TricB is somehow directly involved in regulation of procollagen folding through interactions that are still unknown.

Protein	Role in control of procollagen folding in the ER	References
PDI	Formation of disulfide bonds in C-propeptide domain, subunit of P4H1	(20,52,53)
Calnexin/Calreticulin	Chaperone, procollagen export from ER?, calcium regulation	(54,56)
General HSPs	Chaperone for propeptide domains	(60,89)
HSP47	Stabilizes folded triple helix, prevents aggregate formation, procollagen export from ER?,	(30,63-66,68,69)
FKBP65	Mild prolyl cis-trans isomerase activity, mediates posttranslational modifications, calcium regulation	(71-75)
Cypb	Prolyl cis-trans isomerase activity, mediates posttranslational modifications, assists in propagation of triple helix folding?	(76-82)
P3H1	Posttranslational modification, assists in propagation of triple helix folding?, stabilization of other complex members	(78-83)
CRTAP	Mediates posttranslational modifications, assists in propagation of triple helix folding?, stabilization of other complex members	(78-83)
TricB	Calcium regulation, ??	(86)

Table 1. Summary of proteins described in current section with procollagen folding roles in the ER.

Chapter 3: Osteoblast Formation and Function

DIFFERENTIATION

Most osteoblasts are derived from mesenchymal stromal cells (MSC) or bone marrow stromal cells (BMSC) that can originate from a variety of sources including bone marrow, adipose tissue, umbilical cord blood, and others (90). MSCs are multipotent cells that can produce osteoblasts, chondrocytes, adipocytes and myoblasts (91). There is currently no single marker to identify a MSC, however a panel of cell surface markers is continuously being developed in order to enrich for MSC populations.

MSC differentiation toward an osteoblastic lineage may be stochastic, with the potential cell designation narrowing and becoming more restricted as the process continues (92). It may also be driven by outside stimuli that guide the cell into an increasingly restrictive lineage (90). The latter concept has been supported by studies showing how extracellular stimuli such as cytokines direct and restrict cell differentiation toward an osteoblast (93). However, these effects are complicated by many biphasic and multiphasic effects of outside stimuli (91).

Like for many other cell types, osteoblast differentiation is a dynamic continuous process without distinct steps. Furthermore, not all cells may require the same regulatory pathways to become a properly differentiated osteoblast (91). Yet, for practical convenience, different steps of MSC differentiation toward osteoblasts are often identified (Illustration 6), and the process is divided into proliferation, extracellular matrix development, and mineralization stages. Once an osteoblast has matured, it may turn into an osteocyte, become a bone-lining cell, or undergo apoptosis.

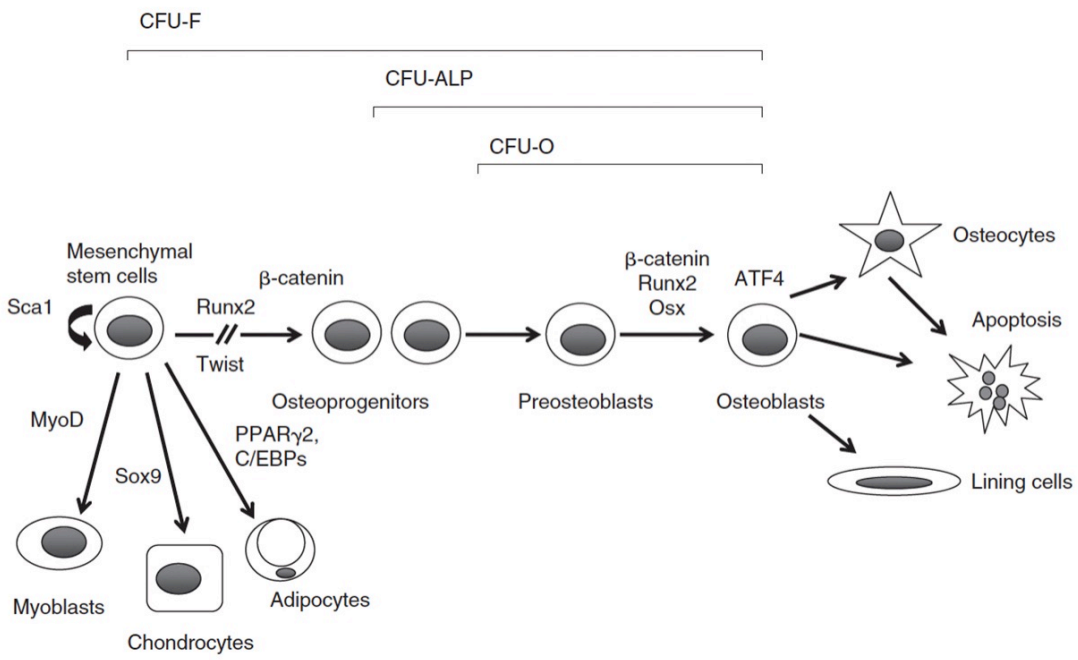

Illustration 6. Osteoblast differentiation.

Mesenchymal stem cells (MSCs) differentiate into many cell types. Described in detail below. Reprinted from Principles of Bone Biology, 1/3, Mammen, J., Jan de Beur, S.M. Chapter 4- Mesenchymal stem cells and osteoblast differentiation by Jane Aubin, 85-107, Copyright (2008), with permission from Elsevier.

PROLIFERATION

During this stage, osteoblast precursors upregulate expression of common genes associated with proliferation, such as histone proteins and proto-oncogenes c-fos and c-myc as well as a more specific osteoprogenitor transcription factor Runx2 (runt related transcription factor 2) (94). Runx2 is the earliest known marker of osteoblast differentiation. Its deletion completely prevents bone formation (95). However, Runx2 is also expressed in other MSC-derived cells such as hypertrophic chondrocytes (96) and it is not the sole determining factor on whether a MSC will become an osteoblast. Downstream of Runx2 expression is the transcription factor Osterix that further restricts the cell

fate. The expression of both Runx2 and Osterix during the proliferation stage suggests that the progenitor, under normal circumstances without a change in extracellular environment, will become an osteoblast. In culture, osteoprogenitors may divide on average up to 8 times before becoming differentiated osteoblasts (97). The expression of type I collagen and other components of bone matrix gradually increases toward the end of the proliferative stage (91).

MATRIX DIFFERENTIATION AND MINERALIZATION

As the osteoblastic precursor matures and enters into the latter phases of differentiation, expression of other genes increase and then fade at different time points. These genes include alkaline phosphatase, collagens, osteocalcin, osteopontin, parathyroid hormone receptor 1, and others (91). Each cell may take a different route to becoming an osteoblast, so that expression patterns of these genes may vary (98,99). A mature osteoblast is defined by its ability to produce and mineralize bone matrix. The exact mechanism of mineralization is not fully understood, yet it is often assumed that osteoblasts regulate this process by producing a variety of non-collagenous proteins that catalyze and inhibit this process (100).

A mature osteoblast is considered to be post proliferation. Some of mature osteoblasts further differentiate into stationary osteocytes that are embedded in bone matrix (101). The prevailing hypothesis is that some osteoblasts becomes buried in the osteoid (unmineralized matrix) they are producing before the mineral is deposited (102,103). To become an osteocyte, the motile osteoblast must stop moving, produce dendritic processes, and shrink its cytoplasmic volume (104). The dendritic processes form an extended network connecting osteocytes with each other and with cells on the bone surface. Their formation

requires cleavage of collagen by secreted proteins from the osteocyte (104). A mature osteocyte has limited synthesis capabilities, but it does secrete important factors for maintaining bone homeostasis (105). It also has a different gene expression profile, down-regulating most osteoblastic genes, and upregulating mostly osteocyte specific genes such as Phex and Sclerostin (105).

Alternatively, a post-proliferative osteoblast may become a bone lining cell or undergo apoptosis. Bone lining cells are found at the surface of bone that does not undergo active matrix deposition. They are identified primarily by morphological characteristics, being flat as opposed to cuboidal shape of active mature osteoblasts, and with relatively few dendritic processes compared with osteocytes. They are thought to be relatively inactive, but may have some important functions, including support for osteoblasts and osteocytes (106) and recruitment of osteoclasts (107).

Apoptosis may occur at any point during osteoblastic differentiation, not only at the end of the osteoblast lifetime (108). Apoptotic cells undergo morphological changes including cytoplasm shrinkage and membrane blebbing, chromatin condensation, DNA degradation, fragmentation, and detachment from surrounding objects (109)

REGULATION

The processes of precursor recruitment from MSCs, osteoblast maturation, bone deposition, and terminal differentiation of the cells are affected by a multitude of stimuli that include a variety of endocrine and paracrine factors, direct interactions with other cells, and parasympathetic nervous system signals (110,111). Here we briefly discuss several of the most studied pathways of osteoblast regulation.

Transforming Growth Factor Beta

TGFβ functions both through autocrine and paracrine signaling mechanisms (112). TGFβ is secreted by osteoblasts and other cells in either an inactive (latent) pro-TGFB form by itself or as a complex with inhibitors, or as active TGFβ; its synthesis and activation do not necessarily correlate (113). Latent TGFβ form reservoirs within the collagen matrix. It is released and activated upon bone resorption by osteoclasts, which is one of the signals for new osteoblasts to form and build new bone during bone remodeling (114-116). TGFβ promotes proliferation of preosteoblasts and is actively involved early in commitment of precursor cells to an osteoblast lineage (117,118). Though TGFβ stimulates osteoblast differentiation early in osteogenesis, it suppresses the differentiation at later stages and couples bone formation with bone resorption (119).

TGFβs, of which there are three, coordinate and interweave numerous signaling pathways important to procollagen biosynthesis and osteoblast function. TGFβ increases procollagen expression, both by increasing transcription and stabilizing mRNA transcripts (7). It is also part of a cytoprotective feedback loop where TGFβ induced increase in procollagen synthesis causes accumulated, aggregated intracellular procollagen which is removed via TGFβ induced activation of autophagy (120). Another connection between TGFβ signaling and procollagen biosynthesis is an ER resident chaperone calreticulin important to procollagen folding may regulate TGFβ signaling via calcium signaling mechanisms in times of cell stress (121). In fact, TGFβ and calcium signaling are intricately connected, as normal TGFβ signaling triggers a release of calcium from the ER into the cytoplasm (122).

Canonical TGFβ signaling occurs through the following mechanism (Illustration 7). Activated TGFβ binds to form a heterotetrameric complex of two type II and two type I receptors, of which there are many. The activated complex phosphorylates receptor Smads 2/3, which then associates with Smad4, and enters into the nucleus to mediate transcription of selected targets (123). Inhibitory Smads 6 and 7 mediate TGFβ signaling by inhibiting the association of Smad4 with Smad2/3, and also target TGFβ receptors for degradation (117). As described earlier TGFβ also can inhibit osteoblast differentiation via activation of a noncanonical pathway mediated by TAK1 (transforming growth factor β kinase 1) (117).

Bone Morphogenetic Protein

Most bone morphogenetic proteins (BMPs) belong to the same superfamily of proteins as TGFβ and play crucial roles in regulating osteoblast differentiation and function. MSCs, osteoblasts, chondrocytes, macrophages, and endothelial cells all secrete precursor BMPs, which are either stored in inactive form by binding to the matrix or effect action on surrounding cells (124). BMPs are essential for committing MSCs to an osteoblastic lineage (125). Briefly, BMPs act as osteoinducers by the canonical signaling pathway described here (Illustration 7). BMP binds to type I and type II BMP receptors to induce formation of an activated heterotetrameric complex (124). This interaction causes phosphorylation of receptor Smads 1/5/8, which then associates with co-Smad4, and translocates into the nucleus to target specific osteoblast target genes. BMPs can also indirectly promote osteoclastogenesis via production of osteoclast recruitment signals and indirect inhibition of Wnts (124). Action of BMP can be inhibited by activation of inhibitory Smads 6/7.

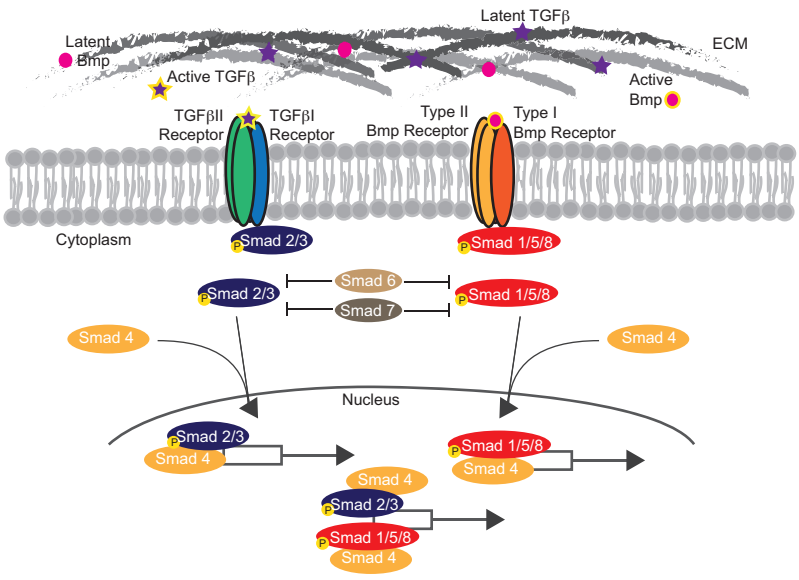

Illustration 7. TGFβ and BMP signaling.

The TGFβ superfamily contains most of BMP family, and their relatedness may explain how their signaling occurs via similar mechanisms described in the text. There is much functional overlap in the genes that TGFβ and BMP regulate, including a key osteoblast inducer Runx2. ECM-extracellular matrix.

BMP signaling is also interconnected between osteoblast function and cellular/ER stress/nutrient signaling via arms of the canonical unfolded protein response (UPR) (Illustration 8). BMP can function through activation the PERK/eIF2α/ATF4 arm of the UPR, a pathway that also signals ER stress in the cell (126,127). ATF4 (activating transcription factor 4) induces transcription of osteogenic genes bone sialoprotein, and osteocalcin (127). It was shown that PERK (doublestranded RNA-activated protein kinase-like ER kinase) null mice cannot activate ATF4 in osteoblasts, which is necessary for osteoblast maturation and function (127). Activation of PERK leads to phosphorylation of the α-subunit of eIF2α (eukaryotic initiation factor 2), which reduces protein synthesis in response to depleted amino acid sources (127). ATF4 is able to escape eIF2α action because of an upstream open reading frame in the 5' UTR,

which is bypassed except when eIF2α is phosphorylated (127). Activation of PERK is required for productive ATF4 translation in osteoblasts, even though there are other kinases that can phosphorylate eIF2α.

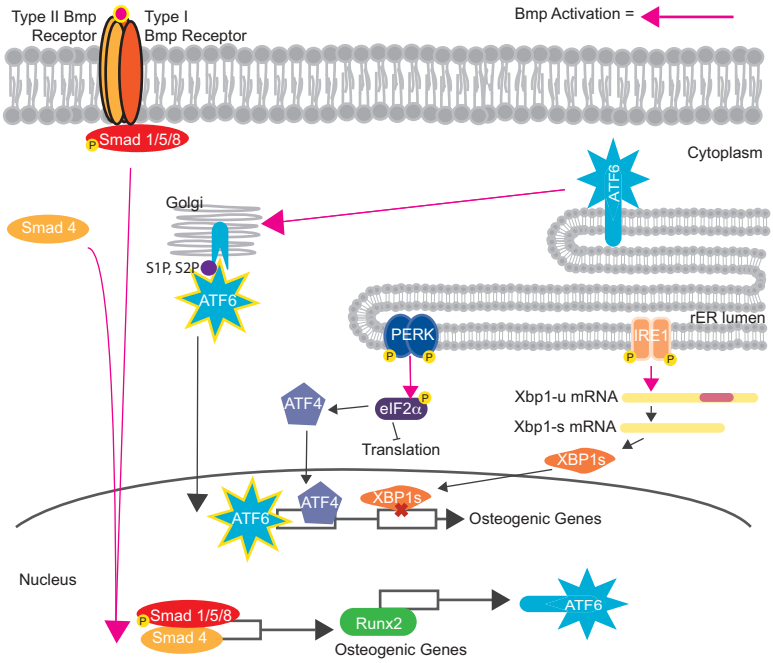

Illustration 8. BMP signaling through the ER stress proteins affects osteogenic gene transcription.

BMP phosphorylates and activates Smads 1/5/8, which translocate into the nuclease with Smad4 and activates transcription of many osteogenic genes, including Runx2. Runx2 is a transcription factor for ATF6 and increases expression of ATF6. Through other, unknown mechanisms, BMPs also mediate cleavage of ATF6, releasing the active-cleaved form of ATF6 to translocate into the nucleus and increase expression of osteogenic genes. In another ER stress pathway, BMP increases activation of PERK, which phosphorylates eIF2α and allows ATF4 translation to occur, but blocks translation of other proteins. ATF4 translocates into the nucleus and increases expression of osteogenic genes. In another ER stress pathway, BMPs increase splicing of XBP1 mRNA, which is mediated through IRE1 activation. Spliced XBP mRNA is translated, and the resulting protein is translocated into the nucleus and blocks expression of osteogenic genes.

BMP2 treatment increases expression and activation of ATF6 (activating transcription factor 6), which is another ER stress activator and transcription factor part of the UPR (125). ATF6's promoter has a Runx2 binding region (125), but actual ATF6 activation mediated by its cleavage requires BMP2, meaning BMP2 has another function besides to indirectly induce transcription of ATF6 (125). Inhibiting ATF6 activation prevents osteocalcin expression, a necessary protein for osteoblast function (125).

BMPs also are known to increase the level of XBP1 (x-box binding protein 1) splicing, caused by IRE1 activation of the UPR (128). This is actually a negative feedback loop, as over-activation of IRE1 by Bmp addition inhibits osteoblastogenesis (128). Some basal level of ER stress induced by BMP2 activation of all three UPR signaling arms (PERK, ATF6 and IRE1) is known to promote for bone formation, however, excessive ER stress is detrimental, indicating that tight regulation of ER stress is essential for normal osteogenesis (127-129).

Wingless Proteins (Wnt)

WNT signaling is important for increasing preosteoblast proliferation, selecting osteogenic cell fate, and reducing apoptosis of osteoblasts and their precursors (130). It inhibits adipogenesis by blocking key adipogenic transcription factors C/EBPβ (CCAAT/enhancer binding protein β) and PPARγ (peroxisome proliferator-activated receptor protein γ), which is important to bone strength as there is a positive clinical correlation between increased fatty marrow content and bone fracture (131,132). WNT signaling prevents apoptosis in osteoblasts (133). Finally, it regulates expression of osteoprotegerin, a competitive inhibitor of

osteoclast inducing protein Rankl (receptor activator of nuclear factor kappa-B ligand), to prevent bone resorption (134).

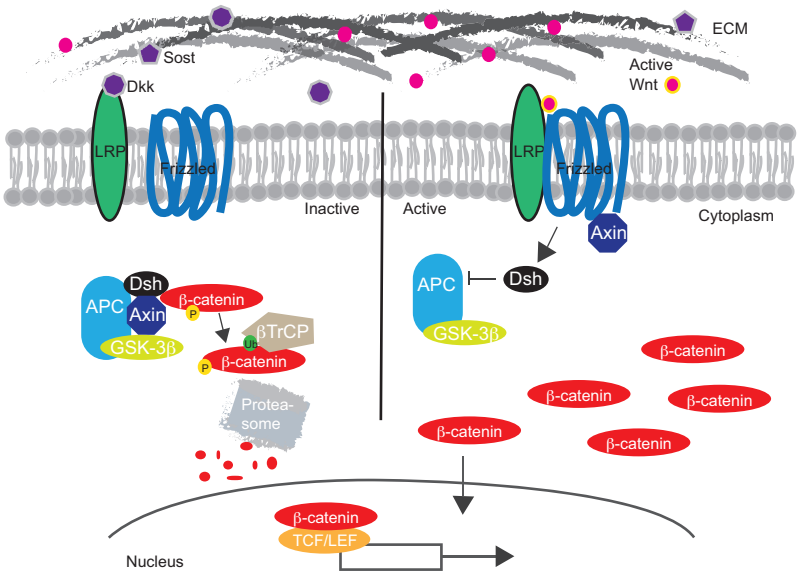

Illustration 9. Canonical Wnt signaling in bone.

Described in text. Inhibition of Wnt signaling, left. Activation of Wnt signaling, right.

There are 19 Wnt proteins that function through either a canonical pathway requiring β-catenin, a noncanonical planar cell polarity pathway, and/or a pathway that involves calcium signaling (135). With respect to bone and osteoblast function, perhaps the most well studied pathway is the canonical Wnt/β-catenin pathway (Illustration 9). It is activated by Wnt binding to frizzled transmembrane receptors and LRP5 and LRP6 (low-density lipoprotein receptor-related protein 5 and 6) co-receptors. β-catenin disassociates from the GSK3B/Axin/APC complex, accumulates in the cytoplasm, enters the nucleus, associates with other cofactors, and induces transcription of its target proteins (135,136). Activation of Wnt signaling is prevented by antagonists in the Sost (Sclerostin) and Dkk (Dickkopf) family, which bind to the LRP5 and LRP6 to

prevent association of the receptor complex. In the absence of Wnts or presence of competing antagonists, LRP5/6 cannot associate with Frizzled, β-catenin is phosphorylated by forming a complex with GSK3β (glycogen synthase kinase 3 β), Axin, and APC (adenomatous polyposis coli protein) and targeted for subsequent ubiquitination by βTrCP (β-transducing repeat containing E3 ubiquitin protein ligase) and degradation by the proteasome (135). Nonfunctional LRP5 leads to low bone mineral density and bone (137), probably due to reduced proliferation of osteogenic precursors (138). Reduced Dkk binding to LRP5 or overexpression of LRP5 have an opposite effect of increasing bone mass (139,140).

Chapter 4: Osteogenesis Imperfecta

Studies of rare genetic abnormalities are crucial for identifying genes and molecular mechanisms involved in human development and pathology. Hereditary abnormalities in bone formation that cause skeletal deformities and bone fragility (OI or osteogenesis imperfecta) occur approximately in 1 out of 10,000 births regardless of ethnicity or gender (141,142). [To the best of our knowledge, the penetrance of OI mutations in different mitochondrial haplogroups has not been studied]. Yet, OI shares multiple features with more common disorders such as age-related osteoporosis. Better understanding of OI may therefore not only clarify still poorly understood aspects of bone biology but it also offer novel approaches to treatment of common bone pathologies.

MOLECULAR GENETICS

Over 80% of OI cases are caused by mutations in the genes that encode type I procollagen chains (143). Mutations that reduce synthesis of the procollagen α1 chain without altering its sequence, e.g., by reducing mRNA stability, cause mild OI (143). Similar mutations in the type I procollagen α2 chain (pro-α2(I)) chain have almost no effect on bone, even when procollagen α2 chains are not translated at all and normal type collagen is completely replaced by homotrimers of the α1(I) chain (144,145).

Mutations that lead to amino acid substitutions, deletions, and insertions in type I procollagen or result in synthesis of chains not capable of incorporating into procollagen trimers typically result in more severe or even lethal OI (143). The pathology may be caused by effects of abnormal procollagen homeostasis in

the cell on osteoblast function as well as by effects of secreted mutant procollagen on bone matrix formation and properties.

Affected protein	Inheritance	Direct effects on secreted collagen and bone matrix	Effects on osteoblast function
Type I collagen	Dominant with few exceptions	Collagen deficiency, abnormal collagen interactions	Abnormal procollagen folding and resulting cell stress
HSP47	Recessive	Secretion of misfolded procollagen	Abnormal procollagen folding and resulting cell stress
FKBP65	Recessive	Abnormal lysyl hydroxylation in collagen and matrix crosslinking	Possible cell stress
LH2 (PLOD2)	Recessive	Abnormal lysyl hydroxylation in collagen and matrix crosslinking	Unknown
CRTAP	Recessive	Abnormal posttranslational modification of collagen	Abnormal procollagen folding and resulting cell stress
P3H1	Recessive	Abnormal posttranslational modification of collagen	Abnormal procollagen folding and resulting cell stress
Cypb	Recessive	Abnormal posttranslational modification of collagen	Abnormal procollagen folding and resulting cell stress
TricB	Recessive	Secretion of misfolded collagen	Altered intracellular calcium signaling
OASIS	Recessive	Unknown	Altered cell stress, signaling
PEDF	Recessive	Unknown	Unknown
Bril	Dominant	Unknown	Unknown
Bmp1	Recessive	Unknown	Unknown
Osterix	Recessive	Unknown	Abnormal differentiation
Wnt1	Recessive	Unknown	Abnormal Wnt signaling

Table 2. Mutations that cause OI.

Extracellular effects are defined as alterations in procollagen that affect fibrillogenesis and matrix protein binding interactions. Intracellular effects are defined by disruption in procollagen biosynthesis that lead to cell stress and altered osteoblast function. Many mutations functions are incompletely characterized, or unknown. OASIS- cAMP-responsive element-binding protein 3-like protein 1. PEDF- pigment epithelial derived factor protein

About 10% of OI cases are caused by mutations in proteins important for procollagen biosynthesis, most of which cause severe or lethal OI (Table 2). Mutations in HSP47 disrupt procollagen folding and cause ER accumulation as well as secretion of misfolded procollagen (69,146). FKBP65 mutations cause posttranslational overmodification but do not appear to affect procollagen folding (74). FKBP65 may directly affect collagen lysine hydroxylation, but it may also affect the activity of lysine hydroxylase 2 (LH2) since patients with FKBP65 and LH2 mutations have overlapping symptoms (147,148). In addition, FKBP65 regulates calcium release from the ER, which is important to osteoblast function (75). Mutations in each of the proteins of the CRTAP/P3H1/Cypb complex affect 3-hydroxylation of Pro in the triple helical region of procollagen α1 chain and may alter folding and other modifications of procollagen as well (80,81,84,85,149,150). Surprisingly, mutations in an ER ion channel TricB cause secretion of misfolded procollagen, but these mutations may also lead to OI by disrupting calcium regulation in osteoblast ER, as discussed earlier in chapter 3 (86,151,152). PEDF (pigment epithelial derived factor) is a collagen-binding protein secreted by a variety of cells, but it may also act as a signaling molecule affecting osteoblast function (153). PEDF deficiency causes a distinct OI phenotype, the pathophysiology of which is unclear (154,155). Bril is a plasma membrane protein expressed by mature osteoblasts (156). Mutations in Bril cause two distinct types of OI, one that is Bril-specific and the other that involves PEDF deficiency in osteoblasts and has the corresponding phenotype (157,158). BMP1 is a procollagen C-proteinase, but it may also have other functions in bone (159). Surprisingly, its mutations appear to affect mineralization rather than deposition of bone matrix (expected in the case of abnormal C-propeptide cleavage) through an unknown mechanism (160).

A number of patients with severe OI or OI-like bone pathology caused by mutations that have no direct effect on procollagen biosynthesis have been reported, but the penetrance of these mutations is presently unclear. A mutation in osterix, a key osteoblast transcription factor is likely to cause OI by affecting osteoblast differentiation (161). Mutations in Wnt1 might also affect osteoblast differentiation and function by altering Wnt signaling (162-165). Mutations in OASIS (cAMP-responsive element-binding protein 3-like protein), a family member of the ER stress transducer ATF6, might cause OI by altering cell stress signaling (166).

Overall, many more severe cases of OI are caused by missense mutations that replace a single amino acid within the collagen triple helix than by all other collagen and non-collagen mutations combined. Most of these mutations are substitutions of obligatory Gly within the Gly-X-Y sequence. The only other ones are substitutions of arginine in Y positions and proline (hydroxyproline) in X and Y positions (67). Notably, all of these amino acids substitutions disrupt proper folding and affect stability of the triple helix. The role of Gly was discussed earlier in chapter 3. Proline and hydroxyproline strongly favor the triple helix formation; Gly-Pro-Hyp triplets are the most stable regions of the triple helix; but Pro and Hyp are not required in every triplet. Y arginine is essential for HSP47 binding during triple helix folding and it also stabilizes the triple helical structure through hydrogen bonding (62,65).

The lack of OI cases caused by substitutions of other amino acids, even in regions known to be important for collagen interactions with collagen or other extracellular matrix molecules is quite revealing. We cannot exclude contribution of collagen malfunction in the extracellular matrix to OI pathology, but we would expect the latter mutations to play a prominent role in OI if such malfunction were the main cause of pathology. We also would not expect such mutations to be

dramatically more severe than Gly substitutions, which could explain the lack of reported cases by early embryonic lethality.

At least in the case of single amino acid substitutions, OI pathology is more likely to be related to procollagen misfolding inside the cell. This interpretation explains the prominence of mutations that cause procollagen misfolding in severe OI. It also suggests that better understanding of procollagen misfolding and its effects on osteoblast function is particularly important for unraveling OI pathophysiology.

PHENOTYPIC VARIABILITY

Another important observation suggesting the importance of osteoblast malfunction in OI pathophysiology is the wide range of clinical severity in OI patients with collagen mutations, from barely detectable to lethal (167). A full range of phenotypes from relatively mild to lethal caused by the same mutation was reported (167). Within groups of consanguineous patients or family members containing the same mutation, there is still variability in clinical outcome (168,169).

This phenotype variability might be related to differences in the genetic background and to epigenetic variations. At the present time, the genetic and epigenetic factors in human patients are difficult to separate. There are only a few case reports of identical twins with OI in literature, in most of which the causative mutation has not been identified. In particular, we found no reports of identical twins with OI caused by Gly substitutions in the triple helix. Yet, it is interesting to note three case reports of similar (170,171) and two case reports (172,173) of different OI severity in identical twins.

At least in the case of collagen mutations, variations in other genes and epigenetic factors are more likely to affect osteoblast response to procollagen misfolding than the function of mutant procollagen molecules secreted into bone matrix. This response, resulting cell stress and cell adaptation to this stress are mediated by multiple proteins and may vary significantly with even small changes in expression and sequence of the corresponding genes.

PROCOLLAGEN MISFOLDING

Procollagen misfolding affects osteoblast differentiation and function for two main reasons. (1) Mature osteoblasts synthesize their cell weight of collagen in one day. Retention of misfolded procollagen in the cell results in dramatic misfolded protein load, which is observed in OI. (2) Procollagen folding presents a challenge for cells to begin with, as discussed earlier in this chapter, complicating handling of the misfolding compared to other proteins.

Procollagen misfolding is caused by amino acid alterations in the molecule itself and in proteins that affect its folding in the ER, including HSP47 (70), FKBP65 (72), CRTAP/P3H1/CYPB complex (76,85,143,149), and TRICB (86). Gly substitutions, which are the focus of the present study, are by far the most common cause of procollagen misfolding in OI.

Gly substitutions disrupt the triple helix folding as shown in Illustration 10 (67). As the triple helix folds and propagates from C- toward the N-terminus, it stalls upon reaching the mutation site, because side chains of other amino acids cannot be accommodated inside the core of the triple helix. Subsequent folding requires renucleation of the triple helix with proper chain alignment past the mutation site. The length of the pause at the mutation site may dependent on how severely the side chain of the substituting amino acid disrupts the triple helix

structure, propensity of the sequence beyond the mutation site to triple helix renucleation, and availability of binding sites for HSP47 and other proteins that may assist in the renucleation and other factors.

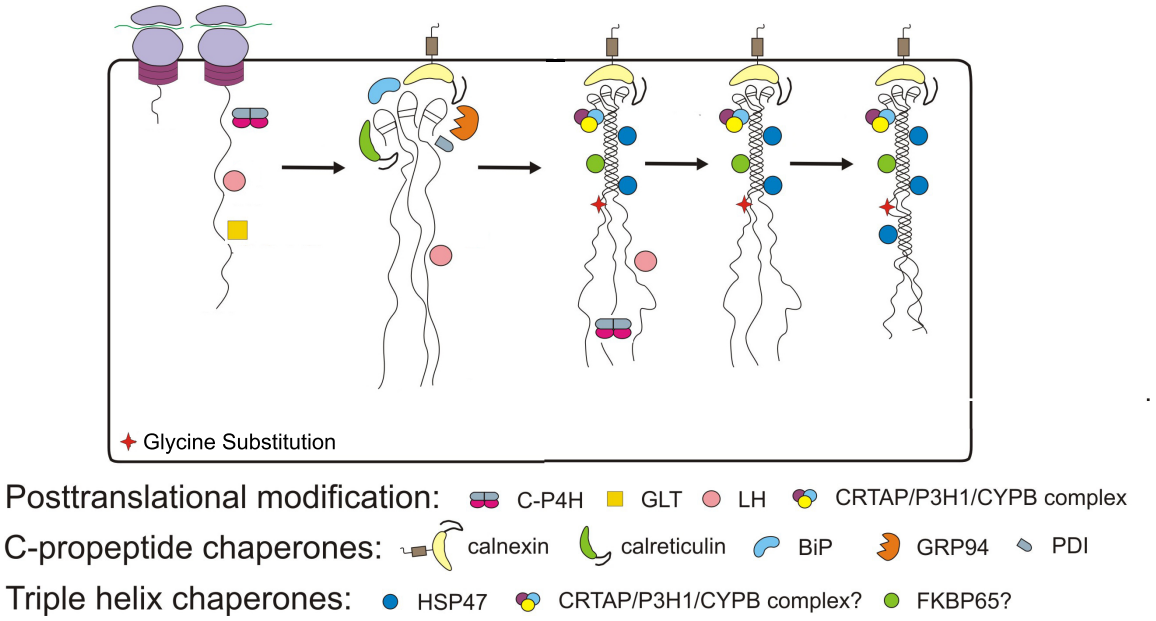

Illustration 10. Procollagen misfolding due to a glycine substitution in the triple helix.

Procollagen is cotranslated into the ER (box), and the C-propeptide folds using C-propeptide chaperones. Triple helix folding commences until the point of the glycine substitution, where it stops. During this time posttranslational modifications continue to occur on unfolded procollagen chains, resulting in overmodification. Eventually folding continues on by renucleation of the triple helix past the substitution. The newly forming triple helix is stabilized by a HSP47 stabilizing chaperone. C-P4H1- prolyl 4-hydroxylase. GLT- glycosyl transferase. LH- lysyl hydroxylase.

Gly substitutions might cause a variety of misfolded procollagen conformations. In particular, a long pause in triple helix folding may increase the probability on nonproductive interactions and aggregation of unfolded chains from different procollagen trimers. Formation of insoluble procollagen aggregates was reported for Gly substitutions (174), HSP47 deficiency (70,174), and

FKBP65 deficiency (72). Gly substitutions cause destabilization and local unfolding of the triple helix, which may affect a large region of the molecule depending on the substitution location (34). Triple helix renucleation may result in improper register of procollagen chains affecting the stability and conformation of the entire collagen molecule, e.g. producing a kink (175,176).

These and other potential misfolded conformations of procollagen are recognized by the cell, retained in the ER and targeted for degradation, as shown by a variety of experimental techniques in multiple studies (174,177).

In general, accumulation of misfolded proteins in the ER is detrimental for cells, which utilize several different approaches to prevent it. The best studied mechanism involves activation of one or more of the three (IRE1, ATF6 and PERK) receptors of unfolded protein response (UPR) through sequestration of BIP at hydrophobic regions of misfolded protein chains (178). UPR restores ER homeostasis by targeting misfolding molecules for ERAD (ER associated degradation) in proteasomes, reducing translation of most proteins and upregulating chaperones, with eventual activation of apoptosis if the ER stress cannot be resolved (178). This conventional UPR is often equated with ER stress response of cells.

However, accumulation of some misfolded proteins does not trigger conventional UPR. An alternative “ER overload” cell stress response was first described as a response to accumulated ER membrane proteins that triggered calcium release and activation of nuclear factor κB (NFκB) (179,180). ER overload has also been described in disorders caused by misfolding of serpin family proteins such as α1-antitrypsin (181-184). Nonproductive polymerization of misfolded serpins in the ER does not cause BIP sequestration, activation of conventional IRE1/ATF6/PERK signaling, or upregulation of ERAD. Characteristic signatures of this response are: Ca2+ release from the ER,

reduced calnexin concentration in the ER, upregulation of NFκB signaling, and degradation of misfolded protein aggregates in lysosomes through macroautophagy (182-186). Interestingly, there is likely some overlap between standard UPR and ER overload, as eIF2α phosphorylation by PERK may be necessary for activation of NFκB by ER stress (187).

Some involvement of cell stress response to procollagen misfolding was suspected beginning from early studies of collagen mutations in OI (188,189). However, conventional UPR was observed only for C-propeptide mutations, while Gly substitutions in the triple helix were not found to sequester and upregulate BIP, which is the key mediator of the UPR (60,190,191).

Evidence of cell stress was found in several studies of OI caused by Gly substitutions, including retention of misfolded molecules in the ER and ER dilation (174,192-194), upregulation of CHOP and αB crystalline (195), degradation of misfolded procollagen through macroautophagy (174), and upregulation of key macroautophagy markers (196). These studies provided important clues, but molecular mechanisms of osteoblast cell stress response to Gly substitutions were unresolved and the role of this stress response in pathology remained unclear.

OSTEOBLAST MALFUNCTION

While the pathways and role of the cell stress response to procollagen misfolding are still poorly understood, abnormal differentiation and function of osteoblasts has been documented in many OI studies. In particular, reduced proliferation was observed in osteoblasts derived from patients with dominant OI caused by collagen mutations compared with normal control within the same age range (197). Interestingly, reduced proliferation compared to normal control was

only observed in younger OI patients. With increasing age, normal control osteoblasts experienced a reduction in proliferative capacity, yielding levels similar as OI patients, indicating that the proliferative capacity of OI cells was similar to aged osteoblasts (197). Studies of the Brtl mouse model of OI showed fewer preosteoblast cells in the pool of MSCs and that MSCs were more likely to undergo adipogenic than osteogenic differentiation (196). Notably, proliferative capacity of OI osteoblasts appears to be lower compared to normal cells in culture, yet more osteoblasts per bone surface is often found in OI *in vivo*, indicating complex dysregulation of osteoblast differentiation (198).

Further evidence of osteoblast dysregulation is provided by studies of abnormal response of OI osteoblasts to TGFβ. In particular, TGFβ receptor (TGFβR) expression in human OI patient osteoblasts was found to be more than two-fold higher than in age matched normal controls (199). Ligand binding to TGFβR did not reduce the number of the receptors on the cell surface in OI osteoblasts, in contrast to normal controls (199). Stimulation of cultured OI osteoblasts with exogenous TGFβ had smaller effects on collagen production compared to control cells (200). More recently, increased phosphorylation of Smads and expression of TGFβ target genes was reported in mouse models of CRTAP deficiency and Gly substitutions (201). The apparent overactivation of the signaling could be at least in part explained by adaptation to reduced collagen production at normal concentrations of active TGFβ in OI. However, the authors interpreted their observations by assuming that extracellular matrix produced by OI cells contains fewer proteoglycans that bind and sequester active TGFβ (201).

BONE MATRIX PATHOLOGY

Deficient procollagen biosynthesis and osteoblast dysregulation caused reduction in the capacity of osteoblasts to produce bone matrix (202,203). However, OI severity does not appear to be related simply to insufficient bone matrix synthesis, e.g. similar bone formation rate per osteoblast was observed in mild and severe forms of OI (203).

Incorporation of mutant collagen and malfunction of osteoblasts may also both affect the composition and structure of the bone matrix. One clue to the importance of osteoblast malfunction in matrix pathology is that OI mutations alter how bone matrix is deposited at different ages while the fraction of secreted mutant molecules does not depend on age. For instance, in osteoblasts derived from human normal controls of various ages, extractable collagen from matrix increased with age through puberty then decreased back to fetal levels, but this trend was not observed in osteoblasts derived from OI patients of the same age (204). Altered proteoglycan synthesis was reported in several studies as well. Similar to collagen, normal osteoblasts were observed to have more proteoglycans in the intracellular and matrix fraction after 2 weeks in culture, whereas OI osteoblasts had decreased proteoglycan levels (202). Reduced osteonectin, chondroitin sulfate proteoglycan (CSPG), hyaluronan sulfate proteoglycan, biglycan, and decorin were found in OI osteoblasts, while thrombospondin increased 2-4 fold compared with normal control, which was most obvious in patients 10 years and younger (197). Relative CSPG and hyaluronan fractions in matrix produced by osteoblasts from OI patients were not reduced with patient age in a similar manner to normal control osteoblasts (197).

Abnormal composition and structure of matrix produced by OI osteoblasts likely contributes to its abnormal mineralization. While mineralization of OI bone

occurs slower, the final mineral content of OI bone is generally higher (205,206). It was proposed that posttranslational overmodification of mutant collagen might affect intermolecular crosslinks that are necessary for induction of mineralization (207). However, more recent observations suggest that mineralization defects could be due to a more global bone cell defect not directly related to the presence of mutant molecules in the matrix (208). An increase in mineralization of OI bone makes it brittle, i.e. less able to withstand forces without breaking.

MOUSE MODELS OF OI CAUSED BY TRIPLE HELIX MUTATIONS

Given the apparent role of osteoblast malfunction in OI pathophysiology and very limited ability to understand this malfunction in cell culture experiments, development and studies of mouse models are essential for OI research. Indeed, it is possible to recapitulate and investigate procollagen misfolding in culture; and it is reasonable to assume that the basic principles of this process are similar in culture and *in vivo*. However, osteoblast differentiation, maturation and function *in vivo* involve a multitude of external stimuli, including interactions with other cells and organs that cannot be modeled in culture, at least at the present time. To put it simply, osteoblasts may deposit and mineralize matrix but they are not capable of forming bone and differentiating into osteocytes in culture. Without animal studies, it would be too presumptuous to assume that OI osteoblasts malfunction in cell culture in the same or even similar way to how they malfunction *in vivo*.

Several models that mimic genetic defects found in human OI, including different procollagen, CRTAP (81), P3H1 (82), and CYPB (80) mutations have been developed. Because of our focus on understanding OI caused by Gly substitutions, here we discuss only discuss the models of procollagen mutations.

The Mov13 model is based on blocking transcription of the procollagen α1 chain by a retroviral insertion of the Moloney leukemia provirus in first intron of collagen chain (209-211). Homozygous animals are not viable. Heterozygous animals mimic loss of expression of one of the two COL1A1 alleles caused by some mutations in human OI, but expression of the provirus complicates interpretation of observations in this model (212).

The collagen minigene model expresses human COL1A1 gene that is missing a significant portion of the triple helix, which is encoded on a plasmid that has to be injected into mouse embryos (213). The shortened human procollagen α1 chain associates with normal murine procollagen α1 and procollagen α2 chains, causing incomplete folding and degradation of the resulting trimers. A similar model expressing G859C in the procollagen α1 chain was constructed the same way, resulting in successfully injected mutation carrying embryos that died perinatally. The substitution caused poorly mineralized, highly deformed bone (214). Major drawbacks of this model are high lethality of injected embryos and variations in disease severity related to the amount of plasmid expressed (212).

The oim mouse arose spontaneously as a single nucleotide deletion that alters ~50 terminal amino acids in the C-propeptide of the procollagen α2 chainsthat are translated but unable to associate into trimers with procollagen α1 chains (215). Homozygous oim animals are viable and develop severe OI (212). This is perhaps the most used and best-studied mouse model of OI, but it mimics only one known case of human OI with a similar etiology (145,216). It is not clear to what extent it represents general features of OI rather than consequences of this specific mutation (145,216).

The Aga2 mouse models OI caused by C-propeptide mutations in the procollagen α1 chain. A study of this model provided strong evidence of ER stress involvement in OI pathology (89). However, the mechanisms of cell stress

response to more common Gly substitutions are likely to be different, as discussed earlier in this chapter.

Col1a1(Jrt) mouse produced by ENU-induced mutagenesis has an 18 amino acid deletion in the N-terminal region the triple helix caused by a splicing donor site mutation that results in skipping exon 9 of Col1a1 (217). This model recapitulates combined phenotype of OI and Ehlers-Danlos syndrome found in human patients with mutations in the same region (217).

The only two other mouse models of Gly substitutions reported to date are the Brtl mouse with a knock-in Gly349 to Cys substitution in the triple helical region of the procollagen α1 chain (218) and the G610C mouse with a knock-in Gly610 to Cys substitution in the triple helical region of the procollagen α2 chain (169). Heterozygous Brtl animals range in severity from moderately severe to lethal and homozygous animals are milder, potentially due to stabilization of molecules containing two mutant chains through disulfide bonds between side chains of the inserted cysteine residues (143,219).

Heterozygous G610C animals exhibit more moderate OI phenotype compared to Brtl mice while homozygous animals die during or shortly after birth, more consistent with expected outcome of a dominant negative mutation (169). Benefits of this model include well-characterized and genetically uniform C57BL/6J background. All attempts to transfer the outbred Brtl mice onto a well-characterized inbred background were unsuccessful (private communication with Antonella Forlino). Unlike Brtl animals, G610C mice are commercially available through Jackson Laboratories, enabling any researcher to reproduce and extend experimental studies. Furthermore, this model mimics the genetic defect found in the largest known group of human patients (over 60 patients) with the same Gly substitution in an Old Order Amish community from Lancaster County, Pennsylvania (169).

Similar to the patients, heterozygous G610C animals exhibit a wide range of OI phenotypes from mild changes in bone mineral density to moderately severe skeletal deformities and bone fragility. Furthermore, C57CL/6J G610C animals have been crossed with other mouse strains, resulting in variable bone strength yet similar collagen deposition (169). It is therefore possible that other genetic factors related to key osteoblast stress and function genes are involved in mediating OI severity in these animals, making them particularly well suited for the present study.

SECTION 2: SUMMARY AND OBJECTIVES OF THE PRESENT STUDY

Overall, we interpret the role of procollagen misfolding in bone pathology as follows. (a) Procollagen folding is a major challenge for the cell because of thermodynamic instability of its triple helix at body temperature. (b) Cell stress response pathways are important in normal osteoblast differentiation and function at least partly because osteoblasts are procollagen factories that have to cope with misfolding of some of the molecules. (c) Excessive misfolding and accumulation of misfolded procollagen in the cell disrupts the normal function of cell stress response pathways, altering osteoblast function and causing abnormal deposition and mineralization of bone matrix. (d) This pathology may result from changes in procollagen, its folding pathway, and cell stress response pathways important for handling procollagen misfolding. It may thus be triggered by mutations, age, environment, infection and other factors.

We believe that studies of OI caused by Gly substitutions are important for better understanding molecular mechanisms that underlie osteoblast malfunction and resulting bone pathology caused by excessive procollagen misfolding. We hypothesize that such understanding might lead to novel therapeutic treatments for OI and other bone pathologies based on targeting accumulation of misfolded procollagen and/or related cell stress response pathways. We therefore focused on the G610C mouse as one of the most appropriate and convenient animal models for addressing these questions.

Specifically, the objectives of the present study were: (1) To develop better assays for monitoring procollagen folding and accumulation of misfolded procollagen in the cell. (2) To identify key elements of procollagen misfolding, resulting cell stress response and subsequent malfunction of G610C osteoblasts

in culture and *in vivo*. (3) To identify pathways of misfolded procollagen degradation that may be targeted for preventing or reducing excessive accumulation of misfolded molecules in osteoblasts.

SECTION 3: RESULTS AND DISCUSSION

Chapter 5: Azidohomoalanine (Aha) Pulse Chase Labeling Assay for Analysis of Procollagen Biosynthesis[1]

BACKGROUND

Protein folding, secretion, and trafficking pathways, including procollagen, and their role in pathology are often studied by pulse-chase measurements, in which labeled amino acids are introduced into cell culture media and incorporated by cells into newly synthesized chains (220,221). After the labeling "pulse", synthesis, folding, trafficking, secretion, and tissue integration of the labeled chains is followed by a "chase" in the media that contains only normal, unlabeled amino acids.

The most common approach to pulse-chase measurements utilizes amino acids containing radioactive isotopes. Labeling with 35S-Met is particularly popular since it is easily detected and highly active, and methionine is an essential amino acid that is not synthesized by human cells de novo (222,223). Collagen is also frequently labeled with 3H- or 14C-Pro (224,225). Because of much higher proline content relative to most other proteins, 3H- or 14C-Pro labeled collagen chains may be visualized by gel electrophoresis without purification. Another approach is labeling with non-radioactive, stable isotopes, but detection of such isotopes is more difficult, requires expensive instruments and is challenging for gel electrophoresis measurements (226-229).

---

[1] Portions of this chapter are reprinted from Pulse-chase analysis of procollagen biosynthesis by azidohomoalanine labeling, 2014; 55(5-6): 403-410, copyright © 2014, Informa Healthcare. Reproduced with permission of Informa Healthcare.

A particularly appealing alternative to radioisotopes is non-canonical amino acids that are incorporated by cells into proteins instead of regular amino acids (230). For instance, azidohomoalanine (Aha) is a methionine analogue (Fig. 1A) that is efficiently incorporated into aminoacyl-tRNA and proteins instead of methionine (231). Unlike inorganic azide ions, the azide group of Aha is stable and nontoxic (232-234). It can be efficiently conjugated with fluorescent dyes via highly specific “click chemistry” reactions, even within live cells (232,235). Previously published studies did not reveal any significant effects of this labeling on translation initiation, chain synthesis or protein folding (231,235,236).

We found collagen pulse-chase labeling with Aha to be more economical, efficient and convenient compared to radioisotopes. For instance, it allows analysis of gel electrophoresis results without a one-two week delay for capturing the gel image on an x-ray film or imaging plate for autoradiography. Moreover, we also found no appreciable non-target effects of Aha on the cells, in contrast to significant DNA damage, cell cycle changes and growth arrest reported in studies of radioisotope labeling (237-243).

Given our focus on nonradioactive labeling as well as safety and environmental considerations, we did not perform parallel pulse-chase measurements with radioisotopes. We believe that radioisotopes might be useful for some studies but should not be viewed as a reference standard for other pulse-chase approaches. On the contrary, we argue that well-established and well-published radioisotope effects on cellular function might require one to be more cautious in interpreting the results of radioisotope-based experiments.

Here, we analyze optimal conditions and potential non-target effects of collagen labeling with Aha in human fibroblasts, since previous studies of procollagen folding kinetics by radioisotope labeling were reported for human fibroblasts. To illustrate this assay, we describe procollagen folding kinetics in

fibroblasts from an osteogenesis imperfecta (OI) patient with a Gly766 to Cys substitution in the triple helical region of the procollagen α1 collagen chain of type I collagen (α1(I)). Like in an earlier report for other Gly substitutions (188), we observed a delay in folding of procollagen molecules containing the mutant chain. Besides the analysis described in these chapters, we can use this assay to monitor procollagen biosynthesis in mouse primary parietal calvaria osteoblasts (pOBs) and mouse embryonic fibroblasts (MEFs) in the future.

RESULTS

Azidohomoalanine Conjugation with Fluorescent Dyes

Our attempts to utilize traditional, copper-catalyzed click chemistry for conjugation of Aha incorporated into α1(I) and α2(I) chains of type I collagen with alkyne derivatives of fluorescent dyes (Fig. 1B) were largely unsuccessful due to Cu-induced collagen precipitation. In buffers that inhibit this precipitation, we observed only low-efficiency, inconsistent Aha conjugation (data not shown).

In contrast, Aha conjugation with commercially available dibenzocyclooctyne (DIBO) derivatives of Alexa Fluor dyes (DIBO-AF) provided more efficient and consistent labeling of collagen chains (Fig. 1C). Labeling of collagen with DIBO derivative of Alexa Fluor 555 (DIBO-AF555) reached saturation around 150 μM (Fig. 1D,E). For our experiments, we chose to use 71.4 μM DIBO-AF555, where the conjugation efficiency was approximately 50% to reduce reagent used yet still get efficient labeling.

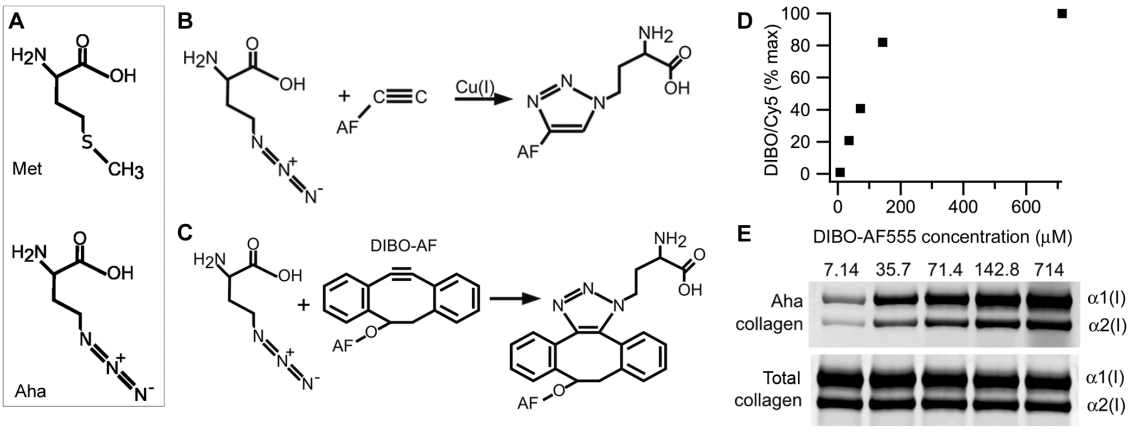

Figure 1. Procollagen labeling with azidohomoalanine (Aha).

(A) Aha and methionine (Met) structures. (B) Cu-catalyzed and (C) Cu-free conjugation of Aha with Alexa Fluor (AF) fluorescent dyes. (D) Aha conjugation efficiency with DIBO-AF555 at different concentrations of the dye calculated from AF555/Cy5 fluorescence intensity ratio in the same gel band (panel E). The conjugation efficiency at 714 μM DIBO-AF555 is assumed to be 100%. (E) Gel electrophoresis of pepsin-treated procollagen (collagen) after Aha conjugation with DIBO-AF555 and Lys conjugation with Cy5. Aha-labeled collagen is revealed by fluorescence scanning at 532 nm excitation and 570±10 nm emission wavelength (AF555) while total collagen is revealed by scanning of the same gel bands at 635 nm excitation and ≥ 665 nm emission (Cy5).

To determine the conjugation efficiency, we also labeled lysine (Lys) with Cy5 (N-hydroxysuccinimide ester) within the same sample and measured the AF555/Cy5 ratio of fluorescence intensities in the same gel electrophoresis bands of α1(I) and α2(I) chains. To correct for possible sample-to-sample variation in Lys labeling, MMP1-cleavage fragments (matrix metalloprotease 1-MMP1) of rat-tail-tendon collagen prelabeled with Alexa Fluor 488 were added to each sample before labeling with Cy5. These fragments provided an internal standard for Lys labeling efficiency, gel loading, and calculation of absolute collagen concentration in the sample; control experiments showed that their ratio to full-length collagen and procollagen remained constant within our purification procedure (244).

Optimization of Aha Incorporation into Collagen

To replace Met with Aha in newly synthesized procollagen chains, we pre-incubated fibroblasts in Met- and Cys-free medium (Met depletion) followed by incubation in the same medium with different concentrations of Aha (labeling pulse). To optimize the replacement, we varied the length of Met depletion, length of Aha pulse, and Aha concentration during the pulse and measured the DIBO-AF555/Cy5 ratio in gel bands of α1(I) and α2(I) chains. We found that 500 μM Aha concentration was sufficient for achieving near maximum Aha incorporation into procollagen newly secreted by fibroblasts (Fig. 2A). A 30 min incubation of the cells in Met and Cys free media prior to the addition of Aha was necessary and sufficient for maximum Aha incorporation (Fig. 2B). The saturating concentration of Aha was achieved after 4 hours in secreted procollagen (Fig. 2C) and after 2 hours in intracellular procollagen (Fig. 2D).

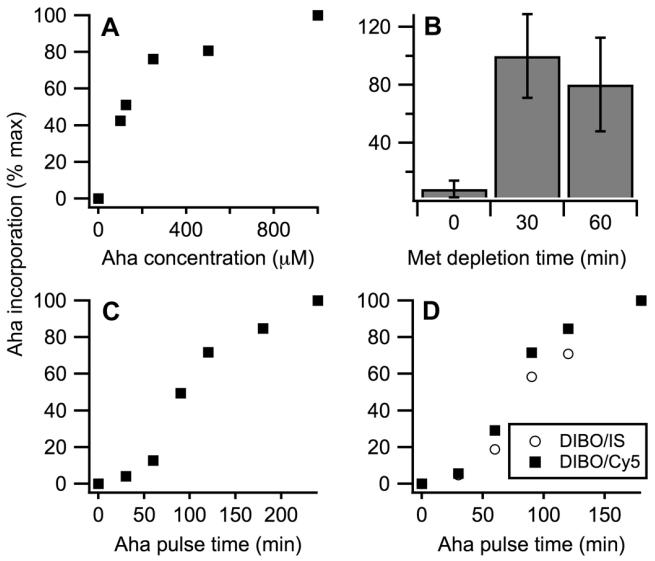

Figure 2. Optimization of Aha incorporation into procollagen.

Aha incorporation is measured from DIBO-AF555/Cy5 fluorescence intensity ratio in secreted (A-C) and intracellular (D) procollagen as described in Fig. 1D. (A) Aha incorporation after 30 min Met depletion followed by 4 h pulses of different Aha concentrations. (B) Aha incorporation after Met depletions of different lengths followed by 4 h 500 μM Aha pulses. Error bars represent standard deviation. (C) Aha incorporation after 30 min Met depletions followed by 500 μM Aha pulses of different lengths. (D) Aha incorporation into intracellular procollagen after 30 min Met depletions followed by 500 μM Aha pulses of different lengths measured from DIBO-AF555/Cy5 (squares) and from DIBO-AF555/IS-AF488 (circles) fluorescence intensity ratios. The latter ratio normalizes the amount of Aha conjugated with DIBO-AF555 by the amount of internal standard (IS) conjugated with AF488, which is added to the cell lysis buffer. The two methods of evaluating Aha incorporation produce consistent results.

Effects of Aha Labeling on Fibroblast Function and Procollagen Biosynthesis

To test effects of this labeling procedure on cell function and procollagen synthesis, we compared: (i) fibroblast cultures in which 30 min Met/Cys depletion was followed by a 500 μM Aha pulse, (ii) cultures in which the same depletion was followed by a 500 μM Met pulse, and (iii) control cultures without the

depletion and Met or Aha pulses. We found no effects of Met depletion and short Aha and Met pulses on transcript levels of key cell stress proteins (Fig. 3A,B). We observed decreased BIP and increased αB crystalline transcription after 24 h pulses, indicating slow activation of some cellular response. The response was similar for Met and Aha and likely associated with low serum concentration in the media (commonly used in pulse-chase studies to promote utilization of labeled amino acids by cells, rather than amino acids from serum proteins). However, the latter response should not pose a significant problem for typical pulse-chase experiments that do not extend beyond 4-8 h.

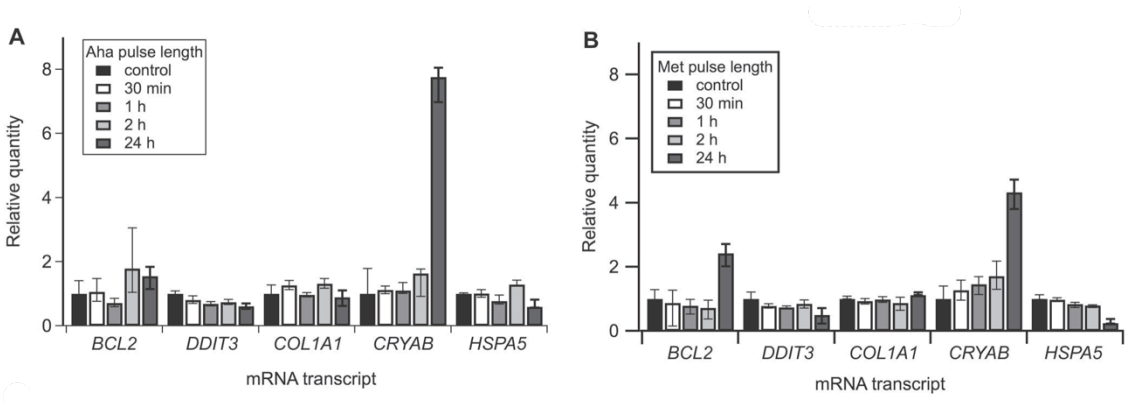

Figure 3. Quantitative real-time PCR analysis of Aha effects on different cell stress markers.

(A) 500 μM Aha pulses of increasing length were compared with (B) 500 μM Met pulses under identical cell culture conditions. Expression of BCL2, DDIT3 (CHOP), COL1A1 (procollagen α1(I)), CRYAB (crystalline αB), and HSPA5 (BIP) transcript levels were measured relative to cells in growth medium (control) and normalized to HPRT1 and B2M as endogenous controls. All error bars represent standard deviation.

We did not observe any detectable effects of Aha labeling on procollagen biosynthesis either. Procollagen transcription and secretion rates as well as the amount of intracellular procollagen remained the same as in control cells for at least 4h (Fig. 4C,D). Normal electrophoretic mobility and thermal denaturation

thermograms of collagen and procollagen indicated that Aha incorporation did not disrupt posttranslational modification, stability or structure of the triple helix (Figure 1E, 4A,B).

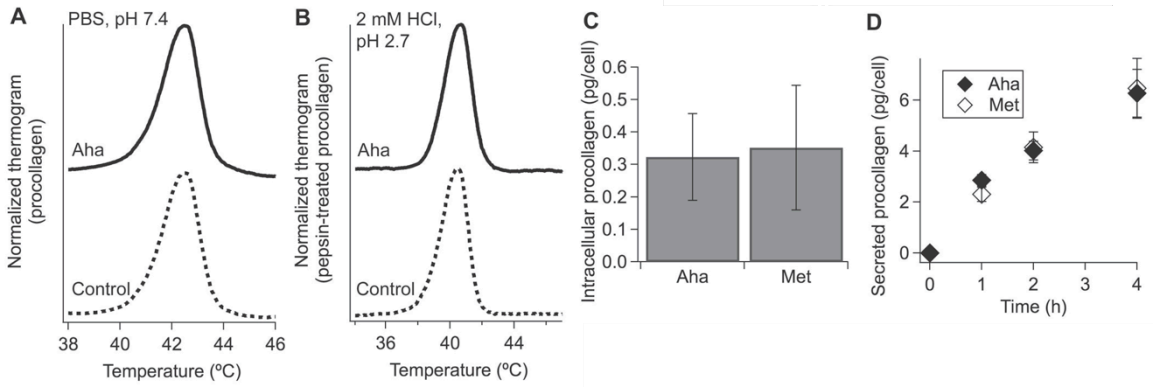

Figure 4. Effects of Aha incorporation on procollagen stability, synthesis, and secretion.

(A,B) Denaturation thermograms of secreted protein after ammonium sulfate isolation of procollagen (A) and subsequent purification of pepsin-treated collagen (B). (C) Amount of procollagen inside each cell after 4 h stimulation with 250 μM ascorbic acid 2-phosphate in growth medium followed by 30 min Met depletion and a 4 h pulse of 500 μM Aha or Met. (D) Amount of procollagen secreted by each cell after the same treatment, except for varying Aha/Met pulse length.

Measurement of Procollagen Folding and Secretion Kinetics

To measure the kinetics of procollagen folding, after depletion of free Met for 30 min, we pulse-labeled newly synthesized molecules with 500 μM Aha for 10 min and measured accumulation of folded procollagen triple helices in a chase medium containing 10 mM Met and no Aha. We isolated folded procollagen triple helices by chymotrypsin/trypsin digestion of cell lysates together with the chase medium as described in Methods (Chapter 10).

We observed significantly slower folding of procollagen molecules in OI compared to control fibroblasts (Fig. 5A,B), consistent with folding of procollagen

with other Gly substitutions studied by pulse-chase labeling with 35S-Met (188). We quantified the kinetics of formation of cleavage-resistant folded triple helices by gel electrophoresis, after other proteins and unfolded procollagen chains in cell lysates were degraded by chymotrypsin and trypsin (188). We detected only full-length helices but not degradation products of partially folded molecules, in which the C-to-N-terminal triple helix propagation paused at the mutation site.

To measure how folded and misfolded procollagen molecules are cleared from the cell, after depletion of free Met, we pulse-labeled newly synthesized molecules with 500 μM Aha for 2 h. After subsequent incubation in 10 mM Met chase medium, we separately purified procollagen triple helices from cell lysates and the chase medium by pepsin treatment. We measured the retention of Aha-labeled procollagen in the cell by comparing the amount of Aha-labeled triple helices in the cell lysate immediately after the labeling pulse and after different incubation times as described in Chapter 10.

We also observed much slower clearance of Aha labeled procollagen from OI compared to normal control fibroblasts. Figure 5C shows the relative content of Aha in triple helices of intracellular procollagen during the chase, which was evaluated from DIBO-AF555/IS-AF488 fluorescence intensity ratio of DIBO-AF555 labeled collagen to AF488 labeled internal standard (IS). These helices were purified by pepsin treatment and salt fractionation from cell lysates free of cell debris and ECM. By directly measuring their Aha content, our assay accurately quantifies the clearance kinetics of labeled procollagen from the cell.

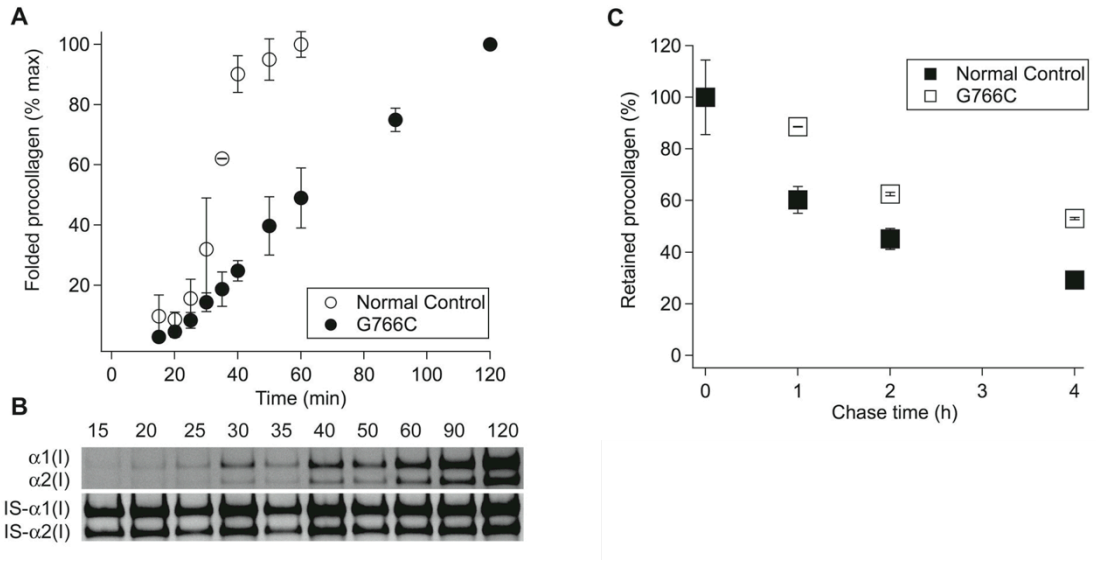

Figure 5. Folding and intracellular retention of procollagen with an α1(I)-G766C substitution.

(A,B) Measurement of procollagen folding kinetics by pulse-chase labeling with Aha. The fraction of fully folded procollagen (A) is calculated relative to the latest time point from DIBO-AF555/IS-AF488 fluorescence intensity ratios of gel electrophoresis bands (B); IS-α1 and IS-α2 are long fragments of α1(I) and α2(I) chains of rat-tail-tendon collagen cleaved with MMP1 used as internal standard (IS). (C). Kinetics of procollagen clearance from cells measured by pulse-chase labeling with Aha from DIBO-AF555/IS-AF488 fluorescence intensity ratios of gel electrophoresis bands of intracellular procollagen after different chase time. The average DIBO-AF555/IS-AF488 ratio at zero chase time is taken as 100%. All error bars represent standard deviation in triplicate experiments.

DISCUSSION

Effects of Pulse-Chase Labeling with Radioisotopes on Cell Function

Pulse-chase labeling of procollagen is most commonly performed with 25-500 μCi/ml 3H-proline (85,224), 0.5-5 μCi/ml 14C-proline (85,225), or 10-200 μCi/mL 35S-methionine (177,188). However, recent studies indicate that these low-energy β-emitters cause significant cell stress and malfunction even at low

concentrations and short exposure (237,238,241-243). Significant fragmentation of DNA was observed after 2h at 10 μCi/ml 35S-methionine and 2-20 μCi/ml 3H-thymidine in the cell culture media (239). Radioisotope incorporation into multiple molecules and subsequent radioactive decay inside the cell was found to cause persistent DNA fragmentation long after replacing the media, suggesting that even short pulse labeling might have severe consequences (237,239). The observed response to radioisotopes was similar in different cell types. Radioisotope labeling at or below typical concentrations was reported to elevate the level of p53, induce formation of reactive oxygen species (ROS), inhibit cell cycle progression, cause growth arrest, and increase apoptosis (237-239,242,243). Gene expression profiling revealed dramatic changes in multiple cell stress response proteins (240).

The observations of significant DNA damage, cell cycle changes, and growth arrest after 3H and 35S exposure indicate that other cellular functions are likely to be altered as well. Radioisotope effects might be particularly severe and difficult to account for in pulse-chase labeling studies of procollagen secretion by cells from patients with procollagen biosynthesis abnormalities. Such experiments require at least 2-4 h equilibration in the radioactive media followed by 2-4 h chase and therefore at least 4-8 h cumulative exposure to radioactive isotopes outside and inside the cells. During this time, DNA damage and ROS might significantly alter procollagen biosynthesis, e.g. because they affect Wnt/β-catenin, TGF-β, BMP and other key signaling pathways (245,246). Retention of abnormal procollagen by the cells might worsen the radioactive damage and its downstream effects by enhancing radioisotope accumulation, particularly in the case of 3H-Pro or 14C-Pro labeling. Combined with differences in the general metabolic activity and susceptibility to radioactive damage, these effects might significantly complicate the comparison between patient and normal control cells.

The response of cells to the DNA damage, ROS and other highly reactive free radicals may therefore affect the interpretation of pulse-chase radioisotope labeling experiments. While these experiments may provide useful information about procollagen chain association, folding and secretion, full understanding of their results requires characterization of potential radioactive damage effects on the cells. Since such damage might depend on specific experimental conditions, its consequences are difficult to predict a priori. One potential alternative is labeling with non-radioactive isotopes, which may be detected by a variety of spectroscopic techniques (227,229,247). Another alternative, which we are pursuing in the present study, is labeling with noncanonical amino acids.

Labeling with Aha as an Alternative Approach

At least for procollagen, replacement of methionine with azidohomoalanine provides a particularly useful labeling approach. It is sufficiently sensitive, utilizes commercially available reagents, reduces environmentally toxic waste, eliminates exposure to radioactivity, and lowers the cost of experiments. Detection of Aha-labeled molecules by conjugation with fluorescent dyes is based on a reaction not found in living systems and is highly specific, eliminating background labeling (232,234). It shortens the time for visualizing labeled proteins on gels. Instead of several days or weeks typically required for x-ray film or imaging plate exposure in autoradiography, fluorescence scanning of gels takes minutes. A pre-labeled internal standard and conjugation of Aha and Lys with different fluorescent dyes allow data analysis with fewer or no assumptions compared to traditional methods that implicitly assume similar procollagen labeling efficiency and extraction yield in patient and control cells, which may not be the case.

In contrast to radioisotopes, Aha does not affect cell viability (231) and has fewer, if any, unintended effects on cell function. In fibroblasts, we found no changes in expression of BCL2, BIP, and CHOP after replacing Met with Aha (Fig. 3), suggesting minimal or no cell stress. We also detected no changes in collagen gene or protein expression (Fig. 3, 4C,D), supporting previous observations of normal protein synthesis rate (235,248) and therefore normal translation initiation at Met codon. Approximately 400 fold slower incorporation of Aha into aminoacyl-tRNA by methionyl-tRNA synthetase does not appear to hinder protein synthesis either (249).

Normal procollagen synthesis rate, concentration in the cell, and lifetime in the cell as well as unaltered triple helix stability, all indicate minimal or no effect of the Met to Aha substitution on procollagen folding, structure or trafficking through the cell. Normal expression of the key regulator of unfolded protein response, BIP, suggests normal folding, structure and trafficking of other proteins as well, consistent with previously reported studies of Aha effects (231,235,236). Because Met residues within the triple helix are exposed to the solvent, it is not unexpected that their replacement with Aha has no significant consequences for the triple helix folding or structure. More surprisingly, this substitution appears to have no effect on folding and structure of even the globular C-propeptide and other globular proteins (236), in which Met is buried inside the protein core.

Apparently, Aha is not just a safer, cheaper, and more convenient alternative to radioisotopes for pulse-chase studies of procollagen biosynthesis, but it also has fewer unintended consequences and its results are easier to interpret. On a cautionary note, however, our and previously published studies do not exclude unintended consequences of Aha labeling for proteins and cell functions that have not been examined so far. For instance, our study revealed no effects of Aha on procollagen biosynthesis or function of fibroblasts.

Previously published studies revealed no effects of Aha on other proteins and other types of cells (231,233,235,236,248). Yet, this evidence is not sufficient to exclude all potential effects of Aha. Further characterization of potential unintended consequences might be necessary for other applications of Aha labeling or for making conclusions that extend beyond procollagen synthesis, folding, and trafficking. At the same time, it is important to keep in mind that such a characterization is even more critical for radioisotope labeling, since the latter does lead to multiple known problems discussed above.

Procollagen Misfolding in OI Fibroblasts

To test whether pulse-chase labeling with Aha is sensitive and accurate enough for measuring procollagen folding and accumulation in cells, we compared cultured dermal fibroblasts from an OI patient and normal control, with the caveats discussed above, previously reported similar studies conducted with radioisotope pulse-chase labeling provided the reference point for evaluating the assay capabilities.

We were able to detect abnormal folding and clearance of procollagen with Cys substitution for Gly766 in the α1(I) chain (Fig. 5). Consistent with a previous, radioisotope-based study of fibroblasts from OI patients with other Gly substitutions (188) and the established role of obligatory Gly residues (142), we observed significantly slower triple helix folding in OI compared to normal control cells (Fig. 5A). Our assay did not detect a folding intermediate paused at the mutation site. Note that in (34), such an intermediate was detected only for a Gly94 substitution at the N-terminal end of the triple helix but not for Gly substitutions located closer to the C-terminal end. In the latter mutations, the folding intermediates might not have sufficiently long lifetimes to be detected by

the trypsin/chymotrypsin digestion assay or the corresponding collagen digestion products might not co-purify with full-length triple helices.

Slower folding likely contributes to slower clearance of Aha-labeled procollagen molecules from OI fibroblasts (Fig. 5C). However, less than 50% decrease in Aha-labeled molecules inside the cells after 4 h chase is difficult to explain just by the delay in their folding. The dramatic increase in the lifetime of a labeled molecule inside the cell points to a delay in trafficking through or export from the cell. In particular, misfolded molecules with Gly substitutions might be selectively retained and targeted for intracellular degradation (174,177,224,250,251). Cell stress response to such misfolding and accumulation of mutant procollagen molecules in osteoblasts might contribute to bone pathology in OI, and is discussed in later chapters .

Chapter 6: G610C Procollagen Folding, Secretion, and Incorporation into Extracellular Matrix

BACKGROUND

Like all Gly substitutions in the triple helix, the Gly610 to Cys substitution in the triple helical region of the collagen α2(I) chain (G610C substitution) may have several different effects contributing to OI. (a) It might affect the function of osteoblasts by disrupting procollagen folding in the cell. (b) It might affect how secreted collagen molecules are incorporated into the matrix outside the cell by altering the stability of secreted molecules and their interactions with other molecules involved in matrix assembly. (c) It might affect how incorporated molecules function in the matrix by altering matrix integrity and interaction with important ligands and cells.

For reasons discussed in Section I, here we focus on the effects of the mutation inside the cell by utilizing cultured calvarial osteoblasts (pOBs) and mouse embryonic fibroblasts (MEFs) from G610C animals. Specifically, we measure how the mutation affects synthesis, folding, and intracellular retention of procollagen chains. However, to better understand the relative role of these effects in OI pathology, we also measure how efficiently the mutant molecules are secreted and incorporated into extracellular matrix.

pOBs isolated from parietal bones of young (3-8 day old) mice represent a convenient model for studies of procollagen misfolding effects in cell culture. Parietal bones are formed by intramembranous ossification by cells that originate from mesoderm, unlike frontal bones that may contain cells derived from neural crest, or occipital bones that are partially formed through a mix of endochondral and intramembranous ossification and contain chondrocytes (252,253).

Furthermore, as discussed later in this section, parietal bones very rapidly grow, hence providing a rich source of osteoblasts, and show clear formation pathology in G610C animals. The main disadvantage of parietal OBs is that they cannot be isolated from homozygous G610C mice that die during or shortly after birth. Therefore, to compare effects of the mutation in wild type, heterozygous and homozygous cells, we utilize MEFs. We demonstrate that procollagen biosynthesis abnormalities observed in heterozygous COBs and MEFs are similar, suggesting that the latter cells may be used to understand at least some of the effects of procollagen misfolding caused by Gly substitutions.

RESULTS

Transcription

We first evaluated whether collagen transcription was affected due to the G610C mutation. We analyzed mRNA from cultured pOBs, mRNA extracted directly from parietal bones, and mRNA extracted from cultured MEFs. While bones contain a heterogeneous population of cells, osteoblasts provide dominant contribution to procollagen synthesis. We found no statistically significant effects of the G610C substitution on Col1a1 and Col1a2 mRNA transcript levels in any of the samples (Fig. 6).

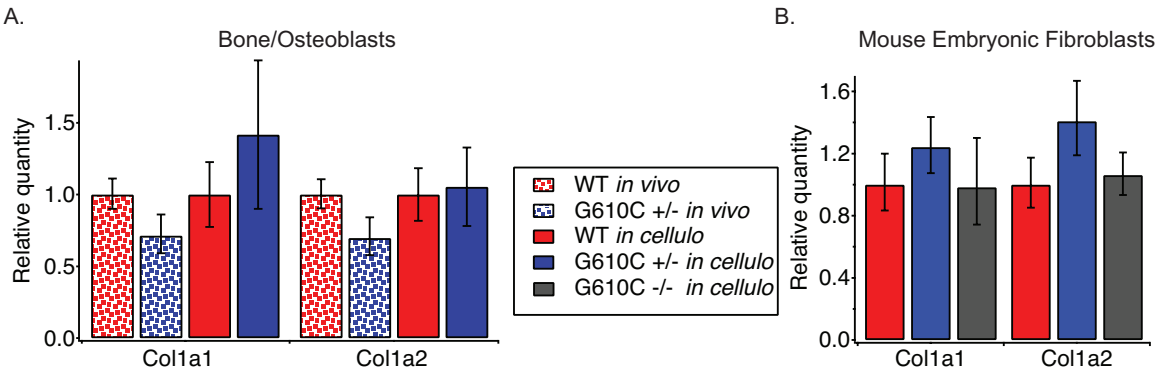

Figure 6. Transcription levels.

Col1a1 (procollagen α1) and Col1a2 (procollagen α2) mRNA transcript levels were measured relative to WT. In (A.), HPRT1 and B2M were used as endogenous controls. In (B.), HPRT1, B2M, and Gapdh were used as endogenous controls. Error bars represent standard deviation of biological replicates.

Folding

We then measured procollagen folding rates to determine whether the G610C substitution delayed folding and to what extent. We exploited the resistance of the procollagen triple helix to trypsin/chymotrypsin treatment for determining the fraction of fully folded molecules after a brief pulse of Aha, utilizing the assay described in Chapter 5.

We found significantly slower folding in G610C heterozygous (G610C/+) pOBs (Fig. 7A). The folding delay was similar in heterozygous MEFs and larger in homozygous (G610C/G610C) MEFs (Fig7C). The latter observation corroborated that the folding delay was caused by the mutation. Indeed, heterozygous cells produce faster folding molecules without the mutant chain and slower folding molecules with the mutant chain, while homozygous cells produce only the slower folding molecules. Since our assay does not distinguish

procollagen with and without the mutant chain, it measures an effective, average folding rate of all molecules.

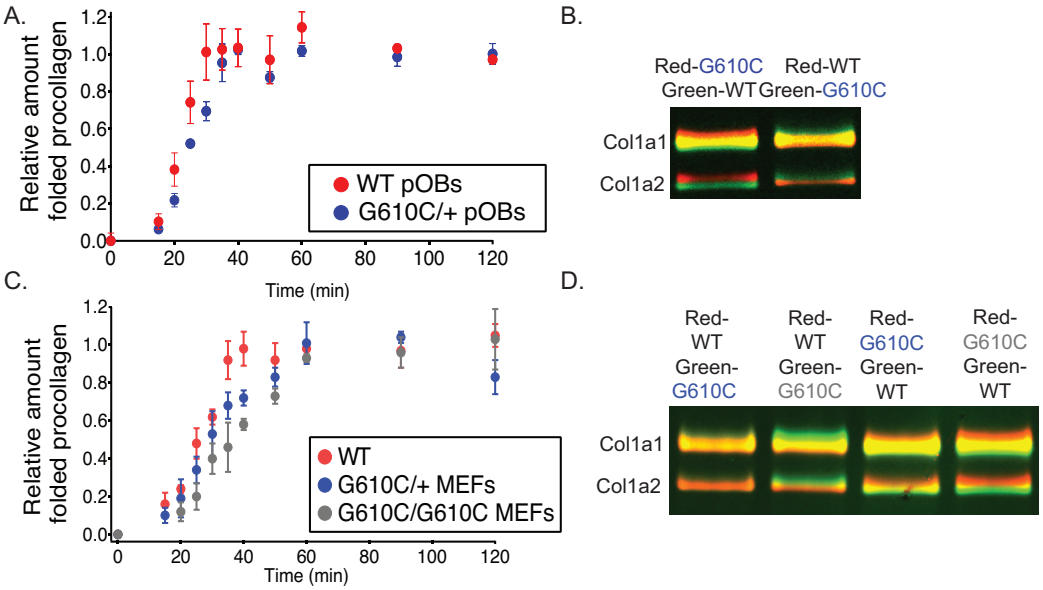

Figure 7. Delayed folding and over-modification of procollagen chains in G610C pOBs and MEFs relative to WT.

(A, C). Measurement of procollagen folding kinetics via pulse-chase labeling with Aha. The fraction of fully folded procollagen produced by pOBs at passage 2 (A) and MEFs (C) was calculated relative to the latest time point from DIBO-AF555/IS-AF488 fluorescence intensity ratios of gel electrophoresis bands. All error bars represent standard error in triplicate experiments. (B, D). Gel electrophoresis of pepsin-treated triple helices labeled with AlexaFluor 488 (Green) or Cy5 (Red). The triple helices were purified by pepsin treatment from procollagen secreted by pOBs (B) and MEFs (D). To reveal relatively small gel migration differences, AlexaFluor-488-labeled WT helices were mixed with Cy5 labeled G610C/+ or G610C/G610C helices at equal concentration and run in the same gel lane. The dyes were then switched to account for effects of the fluorophore on gel migration. Slower gel migration reveals overmodification. Yellow color is where the bands overlap.

When the rate of folding is slower, unassociated chains remain available for proline hydroxylation as well as lysine hydroxylation and subsequent glucosylation for longer, leading to over-modification of the chains (254). This

over-modification of procollagen can be observed by decreased gel mobility via gel electrophoresis, which we confirmed in G610C pOBs and MEFs (Fig. 7B,D). This measurement also does not distinguish between the molecules with and without the mutant chains produced by heterozygous cells. Consistently, we saw more over-modification in collagen produced by homozygous than heterozygous MEFs (Fig. 7D). Interestingly, overmodification of heterozygous pOBs was more comparable to homozygous MEFs than heterozygous MEFs.

Intracellular Procollagen and Secretion

The amount of total intracellular procollagen protein was increased in G610C/+ pOBs by ~50% compared to WT pOBs (Fig. 8A). At the same time, G610C/+ pOBs secreted ~35% less procollagen than WT pOBs, indicating significant retention of procollagen in mutant cells (Fig. 8C).

It is important to note that the secretion rate measured based on procollagen released by pOBs into cell culture medium does not represent the total amount of procollagen secreted by osteoblasts, since it does not account for procollagen retained under cells in the cell layer and collagen deposited into matrix. In osteoblast cultures, procollagen released into the medium may represent a minor fraction of all secreted molecules.

Heterozygous MEFs also accumulated significantly more intracellular procollagen (Fig. 8B), but they secreted approximately the same amount of procollagen into the medium as wild type MEFs (Fig. 8D). Interestingly, homozygous MEFs accumulated and secreted less procollagen than the heterozygous cells.

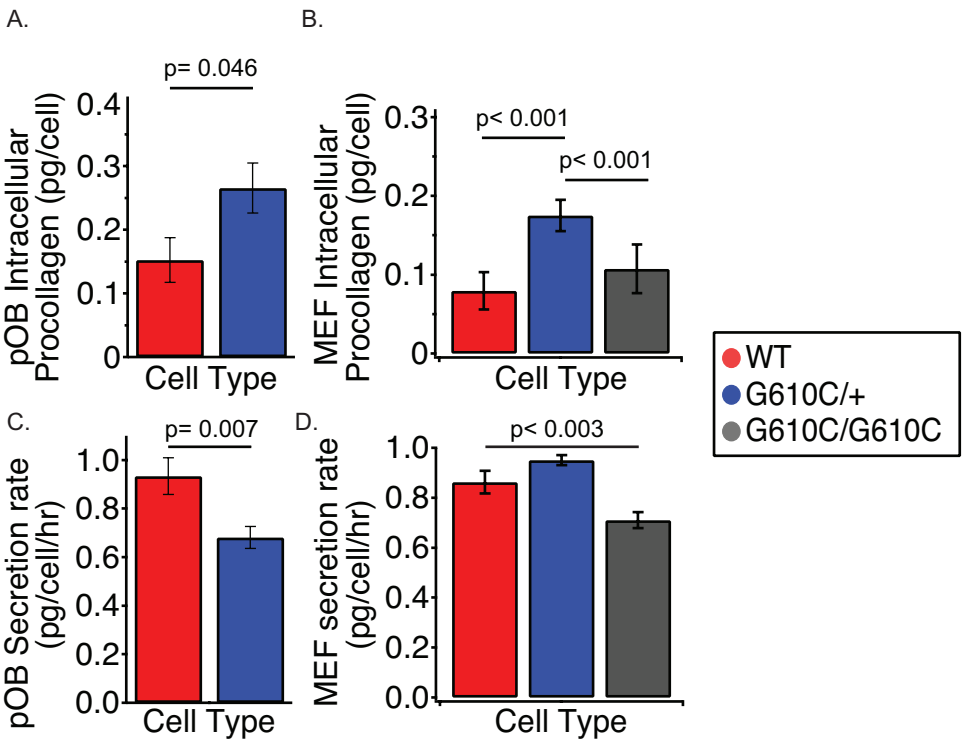

Figure 8. Intracellular procollagen concentration and procollagen secretion rate into cell culture medium measured in G610C pOBs and MEFs

(A.) pOB and (B.) MEF intracellular procollagen levels were measured by ammonium sulfate precipitation followed by pepsin digestion of intracellular procollagen. Absolute procollagen concentration in pg/cell was quantified by normalizing to internal collagen standard added to cell lysates as described in Chapter 10. The rate of procollagen secretion by pOBs (C) and MEFs (D) was measured by quantifying procollagen concentration in cell culture medium collected hourly for four hours. All error bars represent standard error in at least sextuplicate experiments. The p-values were calculated from a two-tailed t-test.

Residence Time

Pulse-chase measurements of the residence time of Aha-labeled procollagen confirmed that mutant cells retain a larger fraction of procollagen they produce than wild type cells. The Aha-labeled molecules remained longer inside heterozygous pOBs and MEFs compared to wild type cells (Fig. 9). Their

residence time was even more dramatically increased in homozygous MEFs (Fig. 9B).

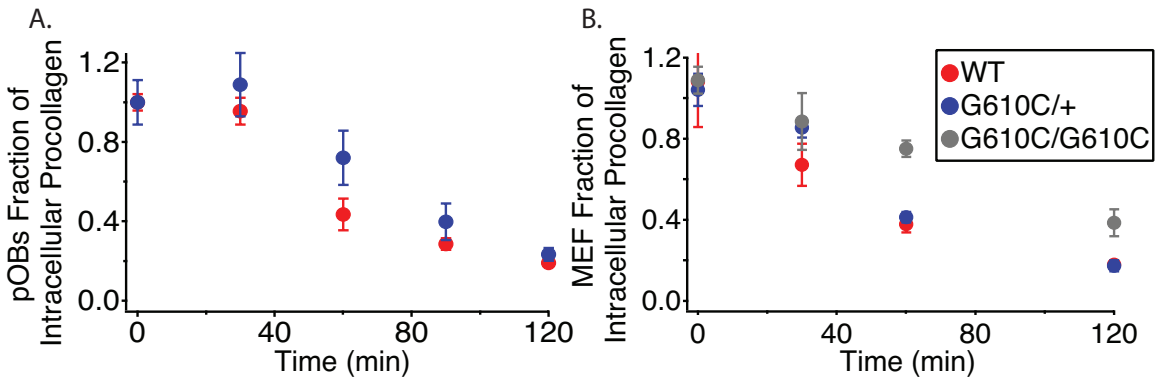

Figure 9. Residence time of procollagen in the cell in G610C pOBs and MEFs. (A,B). Kinetics of procollagen clearance from cells measured by pulse-chase labeling with Aha from DIBO-AF555/IS-AF488 fluorescence intensity ratios of gel electrophoresis bands of intracellular procollagen after different chase time in pOBs at passage 1 (A.) and MEFs (B.). The average DIBO-AF555/IS-AF488 ratio at zero chase time is taken as 100%. All error bars represent standard error in triplicate experiments.

Fraction of Mutant Molecules

Measurement of the composition of procollagen secreted into the media, however, suggested that G610C cells retained molecules with and without the mutant chains non-selectively. Indeed, secreted procollagen collected hourly in the cell culture media of G610C/+ pOBs had ~50:50 ratio of molecules with and without mutant chains (Fig. 10A) consistent with the expected 50:50 ratio of molecules produced by the cell (assuming similar expression of the normal and mutant alleles of Col1a2).

A higher fraction of molecules with the mutant chain irreversibly denatured within several hours after secretion into cell culture media, as expected (26)

based on their lower thermal stability (169). Indeed, when we collected the secreted fraction of collagen after 16 hours, we observed close to 60:40 rather than 50:50 ratio of normal to mutant molecules (Fig. 10B). Rapid thermal denaturation was likely responsible for preventing incorporation of the mutant molecules into slowly forming extracellular matrix, in which the ratio of normal to mutant molecules was close to 70:30 (Fig. 10C).

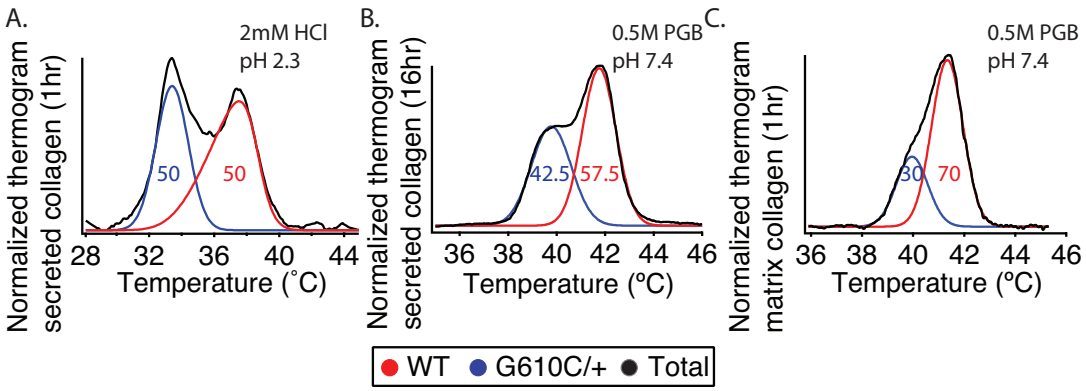

Figure 10. Composition and thermal stability of procollagen secreted into cell culture media and collagen deposited into extracellular matrix by G610C/+ pOBs measured by differential scanning calorimetry

(A.) Denaturation thermogram of ammonium sulfate precipitated and pepsin digested procollagen collected hourly in cell culture media. Purified triple helices were resuspended in 2 mM HCl, which allows better separation of denaturation peaks from mutant (blue) and normal (red) molecules. The thermal stability of pepsin-treated triple helices is identical to that of full-length procollagen, except for molecules with mutations at the interface with N- and C-propeptides (34). (B.) Denaturation thermogram of ammonium sulfate precipitated and pepsin digested procollagen collected in cell culture media after 16 hour incubation. Purified collagen was resuspended in phosphate glycerol buffer (PGB), pH 7.4, which better represents physiological thermal stability of the molecules (26). (C.) Denaturation thermogram of ammonium sulfate precipitated and pepsin digested matrix collagen in PGB. Relative percent of normal (WT) and mutant (G610C/+) molecules was calculated by deconvolution of lower temperature mutant and higher temperature normal denaturation peaks with PeakFit software and measuring the area under each peak. The maximum of each peak represents the apparent denaturation temperature (T_m) in the corresponding buffer at the heating rate (0.125 ^{o}C/min or 0.25 °C/min) used in the DSC experiment. The apparent T_m in physiological saline at the same heating rate may be recalculated from the T_m measured in PGB by subtracting 1.7 ^{o}C (26).

Extracellular Matrix Formation

We next analyzed the total amount of collagen incorporated into matrix by pOBs and MEFs using Raman spectroscopy. Procollagen has a unique Raman scattering spectrum compared to the Raman scattering spectrum of other proteins and cell cytoplasm, allowing us to compare the ratio of collagen to organic material inside cells within different matrix regions (74). After 3 weeks, WT and G610C/+ pOBs had deposited 4 and 7 times more collagen than WT and G610C/+ MEFs cultured for 8 weeks, respectively (Fig. 11). MEFs had to be grown for at least 8 weeks to obtain a measurable amount of matrix. We observed significantly less collagen deposited into the matrix by G610C/+ than WT pOBs (Fig. 11A). There was even less collagen deposited into the matrix in G610C/+ and G610C/G610C MEFs compared to WT MEFs, but no difference between the heterozygous and homozygous MEFs (Fig. 11B).

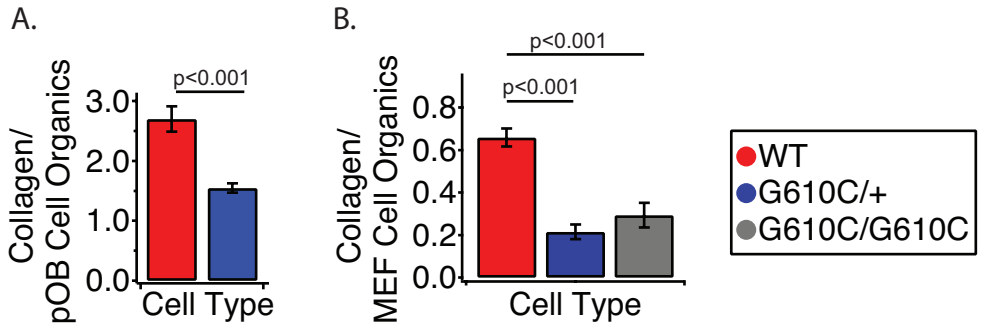

Figure 11. Levels of collagen deposition into matrix in pOBs and MEFs.

Raman spectroscopy measurements of collagen/cell organic material in matrix grown for 3 weeks by pOBs (A.) or 8 weeks by MEFs (B.). Error bars represent standard error and statistical significance was determined by a two-tail t-test. Each bar represents the ratio of intensities of characteristic Raman peaks for collagen and organic material inside cell cytoplasm, which is proportional to the amount of collagen deposited in the matrix by a cell.

DISCUSSION

Procollagen Misfolding

In G610C cells, we observed significantly slower folding of procollagen proportional to the fraction of mutant molecules they made (Fig. 7A,C). The folding rate was not as dramatically decreased as observed by some Gly substitutions in human fibroblasts (188), indicating that folding of G610C procollagen was re-nucleated faster than in the case of the latter mutations. In general, the effect of a Gly substitution on the folding may vary significantly, depending on the presence of HSP47 binding sites and other variations in the amino acid sequence surrounding the mutation (67). The slower folding caused posttranslational overmodification of procollagen, consistent with observations for Gly substitutions in human cells (255).

Folding disruption by the G610C substitution resulted in procollagen accumulation in the cell. (a) The total amount of intracellular collagen was higher (Fig. 8A,B) while the secretion rate was lower or similar (Fig. 8C,D) in G610C compared to WT cells. (b) Newly synthesized procollagen remained longer in G610C cells than in WT cells (Fig. 9). These observations were consistent with published reports for human fibroblasts with other Gly substitutions in the α2 (I) chain of type I collagen (256,257).

While this general qualitative conclusion holds for both pOBs and MEFs, we observed peculiar quantitative “inconsistencies” in how MEFs accumulated and released procollagen into the medium. The apparent inconsistencies between the behavior of pOBs and MEFs might be related to major differences in the amount of procollagen these cells produce and the direction in which they secrete it. In general, osteoblasts produce much more procollagen than less

differentiated MEFs. The similarity between the amounts of procollagen released by pOBs and MEFs into the cell culture medium (c.f. Fig 8C and 8D) is misleading. In contrast to MEFs, only a small fraction of the total procollagen secreted by pOBs was found in the medium. Osteoblasts secrete procollagen primarily into the space between the cells and the surface on which they reside, where it is “trapped”, processed and deposited into matrix. It is therefore reasonable to expect the effect of the mutation on procollagen synthesis and secretion to be somewhat different in pOBs than MEFs.

Interestingly, procollagen accumulation in homozygous MEFs was much less pronounced than either in heterozygous MEFs or heterozygous pOBs, we believe that this observation may be explained by reduced procollagen translation in response to cell stress associated with the synthesis of just the mutant molecules. Indeed, the total fraction of Aha-labeled procollagen, which represents newly synthesized molecule, was always lower in homozygous MEFs than in the other cell types (data not shown), indicating reduced procollagen synthesis. At the same time, the transcription of procollagen mRNA did not appear to be affected (Fig. 6B). Much longer procollagen residence time in the cell (Fig. 9B) suggests that intracellular degradation of misfolded procollagen might not be able to keep up with synthesis of just the mutant molecules in homozygous MEFs, potentially causing the reduction in procollagen translation. However, alternative interpretations are possible and full understanding of procollagen synthesis in homozygous MEFs will require future studies.

No Selective Retention of Mutant Procollagen

We initially hypothesized that misfolded procollagen molecules would be selectively retained and degraded by the cell, but this was not the case. G610C

pOBs secreted equal numbers of normal and mutant molecules. Selective retention of mutant procollagen was observed in some mechanistic studies of OI, but in many others it was not present, suggesting that it might depend on many variables (34,177,225,258).

The most important unknown to be addressed by future studies is the conformation of accumulated misfolded procollagen in the ER. In a crowded ER environment, slower triple helix folding increases the probability of nonproductive interactions between unfolded regions of the chains from different procollagen chain trimers, resulting in procollagen aggregation. Nonselective aggregation would trap both molecules with and without the mutant chain, resulting in nonselective procollagen misfolding, although mutant molecules trigger this process. We could not detect the presence of such aggregates, but other OI studies reported misfolded procollagen aggregation (70,174).

Other possibilities include targeting of large chunks of ER for degradation by macroautophagy, which may occur in response to misfolding of mutant molecules but also may trap procollagen without the mutant chain (174). We will return to discussion of the role of macroautophagy in G610C cells in subsequent chapters. Gross enough disruption of ER homeostasis caused by misfolding of mutant molecules may also affect folding and export of normal procollagen. Adaptive and chronic ER stress, which may have profound effects on ER homeostasis, has been discussed in a number of OI studies (23,177,195,259) and it is the focus of Chapter 7 in this thesis.

Matrix Deposition

We observed dramatically reduced matrix deposition by G610C cells, particularly in MEF cultures (Fig. 11). In part, this observation could be explained

by reduced procollagen secretion and lower thermal stability of mutant molecules, some of which denatured before they had a chance to be incorporated into matrix (Fig. 10). However, reduced procollagen secretion was observed most significantly in pOB, not MEF cultures, while the mutation had a stronger effect on matrix deposition by the latter. The fact that ~50% of secreted mutant molecules did not incorporate into matrix (Fig. 10C) could not explain much larger overall change in the collagen deposition either (~ 2 fold in heterozygous pOB and ~ 3 fold in heterozygous MEF cultures). Furthermore, less procollagen was secreted by homozygous compared to heterozygous MEFs and all of the collagen secreted by homozygous MEFs was mutant, but the same amount of collagen was deposited by both types of cells.

Since abnormal matrix deposition could not be explained only by availability and malfunction of secreted procollagen molecules, we concluded that cellular malfunction caused by accumulation of misfolded procollagen contributed to abnormal matrix deposition. Thus, our next step was determining how misfolded molecules are handled by the cell, and whether osteoblast differentiation and function was disrupted by the G610C substitution.

Chapter 7: Osteoblastic Response to Procollagen Misfolding in the Cell

BACKGROUND

In the previous chapter we described that procollagen misfolding led to nonselective retention and accumulation of procollagen molecules in G610C cells, which would be expected to cause cell stress. The cells did not die and proliferated through multiple passages. They appeared to be able to degrade misfolded procollagen, but the ability to deposit matrix and other functions appeared to be altered. The goals of the next step in our study reported in this chapter were therefore (a) To understand whether accumulation of misfolded procollagen causes ER/cell stress. (b) To identify ER/cell stress pathways involved in response to this accumulation and characterize how misfolded procollagen is degraded by the cell. (c) To identify whether and how the ER/cell stress response affects differentiation and function of osteoblasts.

Historically, OI was proposed to be a protein misfolding disease. Yet, the idea of resulting cell stress was not actively pursued for Gly substitutions, because early studies did not reveal involvement of BIP pathways considered to be a hallmark of UPR, which is commonly equated with ER stress response (60). Given multiple recent reports of ER disruption and cell malfunction caused by Gly substitutions (174,177,195,196), we hypothesized that G610C osteoblasts might utilize an alternative cell stress response pathway. One such pathway is ER overload, which can be induced by misfolding of some mutant forms of α1 antitrypsin protein and does not involve conventional UPR signaling, as described in Chapter 4.

We therefore tested whether characteristic features of ER overload are observed in G610C cells. One such feature, which deserves more detailed introduction before we proceed to describing our findings, is degradation of the misfolded proteins via macroautophagy.

Macroautophagy (hereafter referred to as autophagy) is a complex process of bulk degradation of proteins or organelles. A double membrane forms around the target, fuses with a lysosome to degrade its contents, and molecules are translocated out of the lysosome for reuse. Autophagy activation has best been described by nutrient deprivation. Accumulated amino acid reservoirs in the lysosome are depleted upon starvation, allowing for the mammalian target of rapamycin complex 1 (mTORC1) to dissociate from the lysosomal surface and become inactive (260). Another way mTORC1 is inactivated is through recognition of a high AMP: ATP ratio, indicating depleted energy reserves, via AMP-kinase phosphorylation of components of the mTORC1 complex. Inactivation of mTORC1 allows for activation of two kinase complexes, the UNC51 like Serine/Threonine Kinases (ULK) and the class III phosphatidylinositol-3-phsophate kinase complex (PI3K), which phosphorylate proteins required for autophagosome formation (261). Nucleation of the autophagosome is hypothesized to occur at the membrane junction between the ER and mitochondria, providing the newly forming autophagosome access to many necessary Atg (autophagy related) proteins, other cofactors, and associated proteins (261). The ER membrane also forms the autophagosome-cradling omegasome, which contributes to initiation of the autophagosome (261). The double membrane hallmark of an autophagosome elongates by different membrane contributions of the ER, Golgi, endosome, and plasma membrane, potentially requiring Atg9 (261,262). Other Atg proteins are required for autophagosome elongation. For instance, Atg4 is a protease that cleaves a

precursor of microtubule associated protein light chain 3 (LC3) to its cytosolic LC3I form. Then, Atg7 and Atg3 function as ubiquitin-like E1 and E2 ligases, respectively, to allow for the E3-acting ligase Atg5-Atg12-Atg16L complex to mediate conversion of LC3I into phosphatidylethanolamine conjugated LC3II (262). LC3II remains a part of the autophagosome through its fusion and degradation by the lysosome. The Atg5-Atg12-Atg16L complex is also formed through other Atg proteins, ubiquitin-like E1 ligase Atg7 and E2 ligase Atg10, and remains associated with the autophagosomal membrane throughout the elongation process only (262). After closure, fully formed autophagosomes travel along microtubule tracks and fuse with lysosomes, thus allowing their contents to by broken down by lysosomal enzymes that function at low pH.

In addition to nutrients, autophagy is induced or inhibited by a variety of cell stress pathways, many of which involve the ER. First, general expansion of the ER may trigger autophagy induction (263). Second, calcium signaling is intricately connected to autophagy through various mechanisms. Cytosolic calcium concentration increase due to calcium release from the ER causes autophagy activation by inhibition of mTORC1 (264). It can also activate NFκB signaling (179), which in turn can increase autophagy in multiple, context dependent ways (262). Interestingly, calcium phosphate precipitates transfected into cells were found to induce autophagy as well (265). Third, activation of different arms of the UPR mediates some protein degradation via autophagy. Phosphorylation of eIF2α, the downstream effector of PERK and other eIF2α kinases that are activated due to various cellular stresses can stimulate autophagy through mostly unknown mechanisms (262). ATF6 cleavage and subsequent activation can also induce autophagy through downstream inactivation of mTORC1 (261). Ire1, however, is a negative regulator of

autophagy, as when it's downstream effector XPB1 is absent, autophagy is increased (266).

RESULTS

There is ER Dilation in G610C/+ pOBs

To test how slower folding and intracellular retention of misfolded procollagen affected osteoblasts, we examined ultrastructure of pOBs in culture and *in vivo* by electron microscopy (EM). *In cellulo*, pOBs were incubated for 21 days to allow for deposition of extracellular matrix and embedding of some of the cells within the matrix, fixed with 2.5% glutaraldehyde and further processed for EM imaging as described in Chapter 10. *In vivo,* parietal bones were rapidly removed immediately after euthanizing 12 day old mice and fixed in either 2.5% glutaraldehyde or in a mixture containing 2% glutaraldehyde and 2% formaldehyde. Only the cells with well-preserved mitochondria were selected for more detailed ultrastructural examination.

In cultured G610C/+ cells, EM images revealed dramatically dilated and disorganized ER compared to well-organized, mostly undilated ER in their WT counterparts. Figure 12A shows the typical appearance of ER in a WT cell. In some WT cells, slightly dilated regions of ER cisternae were observed, yet many cells did not have any dilated ER regions at all. Figure 12B shows the appearance of severely disorganized and dilated ER in a G610C/+ cells. No WT cells had such grossly distorted ER. In contrast, many G610C/+ had a significant fraction or entire ER with similar appearance. Still, some G610C/+ cells had

better organized and less swollen ER that looked only slightly more dilated than in WT cells. ER occupied a large fraction of the intracellular space in all pOBs.

In fixed parietal bones from G610C/+ animals, all examined osteoblasts had a significant fraction of grossly distorted ER regions as shown in Figure 12E. In bones from WT animals, most cells with well-preserved mitochondria had normal ER appearance as shown in Figure 12D. However, other WT cells did have some regions of dilated ER. Both G610C/+ and WT osteoblasts had much higher ER density and larger number of ER cisternae compared to cultured pOBs, indicating that they produced much more procollagen. We also observed increased ER dilation in G610C/+ fibroblasts and perivascular cells, which were found in soft tissue adjacent to bone (data not shown).

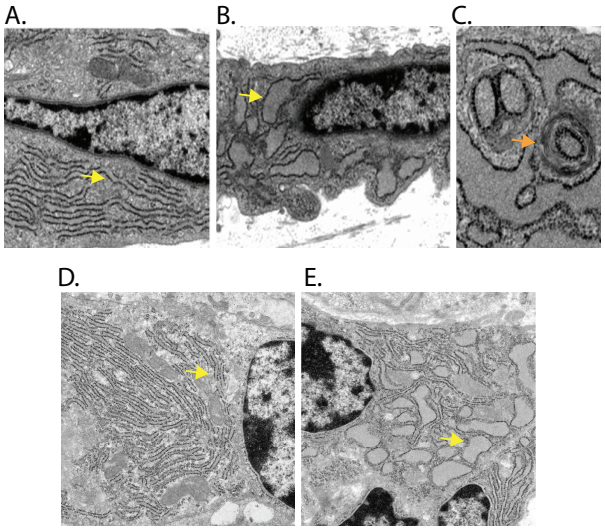

Figure 12. Electron microscopy of WT (A,D) and G610C (B,C,E) pOBs in culture (A-C) and in parietal bone from 12 day old animals (D,E).

Yellow arrows indicate ER. Orange arrow indicates autophagosome. Passage 1 pOBs were used.

In cultured cells, the ultrastructure of which was better resolved, we also identified well-defined and clearly distinguishable autophagosomes. Qualitatively,

we found more autophagosomes in G610C/+ cells, in which we also found autophagosomes encapsulating large ER fragments (Fig. 12C).

Cell Stress Response

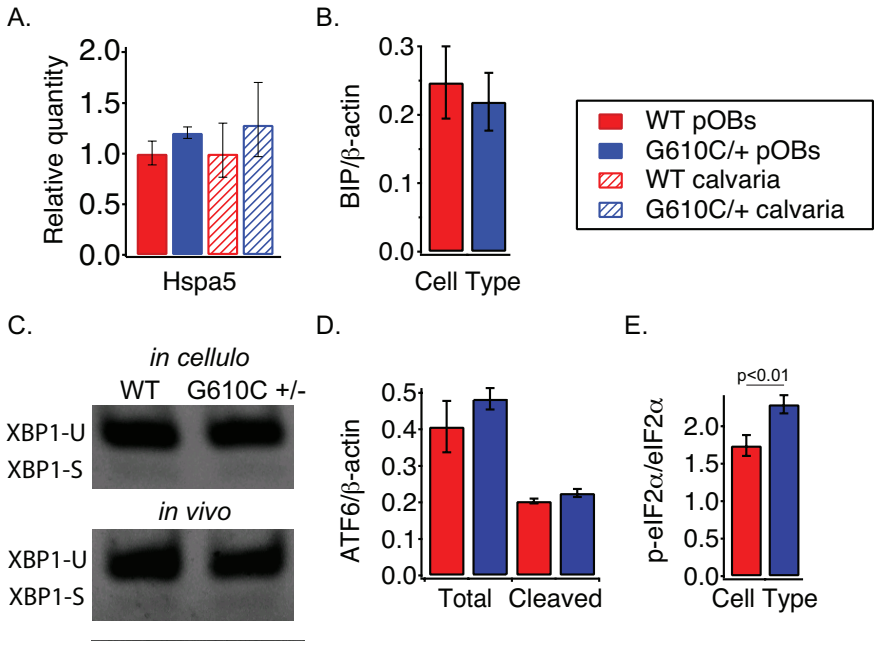

Figure 13. Analysis of Conventional Unfolded Protein Response in WT and G610C/+ pOBs and bone.

(A). Hspa5 (BIP) mRNA transcript levels in cultured pOBs and mouse calvaria from 17 day animals. Transcript levels were normalized to HPRT1/B2M controls and relative to WT. (B). Levels of BIP protein detected by western blot in untreated pOBs. (C). Representative gel electrophoresis image of qPCR of spliced (XBP1-S) and unspliced (XBP1-U) XBP1 mRNA in cultured untreated pOBs (*in cellulo*) and calvaria (*in vivo*). (D). ATF6 levels in untreated pOBs detected by western blot. (E). Ratio of phosphorylated eIF2α to total eIF2α, each first normalized to β-actin, in untreated pOBs. All error bars represent standard deviation of at least three experiments and statistical significance was calculated by a student's two tailed t-test.

Despite significant ER disruption indicative of some form of ER stress experienced by the cells, we found no evidence of conventional UPR by analysis of key UPR markers either in cultured pOBs or in parietal bone *in vivo*. (a) We did

not observe an increase in BIP, which would be expected to be upregulated in UPR (267,268), either at the transcript or protein level (Fig. 13A,B). (b) We did not observe activation of IRE1 or ATF6 arms of UPR signaling, at least one of which is usually activated in UPR (178). Specifically, we found no upregulation of XBP1 mRNA splicing in G610C/+ compared to WT cells, which would be caused by IRE1 activation (Fig. 13C). We also found no upregulation of ATF6 cleavage, which would be caused by ATF6 activation. (Fig. 13D). (c) We did observe an increased ratio of phosphorylated eIF2α to total eIF2α in G610C/+ compared to WT pOBs suggesting activation of PERK (Fig. 13E). However, while PERK is an arm of conventional UPR, increased eIF2α phosphorylation has also been reported in ER overload without UPR.

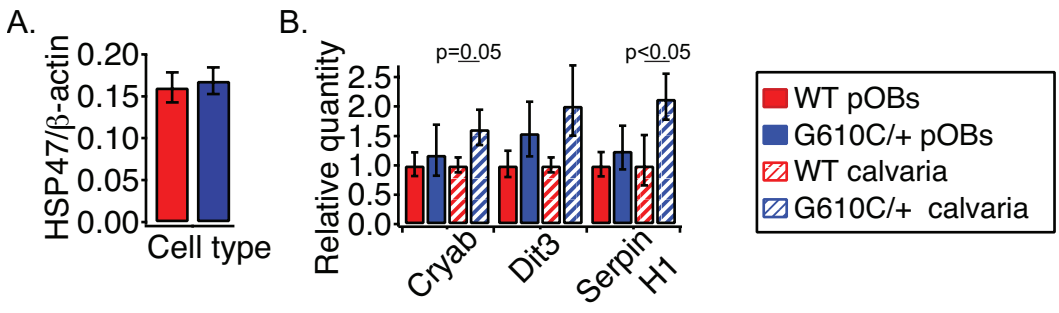

Figure 14. Expression of Serpin H1 (HSP47), Cryab (αB crystalline) and Ddit3 (CHOP) in cultured pOBs and parietal bone

(A). Relative HSP47 protein levels detected by western blot (B). Relative mRNA transcript levels normalized to HPRT1 and B2M and calculated relative to WT.

At the same time, we observed a statistically significant increase in the transcription of SerpinH1 (HSP47) and Cryab (αB crystalline) in parietal bones from G610C/+ vs. WT mice (Fig. 14B). In cultured pOBs, a similar trend did not reach statistical significance. The level of HSP47 protein measured by western blotting was similar in G610C/+ and WT pOBs (Fig. 14A). Ddit3 (CHOP) mRNA

transcription trended higher in G610C pOBs and parietal bones, but the difference with WT was not statistically significant (Fig. 14B).

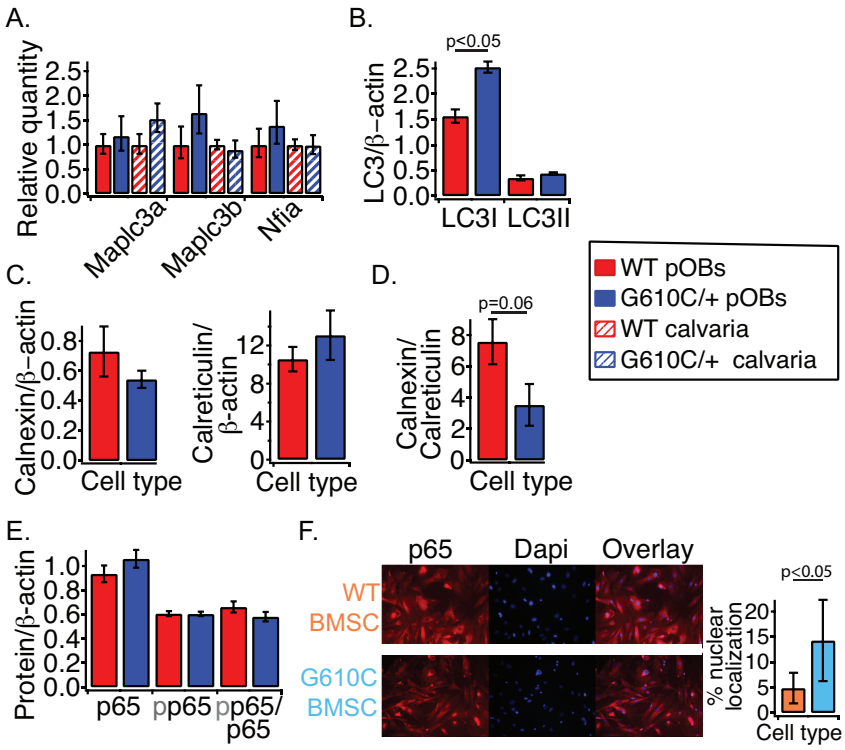

Figure 15. ER-overload response features in G610C/+ cells.

(A,B). LC3I expression measured by qPCR (A) and LC3I and LC3II expression measured by western blotting (B); mRNA transcripts were normalized to HPRT1 and B2M calculated relative to WT. (B). (C,D). Relative calnexin (left) and calreticulin (right) protein levels detected by western blotting in pOBs. Calnexin and calreticulin were detected on the same gel lane and normalized to β-actin with a scaling factor of 100. (E). Relative p65 and phosphorylated p65 (pp65) protein levels measured by western blotting and the pp65/65 ratio in pOBs. (F). Immunofluorescence analysis of nuclear localization of p65 in BMSCs (bone marrow stromal cells) from 4 month old animals. The fractions of cells positive for nuclear p65 are displayed in the graph on the right. All experiments were performed at least in triplicate. Error bars represent standard deviation. The p-values were calculated from a two tailed student's t-test.

Since ER disruption and enhanced autophagy without conventional UPR was previously reported in ER overload response (183), we also examined other

markers of ER overload. We observed more LC3I protein in G610C/+ pOBs while mRNA transcript levels of two LC3 genes were not significantly affected (Fig. 15A,B). We also observed a modest trend for calnexin increase and calreticulin increase with a 2-fold lower calnexin/calreticulin ratio in G610C/+ pOBs (Fig. 15C,D). This trend was consistent between different experiments but did not reach full statistical significance. Finally, we got conflicting results on NFκB activation. In pOBs, we found no changes in the level of either p65 or active, phosphorylated p65 by western blotting (Fig. 15E). In BMSCs from G610C/+ animals, however, we saw an increase in the nuclear localization of p65, indicating activation of NFκB signaling (Fig. 15F).

Degradation of Misfolded Procollagen

To further understand the response of G610C/+ cells to misfolded procollagen accumulation, we examined degradation of the retained molecules. Increased procollagen retention yet similar fraction of Aha-labeled molecules in the cell after 2 hour chase (see Chapter 6) indicated upregulated intracellular procollagen degradation in G610C/+ pOBs.

To clarify the role of the autophagy/lysosome degradation pathway, we first treated the cells with bafilomycin a1 and chloroquine, chemical inhibitors that inhibit parts of this pathway. We observed procollagen accumulation in all cells, but the extent of the accumulation was more significant G610C/+ pOBs (Fig. 16A). Consistently, autophagy enhancement by rapamycin or mild nutrient deprivation in serum-free cell culture media reduced intracellular procollagen in G610C cells approximately two fold to the level found in WT cells. However, we observed virtually no change in WT cells (Fig. 16A).

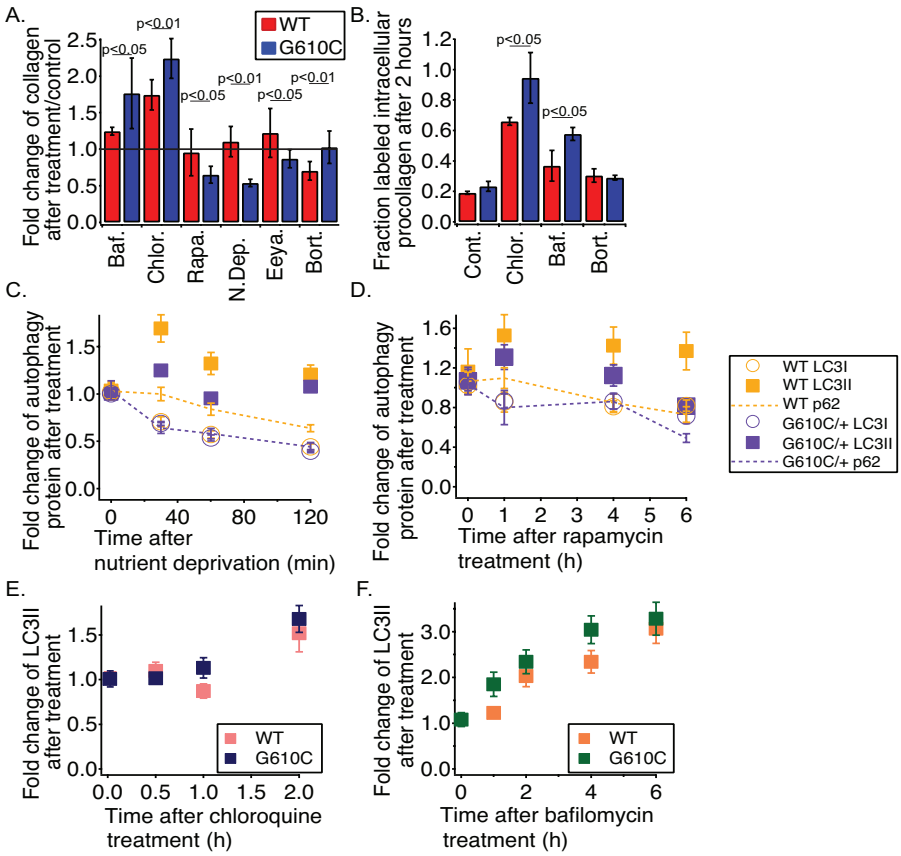

Figure 16. Analysis of procollagen autophagy in pOB culture.

(A.) Effects of treating pOBs with bafilomycin A1 (Baf., 6 h), bortezomib (Bort., 6 h), chloroquine (Chlor., 2 h), nutrient deprivation (N. Dep., 2 h), eeyarestatin (Eeya., 2 h), and rapamycin (Rapa., 4 h) on procollagen accumulation in the cell; measured by western blotting with β-actin as an internal standard. The bars show fold change relative to untreated pOBs. (B) Effects of chloroquine, bafilomycin and bortezomib on the fraction of Aha-labeled procollagen remaining in the cell after a 2 h chase in 10 mM Met medium (preceded by 2 h labeling in 500 μM Aha medium). Passage 1 pOBs were used. (C and D). LC3I, LC3II, and p62 level time course relative to untreated cells in pOBs after nutrient deprivation (C) or rapamycin (D); measured by western blotting with β-actin as an internal standard. (E and F). LC3II level time course relative to untreated cells after chloroquine (E) and bafilomycin (F) treatments. All experiments were repeated at least in triplicate. The error bars represent standard deviation in (A,B) and standard error in (C-F). The p-values calculated from a two tailed Student's t-test show statistically significant differences between G610C/+ and WT pOBs .

Eeyarestatin, which inhibits ERAD by blocking export of proteins from the ER for degradation by proteasomes, had almost no effect on procollagen in

G610C/+ cells and no statistically significant effect in WT cells (Fig. 16A). Bortezomib, which is a proteasome inhibitor, reduced procollagen in WT cells without any effect of G610C cells (Fig. 16A). In contrast to autophagy, ERAD/proteasomes did not appear to be involved in misfolded procollagen degradation.

Changes in procollagen synthesis, degradation and secretion from the cell could contribute to the observations described above. Thus, we also measured the fraction of Aha-labeled procollagen remaining in the cell after a 2 h incubation in 10 mM Met chase media. We found a significant increase in the fraction of procollagen retained in G610C/+ compared with WT pOBs upon treatment with bafilomycin or chloroquine, but not bortezomib (Fig. 16B). Relative to untreated controls, chloroquine and to a smaller degree bafilomycin increased procollagen retention after the 2h chase, even in WT pOBs. Bortezomib did not have a statistically significant effect on procollagen retention relative to untreated cells either in WT or G610C/+ pOBs. Interestingly eeyarestatin increased the amount of Aha-labeled procollagen remaining in the cells after 2h chase (data not shown), even though it did not cause procollagen accumulation upon shorter treatment (4h vs 2h) (Fig. 16A). However, this effect was similar in WT and G610C cells.

To more specifically test the role of macroautophagy vs. a broader range of lysosomal degradation pathways, we measured the autophagy flux. We found that rapamycin treatment (Fig. 16C) and nutrient deprivation (Fig. 16D) had more pronounced effects on LC3II accumulation in WT cells, even though LC3I conversion was the same between WT and G610/+ cells. This indicates increased basal autophagic flux in G610/+ cells, which was further corroborated by faster p62 degradation in G610C/+ cells. Faster accumulation LC3II upon

inhibition of lysosomal degradation with chloroquine (Fig. 16E) and bafilomycin (Fig. 16F) was consistent with higher autophagy flux in G610C/+ cells as well.

Osteoblast Differentiation and Function

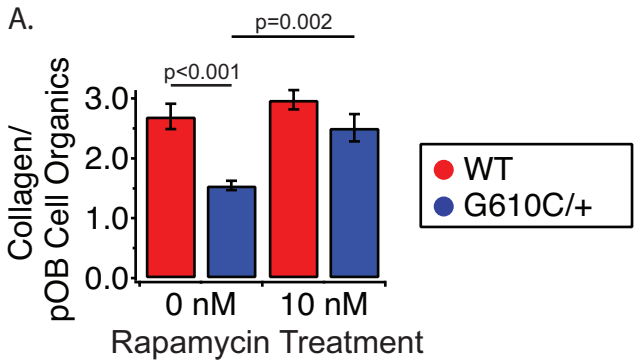

Figure 17. Collagen matrix deposition by cultured pOBs treated with rapamycin. Raman spectroscopy measurements of collagen/cell organic material in matrix grown for 3 weeks by pOBs with and without rapamycin were performed and analyzed as described in Figure 11.

To investigate how misfolded procollagen accumulation affected osteoblast differentiation and function, we first examined its effects on matrix deposition and mineralization by cultured pOBs. As described in Chapter 6, G610C/+ osteoblasts deposited less collagen in extracellular matrix compared to WT osteoblasts, which could be related to malfunction of mutant collagen secreted by the cells, malfunction of the cells themselves or both. Since rapamycin reduced misfolded procollagen accumulation and would not be expected to affect secreted collagen outside the cell, we tested its effects on collagen deposition in the matrix. 10 nM rapamycin did not affect matrix deposition by WT pOBs, yet it normalized collagen deposition by G610C pOBs,

increasing it almost two fold (Fig. 17), Apparently, cellular malfunction did play a major role in deficient matrix deposition by G610C pOBs.

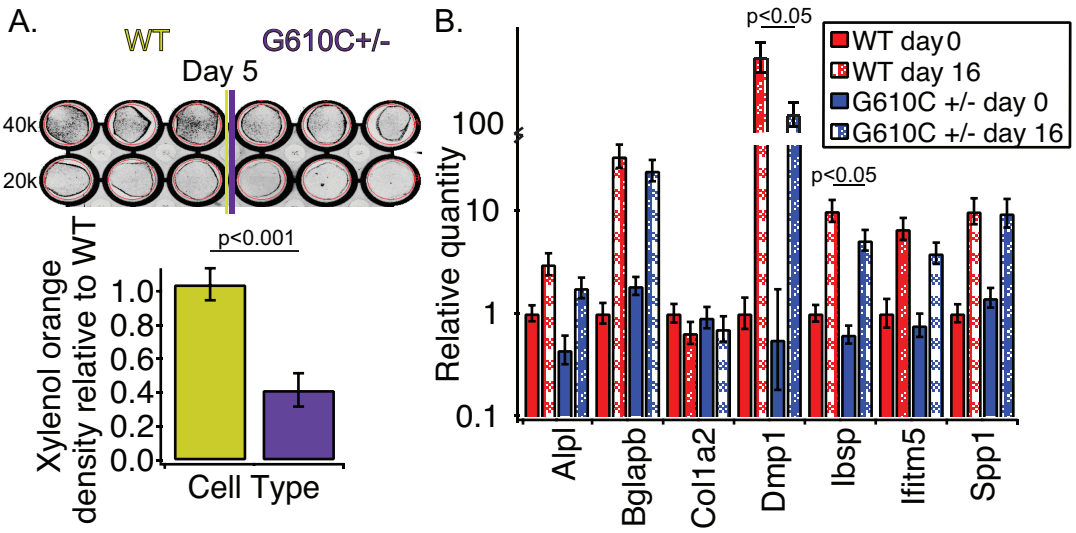

Figure 18. Mineralization of p1 pOBs.

(A) Measurement of average matrix mineralization with xylenol orange. Osteoblasts that were plated at 40,000 cells/well in the top row and at 20,000 cells/well in the bottom row and stimulated with β-glycerophosphate to produce mineralized matrix as described in Chapter 10. Xylenol orange staining was performed at day 5 and day 13. A representative 24 well plate with xylenol orange staining after 5 days of culture is shown. The circles show the area within which xylenol orange intensity was quantified, compared relative to WT and displayed below. (B). Quantity of mRNA transcripts relative to WT cells at day 0 in WT and G610C/+ pOBs before (day 0) and after (day 16) stimulation of matrix mineralization. The qPCR data were normalized to Runx2 and Sp7 mRNA as internal controls for osteoblastic cells. Analysis based on normalizing the data to HPRT1 and B2M produced similar results. Experiments were repeated in triplicate, error bars represent standard error (A) and deviation (B), and statistically analyzed as described in previous figures.

We also found that deficient matrix deposition by cultured G610C/+ pOBs was accompanied by deficient matrix mineralization (Fig. 18). G610C/+ pOBs grown in mineralization media had less xylenol orange staining, which reveals mineral, compared with WT pOBs (Fig. 18A.) This trend was reproduced at each

time point in every experiment (4 cell densities, each in triplicate). Day 5 xylenol orange intensity was quantitated relative to WT at each cell density, and G610/+ mineralization was ~1/2 of what was observed in WT (Fig. 18A, bottom panel). Comparison of mRNA collected after 16 day incubation in mineralizing media revealed reduced Dmp1 and Ibsp transcription in G610C/+ pOBs, consistent with altered osteogenic capacity when stimulated to produce mineralized matrix (Fig. 18B).

Stimulation of cultured pOBs with exogenous TGFβ1 and Wnt3a revealed additional evidence of osteoblast malfunction, G610C/+ pOBs exhibited a blunted response to exogenous TGFβ1 compared with WT cells, as evidenced by almost no increase in intracellular procollagen and reduced Smad2 phosphorylation (Fig. 19A,B). In G610C/+ pOBs, we also observed a reduced response to exogenous Wnt3a via decreased Axin2 transcription relative to WT, a transcriptional target of Wnt signaling (Fig. 19C).

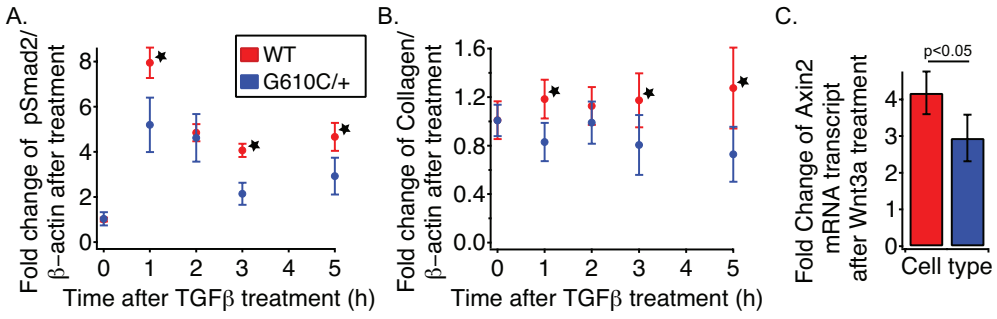

Figure 19. Response to TGFβ1 and Wnt3a.

(A and B). pOBs were treated with 10ng/mL TGFβ1 for up to 5 hours. Phosphorylation of Smad2 (A) and intracellular procollagen content (B) were measured by western blotting with β-actin as an internal standard . Fold change was determined relative to untreated controls. The stars represent statistically significant differences between WT and G610C/+. (C). pOBs were treated with 100 ng/mL Wnt3a for 4 hours and mRNA transcripts were normalized to HPRT1 and B2M as internal controls. The fold change of Axin2 was calculated relative to untreated cells. All experiments were repeated at least in triplicate, error bars represent standard deviation, and statistically analyzed as in previous figures.

Finally, analysis of BMSCs collected from femurs of 4 months old mice revealed severely affected differentiation of G610C cells, which produced approximately 3 times fewer colonies capable of mineralization (Fig. 20), Comparison with less dramatic effects on total and alkaline phosphatase positive colonies indicated disruption of osteogenic differentiation. Interestingly, enhancement of autophagy in animals placed on a low protein diet for 8 weeks (LPD) significantly improved differentiation of G610C/+ BMSCs, even though all cells were cultured in the same medium with full serum.

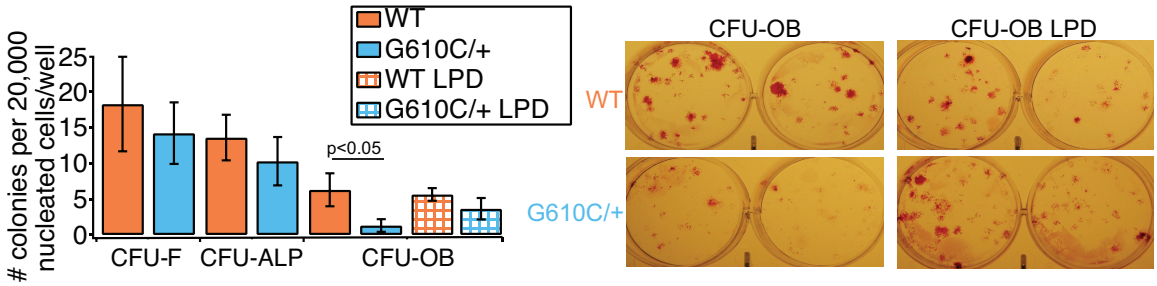

Figure 20. Differentiation of BMSCs from 4 month old animals, half of which were placed on a low protein diet (LPD) for 8 weeks before they were sacrificed.

The number of colony forming units (CFU) was quantified by staining with Crystal Violet (CFU-F), alkaline phosphatase (CFU-ALP) or alizarin red mineralizing colonies, (CFU-OB) as described in Chapter 10. To measure CFU-OB, the cells were grown for two extra weeks in cell culture medium containing β-glycerophosphate and dexamethasone. Representative samples of BMSC colonies stained with alizarin red are shown on the right. The measurements were repeated in biological and technical triplicate and statistically analyzed as described in Chapter 10. Error bars represent standard deviation and statistical significance was calculated by a student's two-tailed t-test.

Auxiliary Observations

In an attempt to more carefully tease out relative contributions of ERAD and autophagy to degradation of misfolded procollagen, we tried experiments

with multiple alternative treatments. Such treatments are known to affect cells in multiple ways beyond their intended targets (260,269,270). Thus, it was not surprising that some of our attempts produced results indicative of significant off-target effects and artifacts, which we did not pursue. Since we could not properly interpret the results of these experiments, we did not discuss them above. However, we believe that it is important to list them and provide brief descriptions of the problems we encountered.

Proteasome inhibition with lactacystin and MG132. These commonly used inhibitors dramatically reduced procollagen transcription by pOBs, similar to transcriptional effects described in (271).

Autophagy inhibition with 3MA. We observed no increase in intracellular p62, which should accompany autophagy inhibition, when we tried 3MA treatment of our pOB and MEF cultures. The action of 3MA in cells that secrete massive amounts of procollagen might be different from other types of cells. Interestingly, 3MA might induce rather than inhibit autophagy in the presence of serum (269). Because serum-free media prevented accumulation of procollagen in G610C, we chose not to use the combination of serum-free media with 3MA.

Inhibition of lysosomal degradation with leupeptin and NH_4Cl. Instead of increasing p62, which is primarily degraded in lysosomes via autophagy, this treatment reduced p62 in our pOB and MEF cultures, suggesting possible complex off-target effects.

Activation of autophagy by complete amino acid starvation. We observed significant pOB detachment from plastic and death after 1h in balanced salt solutions without serum and amino acids, suggesting that such treatment was inappropriate for osteoblasts.

Inhibition of lysosomal degradation with bafilomycin and chloroquine in MEF cultures. Similar to pOBs, we observed an increase in LC3II and p62

consistent with inhibition of lysosomal degradation. Yet, unlike pOB cultures, we did not see an increase in intracellular procollagen in either WT or G610C cells. This observation might point to important differences in procollagen processing by pOBs and MEFs and would be interesting to investigate in future studies.

DISCUSSION

Our experiments described in this chapter show that (a) Procollagen misfolding in the ER of G610C osteoblasts causes ER dilation and disruption, triggering some form of cell stress response. (b) This cell stress response does not conform to conventional UPR and has some, but not all features characteristic of ER overload described in serpinopathies. (c) Osteoblasts adapt by upregulating autophagy and degradation of misfolded procollagen in lysosomes, preventing more severe cell stress and death. (d) Nevertheless, procollagen misfolding disrupts normal differentiation and function of osteoblasts. (e) Enhancement of autophagy may reduce detrimental effects of procollagen misfolding on osteoblast homeostasis.

Cell Stress Response

Similar to the Brtl mouse (177), procollagen misfolding in the G610C model causes ER dilation and disruption without sequestering BIP (Fig. 13A,B), suggesting that canonical UPR is not involved in signaling this disruption to the rest of the cell. Based on previous observations for human fibroblasts (60), this appears to be a general feature of Gly substitutions in the triple helix. The three arms of the canonical UPR are IRE1, ATF6, and PERK. Their activation is most

commonly mediated by BIP. Their signaling is repressed by bound BIP and activated by the release of BIP when BIP is sequestered by misfolded proteins (272,273). IRE1 activation causes splicing of XBP1 mRNA, leading to translation of an active transcription factor that increases transcription of a variety of genes including chaperones (178). ATF6 activation causes translocation of ATF6 to the Golgi, where it is cleaved to yield an active ATF6 transcription factor that also changes expression of a variety of genes including chaperones (178). PERK activation causes phosphorylation of eIF2α, which blocks translation of most proteins except ATF4, which itself acts as a transcription factor (178).

However, as IRE1, ATF6 and PERK signaling pathways of UPR can be activated through other mechanisms than BIP dissociation, it is possible that they may still be involved (178). For instance, each of the UPR arms may be triggered individually depending on the stressor, such as reduced glycosylation efficiency in the ER, or changes in calcium concentration (178). Many ER resident proteins require calcium to function, and altered calcium concentration affects multiple aspects of ER homeostasis (274). ER/cytosolic calcium signaling mechanisms are vast and beyond the scope of this discussion to discuss, but calcium signaling defects are a known cause of OI and lead to misfolded procollagen (151,152). Another potentially relevant consideration is that that IRE1 activation may be turned off in chronic ER stress but PERK activation continues (178). Our more detailed analysis revealed no activation of IRE1 and ATF6 signaling in G610C, either *in cellulo* or *in vivo* (Fig. 13). Yet, we observed increased phosphorylation of eIF2α (Fig. 13E), which could be caused by activation of PERK. Interestingly, a downstream effector of PERK activation was increased in the Brtl mouse as well (195). Thus, it is tempting to speculate that PERK activation causes the increased phosphorylation of eIF2α in G610C cells. However, there are four different kinases that can phosphorylate eIF2α

(262,275). In particular, disruption of ER homeostasis might lead to eIF2α phosphorylation by GCN2 (general control nonderepressible-2) and by PKR (RNA-activated) kinases (276,277). Therefore, further characterization is needed to determine which kinase is responsible for this change, and how it contributes to the overall stress response.

Degradation of misfolded procollagen via autophagy (Fig. 16), a trend toward lower calnexin content in the ER (Fig. 15C,D), and apparent activation of NFκB signaling in BMSCs (Fig. 15F) from G610C mice point to at least some similarities with the ER overload response. The ER overload response was first described as an alternative to conventional UPR nearly twenty years ago, but it is still poorly understood (180). This may in part be due to cell and context-dependent factors that complicate a general mechanism. For instance, the effects and extent of NFκB activation may be mediated by numerous competing signals such as stress, normal development, and inflammation (278).

Given all these complexities, we are reluctant to classify the stress response to procollagen misfolding in the G610C model as a peculiar form of UPR or ER overload. An attempt of such classification is further complicated by the evolving understanding of various possible stress response pathways in UPR and ER overload as well as by different meaning attributed to these terms by different researchers. We hope that future, more in-depth studies of the stress pathways we identified and the pathways we could have missed will provide better clarity. In the meantime, it is clear that the G610C substitution does disrupt ER homeostasis and activates some cell response. For the lack of a better term, we simply refer to it as a cell stress response.

We believe that the trend toward reduced calnexin and increased calreticulin content in the ER of G610C/+ osteoblasts (Fig. 15C,D) opens a particularly interesting venue for future studies. An attractive hypothesis is that

calnexin travels with misfolded protein to the autophagosome, which is observed in the serpinopathies (183). Calnexin may even be involved in targeting misfolded procollagen bound to it in the ER lumen for degradation via autophagy. Together, calnexin and calreticulin are necessary for recognizing N-glycosylation of the C-propeptide of procollagen, and likely to be involved in targeting procollagen for export out of the ER for normal trafficking or degradation (54,56). They also share a dependency on calcium signaling, and their altered expression may indicate altered calcium in the ER and calcium signaling in the cell. All these questions are currently being pursued in our laboratory.

Importantly, we consistently observed greater ER disruption in osteoblasts *in vivo* compared to cell culture, which could be explained by more active procollagen biosynthesis by osteoblasts in their natural environment. Our experiments also provided evidence of stronger cell stress response to procollagen *in vivo*. In particular, we observed greater changes in HSP47 mRNA transcription. As increase in HSP47 and αB crystalline mRNA expression has been observed in OI and it may be involved in cell stress response to excessive procollagen triple helix misfolding (195,279). Ddit3 (CHOP) transcript levels were also more increased *in vivo* than in cell culture, indicating stronger downstream consequences of cell stress. Increased osteoblast turnover rate combined with relatively few mature osteoblasts is a common finding in OI (46), which could be related to osteoblast apoptosis or disrupted maturation through CHOP signaling.

Osteoblast Malfunction

While understanding the exact mechanisms and pathways of cell stress response to procollagen misfolding will require additional studies, it is clear that this response affects differentiation and function of G610C/+ osteoblasts. In

particular, deficient osteoblastic differentiation of G610C/+ BMSCs (Fig. 20) might be related to higher procollagen synthesis in more mature cells. Cell stress caused by increased accumulation of misfolded procollagen with osteoblast maturation might trigger a change in the fate or phenotype that requires lower procollagen synthesis rate. The outcome may depend on multiple factors and differ for different mutations. For instance, an observed shift from osteogenic toward adipogenic differentiation of BMSCs from Brtl mice could be a manifestation of this effect (196).

One potential mediator of such an effect in the G610C model might be activation of NFκB signaling, which we observed in BMSC cultures (Fig. 15F). In general, NFκB activation is detrimental for osteoblast differentiation and function, although this is not always the case depending on factors and mechanisms that are not well understood (280-289). Canonical NFκB activation is contingent on proteasomal degradation of its inhibitors (278). Proteasomal inhibitor bortezomib improved osteoblastic differentiation of BMSCs in Brtl mice and in human bone marrow osteoprogenitor cells (196,290). It would be interesting to find out whether this effect was caused by reduced NFκB activation or by another mechanism, e.g. an increase in autophagy that might accompany proteasome inhibition (291).

Not only does accumulation of misfolded procollagen inhibit osteoblast differentiation, but once differentiated, the osteoblast is also malfunctioning as evidenced by reduced collagen deposition in matrix (Fig. 17), deficient matrix mineralization (Fig. 18) and abnormal response to key cytokines (Fig. 19). This potentially leads to changes in proliferation and disruption of normal intra- and intercellular signaling. For instance, TGFβ signaling is required for normal osteoblast function including inter- and intracellular signaling and proliferation (113). Dysfunctional TGFβ signaling in G610C osteoblasts may therefore

contribute to bone pathology in this model. Interestingly, in a gene expression study of human patients with an aggregation-prone mutant α1 antitrypsin that causes ER dilation, dysfunctional TGFβ target gene expression has been observed as well (292).

Multiple cell stress pathways may contribute to abnormal osteoblast function. For example, an increase in calreticulin concentration in the ER might contribute to pathology since overexpression of calreticulin inhibits mineralization and reduces canonical Wnt signaling (293-295). The decreased matrix mineralization and ability of cultured G610C pOBs to respond to Wnt3a could be in part related to calreticulin upregulation. It would be useful to determine whether this is indeed the case.

Procollagen Autophagy

Our observations suggest that procollagen (macro)autophagy may be a particularly important pathway both for understanding and targeting osteoblast cell stress and malfunction. We discerned that misfolded procollagen in G610C/+ pOBs was primarily degraded by lysosomes via autophagy. Similar findings were reported for HSP47 null cells and Mov13 cells expressing procollagen α1(I) chains with a Gly substitution (174). Potential importance of autophagy can also be deduced from observations in the Brtl mouse model (196). Suppression of autophagy in bone leads to reduced mineralization, proliferation, and bone growth (296,297). The implications of altered autophagic flux may thus be important, as autophagy appears to be essential for osteoblast function. For instance, a normal function of TGFβ in osteoblasts is to increase both collagen expression and autophagy activation; without appropriate autophagy mediation by TGFβ stimulation, even normal procollagen accumulates and aggregates in

the cell (120). An increase in autophagy is also observed during normal osteoblast differentiation into a mature osteoblast, further indicating its importance in normal collagen synthesis (296,297). When collagen synthesis is disrupted by the G610C substitution, the autophagy requirements might supersede what the cell is able to accommodate. The resulting cell stress response crosses with normal cell signaling (like TGFβ), and causes osteoblast malfunction, including the deficient matrix deposition and mineralization we observed.

One of the most exciting results of this study is that the cell stress caused by accumulation of misfolded procollagen and resulting osteoblast malfunction might be reduced by enhancing autophagy. In cell culture, autophagy enhancement was enough to reduce accumulated procollagen in G610C/+ pOBs to WT levels within two hours (Fig. 16). Similarly, autophagy enhancement has been shown to reduce accumulation of other proteins in the ER, including mutant dysferlin and α1-antitrypsin, providing cytoprotective effects (183,185,298). In another collagen disorder caused by deficient type VI collagen synthesis, enhancement of autophagy reduced pathogenic effects of the mutation (299). We plan to pursue whether enhancement of autophagy mediates cell stress mechanisms in G610C pOBs, including its influence on phosphorylation of eIF2α, NFκB activation, and ER protein expression.

To our knowledge, no one has attempted enhancing autophagy as a potential treatment for OI. In our lab, we tested an eight week treatment of G610C mice by low protein diet supplemented with methionine and aromatic amino acids to enhance autophagy. BMSCs isolated from these mice indicated that this treatment improved osteoblast differentiation and its effects were long lasting (observed in cells grown in full nutrient conditions for 4 weeks before analysis). Preliminary analysis of the animals revealed that the bone synthesized

in the G610C mice during the low protein diet was more properly mineralized in a control group of mice on a normal diet (data not shown). An extended low protein diet is not a viable treatment of OI, particularly in children, since nutrient deprivation suppresses growth and overall bone deposition, overriding the benefits of improvements in the bone material properties, However, these results indicate that autophagy might be an important target for improving osteoblast function in OI and potentially other bone disorders.

Chapter 8: Preliminary *in vivo* Characterization of WT, G610C/+, and G610C/G610C Animals

BACKGROUND

Beyond comparing pOB function in cell culture and *in vivo*, we conducted several additional *in vivo* experiments that were essential for interpreting our observations described in Chapters 6 and 7. For these experiments, we utilized primarily E18.5 embryos and newborn pups produced from breeding heterozygous G610C males with heterozygous G610C females. Despite more severe procollagen biosynthesis defects in homozygous vs. heterozygous MEFs we observed similar collagen matrix deposition, as described in Chapter 6, These observation indicated that comparison of homozygous with heterozygous osteoblasts and bone might provide additional insights into the relative role of collagen matrix vs. osteoblast pathology. We could not test pOBs from homozygous animals, all of which die during or shortly after birth (169). Instead, we focused on examining composition and mineralization of extracellular matrix and signatures of osteoblast malfunction *in vivo*.

RESULTS

Embryo and Neonate Viability

At gestational day E18.5 in heterozygous/heterozygous G610C breeding pairs, we observed close to the expected 1:2:1 ratio of wild type : heterozygous :

homozygous embryos, all of which had similar size and appeared to be viable. However, consistent with previous observations only dead homozygous pups were recovered from the breeding cages within hours of delivery. In some litters, we recovered dead heterozygous and wild type pups, and we did not observe increased death rate among the latter. Close to 1:1 ratio of surviving pups from breeding of heterozygous G610C males with WT females was also consistent with minimal or no lethal outcomes of heterozygous G610C, in contrast to about 30% lethality in heterozygous Brtl mice (218). So far, we have not identified the exact time and cause of death of the homozygous pups. The corresponding study is currently in progress.

Extracellular Matrix Composition

A previous study of collagen composition in tail tendon of heterozygous G610C mice revealed approximately 50% of molecules with the mutant chain (169). This observation was consistent with the composition of collagen secreted by cultured pOBs measured in the present study but not with the composition of collagen deposited by pOBs into matrix (Fig. 10). The tail tendon composition suggested that the mutant molecules were capable of normal incorporation into the matrix at the physiological temperature in tail tendon, which is lower than the core body temperature. Matrix composition in the pOB culture could then be explained either by (a) stronger effect of non-physiological matrix deposition in culture on the incorporation of mutant molecules or by (b) denaturation of a significant fraction of mutant molecules at 37 ^{o}C, before they had a chance to be incorporated (because of their much lower thermal stability).

To distinguish between these interpretation, we measured the fraction of mutant molecules in skin of G610C/+ animals collected at E18.5, since the entire

embryo develops at core body temperature. In three G610C/+ embryos from the same liter, we observed 29.6 +/- 2.5% of mutant molecules, in perfect agreement with each other and with the matrix composition in pOB culture (Fig. 21).

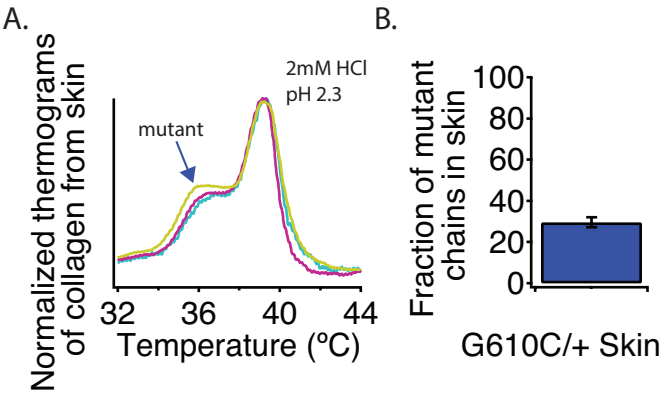

Figure 21. DSC of skin from G610C/+ E18 fetuses.

(A). Measurement of the collagen composition by DSC (c.f. Fig. 10). Normalized thermograms from individual embryos (n=3) are distinguished by color. (B). The fraction of mutant molecules (α2(I) chains) calculated from the DSC thermograms as described in Fig. 10; the error bar represents standard deviation.

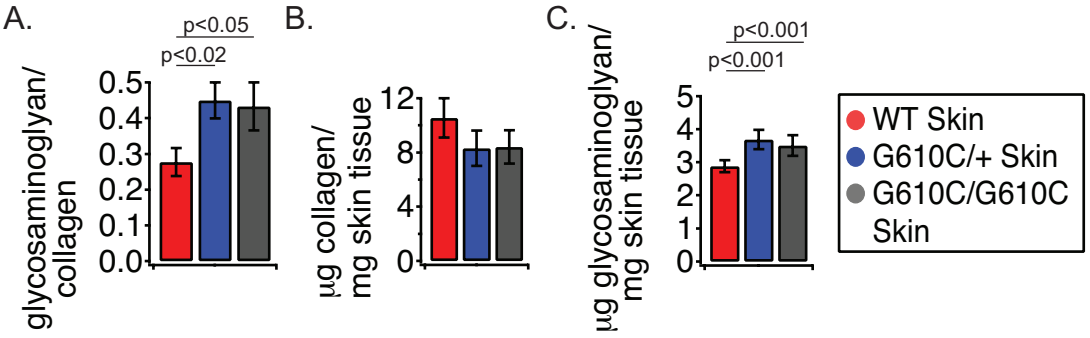

Figure 22. Glycosaminoglycan and collagen content in skin from E18.5 embryos.

Collagen and proteoglycans were extracted from skin of WT (n=2), G610C/+ (n=3) and G610C/G610C (n=2) embryos according to Sircol collagen assay and Blyscan glycosaminoglycan assay instructions. The resulting collagen and proteoglycan concentrations were normalized to the total sample weight.

We next examined collagen and proteoglycan content of skin from E18.5 embryos of all three genotypes (Fig. 22). We observed lower collagen content

and greater ratio of proteoglycans to collagen in G610C/+ and G610C/G610C relative to WT, but no significant difference between heterozygous and homozygous animals. The decrease in collagen content and the similarity between heterozygous and homozygous matrix was consistent with our findings in matrix produced by MEFs in cell culture (Fig. 11B).

Neonatal Bone

Skeletal staining (Fig. 23) and X-ray radiography (Fig. 24) of newborn animals from multiple litters revealed significant variability of bone pathology in animals with the same genotype even within the same litter. We observed severely delayed (virtually nonexistent) mineralization of caudal vertebrae and parietal bones in the skull of G610C/G610C animals (Figs. 23A,D and Fig. 24A, top). To a lesser extent than in the parietal bones, delayed mineralization was also detected in frontal and occipital bones of calvaria. Furthermore, sutures between different calvaria bones were poorly formed, resulting in displacement of parietal bones upon brain swelling in 2% KOH used for skeleton clearing after staining. We observed similar defects in more severely affected G610C/+ animals (Fig. 23F and Fig. 24B, top), but most G610C/+ animals were less affected (Figs. 23K, and Fig. 24C, top) relative to WT (Fig. 23P, and Fig. 24D, top).

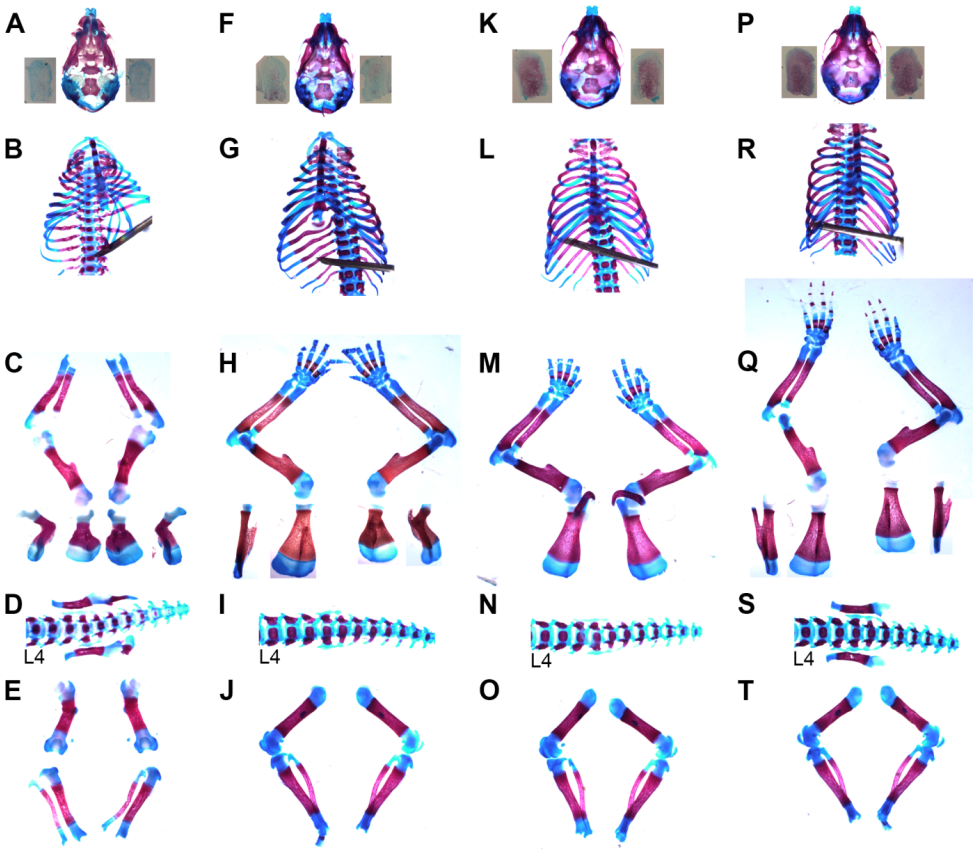

Figure 23. Skeletal staining of homozygous G610C/G610C (A-E), severely affected heterozygous G610C/+ (F-J), moderately affected heterozygous G610C/+ (K-O) and wild type +/+ newborn pups.

A,F,K,P. Skull and parietal bone staining; enlarged images of the corresponding parietal bones separated from the skull are shown on each side of the skull. B,G,L,R. Rib cage staining. C,H,M,Q. Forelimb staining. Each scapula is shown in two projections, to illustrate severe deformities observed in homozygous (C.) and severely affected heterozygous (H.) mice. D,I,N,S. Staining of lower lumbar, sacral and caudal vertebrae; L4 vertebrae is marked on each image. E,J,O,T. Staining of femurs, tibia and fibula. Femurs from the homozygous pups were photographed in a different orientation (~90° rotation) relative to other animals due to their sharp bending.

Comparison of rib cages revealed severe narrowing of the upper part, resulting in a triangular shape of the rib cage outline (flared chest) in G610C/G610C and severely affected G610C/+ animals (Fig. 23B,G and Fig. 24A,B, middle and bottom). Their rib cages were also significantly reduced in

size. Furthermore, G610C/G610C animals had severely deformed ribs with evidence of numerous fractures. WT (Fig. 23R and Fig. 24D, middle) as well as moderately affected G610C/+ (Fig. 23L and Fig. 24C, middle and bottom) animals had normally developed rib cages with no apparent deformities.

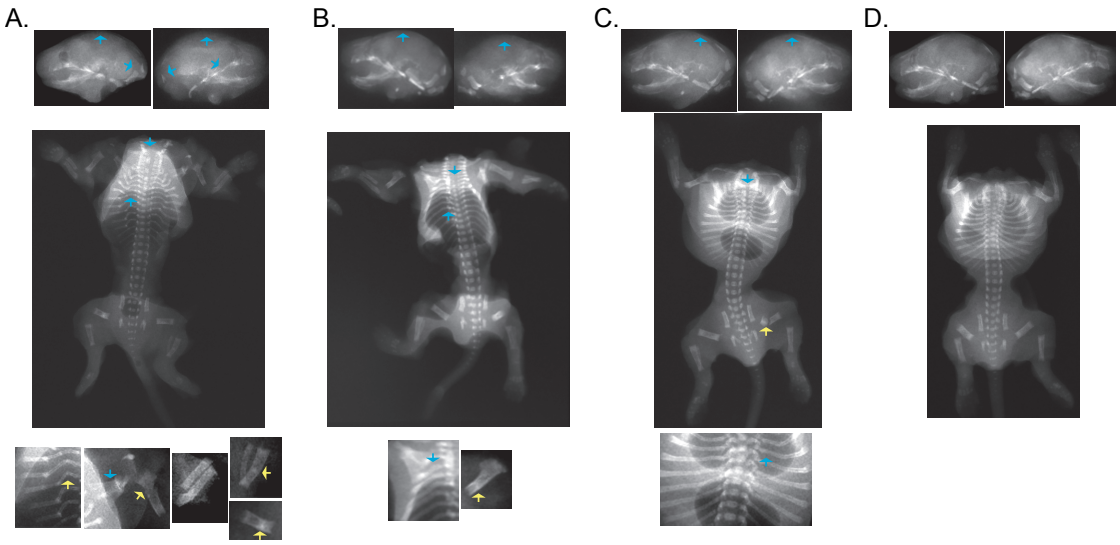

Figure 24. X-rays of homozygous G610C/G610C (A), severely affected G610C/+ (B), moderately affected G610C/+ (C), and WT (D) newborn pups.

Animals are shown with 2x zoom of skeletal defects/deformities at the bottom. Brightness/contrast was enhanced for each panel individually to ensure optimal reproduction of skeletal features. Skeletal features are described in text.

We also observed a range of fractures and deformities in limbs that correlated with the severity of skeletal defects described above. G610C/G610C animals had numerous fractures, and almost all animals had severely deformed scapula and long bone defects (Fig. 23C,E, and Fig. 24A, middle and bottom). Severely affected G610C/+ animals had occasional scapula deformities (Fig. 23H), while moderately affected animals had no major deformities (Fig. 23M). We found fresh long bone fractures only in G610C animals, which indicated increased bone fragility and could result from birth, several hours in the cage, or

sample preparation for x-ray radiography and staining. WT animals had no deformities or fractures.

Expression of TGFβ Target Genes

We observed blunted response to exogenous TGFβ in pOBs cultures (Fig. 19A,B). At the same time, a recently published paper reported hyperactive TGFβ signaling in G610C animals based on transcriptional upregulation of TGFβ target genes Cdkn1a (Cyclin dependent kinase inhibitor 1A) and Serpine1 (Serine peptidase inhibitor, clade e) (201).

We therefore examined expression of the same genes in calvaria and pOB culture. We observed only a trend toward higher Cdkn1a expression in pOB culture, but no statistically significant increase of either target gene (Fig. 25). However, analysis of calvaria revealed a statistically significant upregulation of Cdkn1a, consistent with the results reported in Ref. (201).

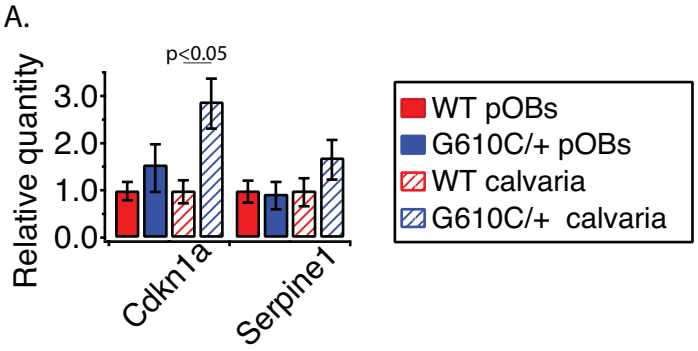

Figure 25. Endogenous TGFβ signaling in culture and *in vivo* characterized by TGFβ transcriptional targets.

Relative quantity of mRNA transcripts isolated from cultured pOBs and calvaria of 17 day old pups was measured by qPCR with HPRT1 and B2M as internal standards and normalized to WT.

DISCUSSION

In vivo observations described in this chapter are consistent with cell culture results and support our hypothesis that cell malfunction plays a major role in OI pathology. (a) Similar collagen and proteoglycan content in matrix from heterozygous and homozygous animals suggest that dramatic differences in OI severity between these genotypes are more likely to be related to cell than matrix malfunction. (b) A wide range of OI severity in heterozygous animals is more likely related to differences in ability of the cells to handle misfolded procollagen load than to differences in the function of matrix that appears to have the same composition in all heterozygous animals. (c) Severely delayed mineralization of immature bone in newborn pups (Fig. 23, 24) and hypermineralization of mature bone in adult animals (169) occur in the context of the same bone matrix but different osteoblast maturity, suggesting that mineralization defects are more likely to be a consequence of dysregulated osteoblast differentiation and maturation.

Importantly, large phenotypic variability is a general feature of OI caused by Gly substitutions. Mild to moderately severe range of OI phenotypes was described for human patients with the same Gly610Cys substitution and moderate to lethal for the Brtl mouse model (169,218). In the latter case, one could assume that at least some variation in the function of bone matrix may be caused by variations in expression of matrix molecules other than type I collagen or by mutations/polymorphisms in these molecules as the Britl mouse is on a heterogenous background. In G610C mice, all of which have the same C57BL/6J genetic background, such variations are much less likely yet the phenotype range is just as wide. In contrast, big differences in ability of osteoblasts to handle the

misfolded procollagen load could be explained by subtle epigenetic and environmental factors. Our observations cannot exclude that malfunction of mutant collagen molecules in bone matrix contributes to bone pathology in OI, which it probably does. However, they suggest that osteoblast malfunction is at least just as important.

Abnormal TGFβ signaling is one manifestation of osteoblast malfunction that may be important in pathophysiology of OI. A recent study described excessive TGFβ signaling in the CRTAP-/- mouse model of recessive OI and in heterozygous G610C mice, which it attributed to the lack of sequestration of active TGFβ on the matrix (201). The pathology appeared to be reduced by treatment with a TGFβ inhibiting antibody (201). We observed a similar increase in expression of TGFβ target genes in bone of G610C mice, but we found the matrix proteoglycan content in G610C animals to be higher rather than lower compared to WT animals. Since active TGFβ is sequestered by proteoglycans, our observations appear to be inconsistent with the interpretation proposed in Ref. (201). However, we estimated the overall proteoglycan content based on a glycosaminoglycan assay. More careful analysis of the content of individual proteoglycans known to sequester TGFβ with more specific assays should clarify this issue. In the meantime, the appearance of overactive TGFβ signaling *in vivo* may also be related to abnormal cell response to this cytokine even without an excess of unsequestered active TGFβ outside. In osteoblasts, TGFβ signaling mediates a transient release of Ca^{2+} from the ER to cytosol (122). As we discussed in the preceding chapter, osteoblast response to procollagen misfolding may also include Ca^{2+} release. The latter could blunt the cell response to actual TGFβ signaling and at the same time create an appearance of overactive TGFβ, particularly in the case of more severe accumulation of misfolded procollagen expected *in vivo*. This is just one out of many possible

speculations that would reconcile the cell culture observations here and in studies of osteoblasts from OI patients (199,200) with an appearance of overactive TGFβ reported in (201). Alternative explanations of the reported beneficial effects of a neutralizing TGFβ antibody for bone in G610C animals (201) are also possible, since global modulation of TGFβ may have multiple complex effects on function of different cells.

Chapter 9: Conclusions and Future Directions

To understand molecular mechanisms underlying OI pathophysiology, we utilized a mouse OI model with Gly610 to Cys substitution in the α2(I) chain in the triple helical region of type I procollagen.

- We developed a novel non-radioactive pulse-chase labeling assay for analyzing disruptions in procollagen biosynthesis and their consequences for cell function with minimal off-target effects.

- Combined with steady-state analysis, pulse-chase experiments demonstrated delayed folding, excessive accumulation and reduced secretion of procollagen by mutant cells.

- We discovered that accumulation of misfolded molecules inside cultured osteoblasts and fibroblasts triggered an unconventional cell stress response, resulting in abnormal differentiation and function of collagen-producing cells.

- Analysis of mutant animals revealed that this cellular malfunction significantly contributed to the disease phenotype.

- Most importantly, we found that misfolded procollagen was degraded primarily by autophagy and that autophagy enhancement might be a promising therapeutic target for reducing OI severity.

Our findings define the following OI pathophysiology pathway. Slower folding and misfolding of type I procollagen caused by Gly substitutions in the triple helix result in excessive accumulation of incompletely- and mis-folded

molecules in osteoblast ER and dilation of ER cisternae. This accumulation does not activate conventional UPR signaling and ERAD; likely because triple helix misfolding does not expose large hydrophobic patches, does not result in sequestering of BIP, and therefore does not signal ER stress through IRE1 and ATF6 (60,300). Instead, increased phosphorylation of eIF2α, decreased calnexin, increased calreticulin, and degradation of misfolded procollagen via autophagy point to cell stress response involving Ca^{2+} signaling that shares some features with "ER overload" in serpinopathies (181-183). Osteoblasts survive and adapt to the increased load of misfolded procollagen. However, their differentiation and response to the surrounding environment as well as their ability to deposit and mineralize bone matrix changes. This osteoblast "malfunction" alters the sites, quantity, and quality of bone deposition as well as disrupts the balance between bone deposition and resorption during remodeling, causing bone fragility and skeletal deformities. The pathology is likely compounded by deficient incorporation and function of mutant collagen in the bone matrix.

We hypothesize that that the extent of osteoblast malfunction may differ depending on genetic and epigenetic variations and this is a key contributing factor to the observed phenotypic variability in OI. Based on the results reported in this dissertation, we propose that the pivotal genes will be related to the cell stress response to procollagen misfolding. Determining the factors that cause greater osteoblast malfunction in more severe patients and lesser osteoblast malfunction in milder patients will be pivotal to developing therapeutic targets to combat cellular stress caused by procollagen misfolding.

Multiple studies of different genetic disorders support the notion of recovering cellular homeostasis as a potential therapeutic approach. In cystic fibrosis, recovering partial function of the mutant protein improved global cellular function (301). In muscular dystrophy caused by type VI collagen mutations,

enhancement of autophagy improved cellular function and reduced the severity of this disorder in mice (299). In Huntington disease, enhanced autophagy reduced accumulation mutant protein aggregates in the cell and reduced pathogenesis in flies and mice (302).

We believe that therapeutic targeting of the osteoblast malfunction is the most realistic approach to reducing OI severity, at least in the short run. Reducing the synthesis of defective molecules would be an ideal solution, which would correct malfunctions of both osteoblasts and collagen secreted by them. However, development of safe and effective approaches to suppressing expression of dominant negative mutations is more difficult and likely to take much longer.

Our idea of targeting osteoblast malfunction is to prevent excessive accumulation of misfolded procollagen in the cell, which appears to be the initial cell stress trigger. Based on the results of the present study, we propose to focus on enhancing the ability of the cell to degrade the misfolded molecules. In culture, both rapamycin and nutrient deprivation reduced intracellular procollagen to almost normal levels in mutant osteoblasts and had almost no effect on intracellular procollagen in normal osteoblasts. *In vivo*, a low protein diet allowed G610C animals to produce BMSCs capable of almost normal differentiation into osteoblasts and had no effect on differentiation of BMSCs from normal animals.

We therefore hypothesize that pharmacological and/or nutritional targeting of autophagy is a promising therapeutic approach to OI. The present work lays the foundation, but more detailed studies of misfolded procollagen accumulation and recognition by the cell as well as of autophagy (both in culture and in vivo) are needed for testing our hypothesis and implementing this idea.

PROCOLLAGEN MISFOLDING AND ACCUMULATION.

Pulse-chase labeling with azidohomoalanine (Aha), which replaces methionine in protein chains and is amenable to highly specific conjugation with a fluorescent probe, revealed slower folding and clearance of procollagen from mutant cells in culture. Ultrastructural examination of ER dilation by electron microscopy suggested that procollagen folding and trafficking is even more severely affected in animals, emphasizing the need for developing approaches to monitoring these processes *in vivo*.

One idea for such future *in vivo* studies is to further exploit the non-toxic nature of Aha as well as its lack of effect on procollagen synthesis and thermal stability. Similar approach to glycoprotein labeling by azides was reported in mouse studies (303). In cell culture, we found that the Aha assay produces fewer (if any) disruptions in cell function compared to radioisotope labeling as well as provides a safer, more cost-effective and more time-efficient way to connect cell stress response with procollagen synthesis in the same experiment (Chapter 5). On a cautionary note, however, potential off-target effects of Met replacement with Aha in animal diet compared to cell culture media will need to be further characterized. For instance, tRNA charging rate of Aha is ~400 times slower than Met, which could activate ATF4 pathway that recognizes uncharged tRNA and signals this information to the cell (249,304).

The decrease in calnexin at the protein level provides a hint that calnexin might be degraded by autophagy together with misfolded procollagen. For instance, slower procollagen folding and misfolding might prevent its timely release from calnexin, resulting in ubiquitination of the cytoplasmic tail of calnexin and targeting of the calnexin/procollagen complex for degradation (183,186,305). Nonselective retention of molecules with and without the mutant chain in

G610C/+ pOBs suggests that increased concentration of partially unfolded procollagen chains in the ER may trigger their nonspecific aggregation, which could be involved in this process (174).

Further studies are also needed to understand how the cell recognizes excessive accumulation of misfolded procollagen, and how these molecules are targeted for degradation by autophagy.

CELL STRESS RESPONSE AND AUTOPHAGY OF MISFOLDED PROCOLLAGEN.

Two important aspects of the cell stress response and its interplay with osteoblast function are the roles NFκB and TGFβ and their contributions to osteoblast malfunction. NFκB activation is a known inhibitor of osteoblast function (280,281), and it would be tempting to speculate that its activation or even dysregulation by the cellular stress response to procollagen misfolding produces the negative effect on osteoblast differentiation that we observed.

Furthermore, NFκB activation can inhibit activity of Smad proteins, which are crucial effectors of TGFβ signaling (287). Thus, there may be significant alterations in normal TGFβ signaling upon cellular stress to procollagen misfolding, which may explain why we observed increased endogenous TGFβ target gene expression *in vivo*, but decreased phosphorylation of Smad proteins upon exogenous treatment of TGFβ *in vitro*. TGFβ is a key regulator of osteoblast differentiation and function, and TGFβ signaling may be a target as well as a reporter of the osteoblast function in the G610C mouse model.

Likely involvement of Ca^{2+} signaling in the osteoblast cell stress response to misfolded procollagen accumulation is particularly interesting to pursue, since it might be a common factor tying together the underlying pathways. For instance, an increase in cytosolic Ca^{2+} caused by its release from the ER

activates autophagy (264). NFκB activation via ER stress is also mediated by Ca^{2+} signaling (179). Canonical cytokine signaling required for proper osteoblast function is at least to some extent mediated by Ca^{2+} signaling as well (122). Taken together, it is tempting to speculate that procollagen accumulation in the ER leads to Ca^{2+} release into cytosol, activating Ca^{2+}-dependent cell stress pathways and interfering with Ca^{2+}-dependent signaling mechanisms involved in normal osteoblast function. We are currently planning a study that would compare Ca^{2+} levels and flux between G610C and WT pOBs. We are then planning to determine Ca^{2+} flux in response to exogenous stimuli such as canonical mediators of Ca^{2+} flux from the ER as well as to TGFβ1 and other cytokines important for osteoblasts and known to affect TGFβ1 signaling.

Another approach to better understanding the cell stress pathways in G610C osteoblasts is to determine how modulation of individual components of the stress response we observed affects osteoblast differentiation and function. A first and probably most important step in this study is to fully characterize how misfolded procollagen is recognized, trafficked and degraded by the cell. (a) Since autophagy appears to be primarily responsible for delivery of misfolded procollagen for degradation and its enhancement improves osteoblast differentiation and function, it is a major focus of our present research as described below. (b) Since calnexin might mediate recognition and targeting of misfolded procollagen for autophagy, as discussed above, testing of this hypothesis is also currently under way. (c) To visualize specific autophagy routes as well as other procollagen trafficking pathways, we are developing approaches to super-resolution imaging of photo-activatable/switchable fluorescently tagged procollagen. Cotransfection of such procollagen chains with fluorescently tagged autophagy, ER, Golgi, and other markers will allow us to monitor trafficking of newly synthesized normal and mutant molecules in real time.

MANIPULATION OF AUTOPHAGY IN VIVO

The present study provides compelling evidence for the role of autophagy in misfolded procollagen degradation and possible autophagy targeting for reducing osteoblast malfunction. This evidence is based on several different approaches to inhibiting and enhancing autophagy, but all of the chemical compounds and nutrient deprivation might affect cell function in multiple ways and produce artifacts, as discussed at the end of Chapter 7. These approaches were appropriate for the initial study reported here. Yet, before focusing more efforts and resources on autophagy as a potential therapeutic target in bone disorders, we are working on validating and extending our findings by more targeted and specific genetic manipulation.

We are presently generating two separate mouse models for manipulating autophagy. The first model is based on existing mice, in which both Atg5 alleles contain loxP sites and can be conditionally inactivated by expressing Cre-recombinase under the control of a lineage-specific promoter (306). Breeding of these mice with G610C animals, transgenic mice expressing Cre under the control of osteocalcin promoter (307), and transgenic mice expressing fluorescent LC3-GFP fusion protein to monitor autophagy (308,309) is almost complete. We expect to obtain the first results within several months.

The second model is based on inserting Atg5 transgene preceded by a loxP controlled stop-cassette into the ROSA26 locus, allowing for conditional overexpression of Atg5 based on the same Cre-expressing mice as for conditional Atg5 knock-out. The corresponding embryonic stem cells have been generated and validated and the last phase of animal generation is presently under way.

The choice of Atg5, which is an essential autophagy gene is based on the following findings. (a) It has been shown that knockdown of Atg5 in osteoblasts causes significant disruption of function and differentiation (296). We expect a significant increase in OI severity upon Atg5 knockdown in G610C osteoblasts. (b) Global Atg5 overexpression has been shown to be beneficial for mice, e.g., extending their life span (310). We expect a significant reduction in OI severity by Atg5 overexpression in G610C osteoblasts. Furthermore, it will be interesting to see how osteoblast specific Atg5 expression or overexpression affects bone in aged mice compared with young mice. By monitoring changes in procollagen folding and cellular stress, this will be a beginning approach for understanding the role of procollagen misfolding and autophagy in osteoporosis.

An additional benefit of this approach is that it will allow to trace autophagy-dependent effects through different stages of osteoblast differentiation. Specifically, if the first phase described above is successful, we plan to exploit existing mouse models, in which Cre expression is controlled by osterix, collagen, Dmp1 and other promoters that are activated at different stages in osteoblast differentiation.

For therapeutic applications, autophagy may be targeted pharmacologically, nutritionally or through a combination of these two approaches. Enhancing autophagy by rapamycin, which inhibits the mTORC1 pathway, is possible but potentially problematic in the context of OI. Rapamycin affects osteoclasts as well as osteoblasts and may have some detrimental effects on bone growth and remodeling (311-314). A low protein diet supplemented with methionine and aromatic amino acids did not have detrimental effects on bone in older mice, and may both reduce synthesis of new proteins and enhance degradation via autophagy (315). Our experiments showed that such a diet improves BMSC differentiation and quality of the bone material, but it also

suppresses growth and overall bone deposition in younger animals. Interestingly, BMSCs from low protein diet animals cultured in 20% FBS were able to "remember" the treatment for at least several weeks, as judged from significantly improved osteoblast differentiation. It would be tempting to speculate that the treatment may cause some epigenetic or other long term changes in induction of autophagy, which means it might be possible to treat intermittently without adverse effects on bone and overall growth.

IMPLICATIONS FOR OTHER BONE DISORDERS

In conclusion, there may be universal benefits of targeting osteoblast malfunction for application to osteoporosis and other bone disorders, all of which may involve excessive accumulation of misfolded procollagen. For instance, it is known that autophagy activity decreases with age (316). Furthermore, chaperone expression is also known to decrease with age, including calnexin (317). As 10-15% of normal procollagen molecules are typically misfolded even in normal osteoblasts, it would be tempting to speculate that the decrease in autophagy with age causes accumulation of normal but misfolded procollagen. Accumulation of misfolded procollagen may underlie many observed similarities between OI and age-related bone pathology. These and other bone disorders may thus have common pathophysiology mechanisms and may be amenable to the same therapeutic interventions.

SECTION 4: MATERIALS AND METHODS

Chapter 10: Methods[2]

ANIMALS

B6.129(FVB)-Col1a2tm1.1Mcbr/J (G610C/+) and C57BL/6J (WT) animals were obtained from The Jackson Laboratory and housed at NIH in a pathogen free room, exposed to a 12 hour light/dark cycle, ambient room temperature and ad libitum access to water and food. G610C/+ animals were bred to produce animals homozygous for the mutation. Animals were genotyped using forward primer (TCCCTGCTTGCCCTAGTCCCAAAGATCCTT) and the reverse primer (AAGGTATAGATCAGACAGCTGGCACATCCA) to generate WT (165 bp), homozygous (337 bp) or heterozygous (both bands) PCR products. All procedures were reviewed and approved by the NIH Institutional Animal Care and Use Committee.

CELL CULTURE

Mouse Primary Embryonic Fibroblasts (MEFs)

Primary mouse embryonic fibroblasts (MEFs) were isolated from E14.5 embryos as described in (318). MEFs were cultured at 37°C, 5% CO2, in

[2]Portions of this chapter are reprinted from Pulse-chase analysis of procollagen biosynthesis by azidohomoalanine labeling, 2014; 55(5-6): 403-410, copyright © 2014, Informa Healthcare. Reproduced with permission of Informa Healthcare.

Dulbeccos modified Eagle's medium (DMEM) with GlutaMAX™ (Invitrogen), 10% fetal bovine serum (FBS, Sigma), and 1% Pen-Strep (Invitrogen). MEFs from P3 to P6 were used for experiments; 0.05% Trypsin-EDTA (Invitrogen) was utilized for cell passage.

Mouse Primary Parietal Osteoblasts (pOBs)

Primary calvarial osteoblasts (pOBs) were isolated from parietal bone of 4-8 day old mice as described in (319). Briefly, the parietal bone of calvaria was removed, cleaned, washed with PBS, and digested with 3mg/mL collagenase in 15 minute fractions at 37°C. Cells from collagenase released fractions 3-5 were plated at a density of 2,000 cells/cm^2 and cultured at 37°C, 5% CO2, 5% O_2 in growth medium containing advanced modified Eagle's medium (αMEM) with GlutaMAX™ (Invitrogen), 10% FBS (Valley Biomedical), 100 μM ascorbic acid 2-phosphate (hereafter ascorbic acid, Sigma), and 1% Pen-Strep (Invitrogen). For all experiments we used FBS from the same lot that was preselected for its ability to support proliferation and osteoblastic potential of pOBs and bone marrow stromal cells. Since presence of ascorbic acid in media resulted in matrix deposition, for passaging the cells were treated with 3 mg/mL collagenase followed by 0.05% Trypsin-EDTA (Invitrogen).

Osteoblasts from p0 (passage 0) to p2 (passage 2) were used. All figures show p0 pOBs, except the following. Figures 9A, 12A-C, 16B, and 18 represent p1 pOBs. Figure 7A represents p2 pOBs.

Mouse Bone Marrow Stromal Cells (BMSCs)

Primary bone marrow stromal cells (BMSCs) were isolated as described in (320). Briefly, femurs of 17 week old mice were cleaned of soft tissue, cut at each

end, and the marrow was flushed with a syringe. For experiments (3 animals from each group), the marrow plugs (accumulated at the bottom) were transferred and treated with 2-3 mg/ml collagenase and 4-5 mg/ml dispase in PBS at 37 °C for 30 min for digestion of stroma. After spinning to remove enzymes, cell pellets were resuspended, strained, and the number of nucleated cells were counted. BMSCs were cultured at 37°C, 5% CO2, 5% O_2 in growth medium containing advanced modified Eagle's medium (αMEM) with GlutaMAX™ (Invitrogen), 20% FBS (Valley Biomedical), 100 μM ascorbic acid 2-phosphate (hereafter ascorbic acid, Sigma), and 1% Pen-Strep (Invitrogen). BMSCs were plated directly from isolation for differentiation experiments, and p2 BMSCs were used for p65 experiments. Since presence of ascorbic acid in media resulted in matrix deposition, for passaging the cells were treated with 3 mg/mL collagenase followed by 0.05% Trypsin-EDTA (Invitrogen).

Human Fibroblasts

Normal control dermal human fibroblasts were generously provided by Dr. Joan Marini, National Institute of Child Health and Human Development, National Institutes of Health. Human dermal fibroblasts containing a type I collagen α1-chain Gly766 to Cys substitution were generously provided by Dr. Peter Byers, University of Washington School of Medicine. Fibroblasts were cultured at 37°C, 5% CO2 for less than 15 passages; 0.05% Trypsin-EDTA (Invitrogen) was utilized for cell passage.

AZIDOHOMOALANINE (AHA) EXPERIMENTS

Cell Culture Media

(a) Growth medium, described above. **(b) Labeling medium,** Met and Cys free DMEM and 250 μM (human fibroblasts) or 100 μM (mouse MEFs and pOBs) ascorbic acid 2-phosphate (Sigma) **(c) Chase medium**, Met and Cys free DMEM, 250 μM (human fibroblasts) or 100 μM (mouse MEFs and pOBs) ascorbic acid 2-phosphate, and 10 mM Met.

Labeling with Azidohomoalanine (Aha)

For determining the appropriate Aha concentration and pulse experiments, confluent human fibroblasts were treated with 250 μM ascorbic acid 2-phosphate (Sigma) in the DMEM growth medium for 1 day, depleted of Met in the depletion medium for described length of time, and incubated with the described concentration of Aha (IRIS) in labeling medium.

Procollagen Isolation and Purification

Media procollagen was precipitated with 176 mg/mL ammonium sulfate. To measure the amount of secreted procollagen, internal collagen standard was added to 0.8 μg/mL final concentration before the precipitation. The internal standard (rat-tail-tendon collagen cleaved with MMP-1 and fluorescently labeled with Alexa Fluor 488) allows accurate measurement of the initial collagen concentration and provides a control for the efficiency of subsequent fluorescent labeling (244). Intracellular procollagen was extracted by washing the cells with

PBS for 10 minutes at 4 °C on a rocker, followed by lysis with cell extraction buffer for 20 minutes at 4 °C on a rocker (1% NP40, 50 mM Tris-HCl, 150 mM NaCl, 5 mM EDTA, 1 mM phenylmethylsulfonyl fluoride, 5 mM benzamidine, 10 mM N-ethylmaleimide, 0.15-0.78 μg/mL internal standard, pH 8.0) and precipitation with 176 mg/mL ammonium sulfate. Note that N-ethylmaleimide covalently modifies cysteine residues, but normal type I collagen chains do not contain such residues and we have never observed any effect of NEM on purification or gel electrophoresis of mutant collagen chains with Gly to Cys substitutions. Collagen was purified from procollagen precipitates by resuspension and overnight incubation in 0.1 mg/mL pepsin in 0.5 M acetic acid at 4 °C followed by precipitation with 0.7 M NaCl (final concentration).

Fluorescent Labeling and Gel Electrophoresis

Click-IT Alexa Fluor 555 dibenzocyclooctyne (DIBO-AF555, Invitrogen) and monoreactive N-hydroxysuccinimide ester of Cy5 (Cy5, GE Healthcare) were suspended in anhydrous dimethylformamide, aliquoted, lyophilized, and stored with desiccant at 4 °C (Cy5) or -20 °C (DIBO-AF555) protected from light. For Aha labeling, collagen resuspended in 0.2 M phosphate, 150 mM NaCl, pH 8.0 was rapidly mixed 10:1 with DIBO-AF555 resuspended in dimethylformamide at concentration indicated, vortexed and incubated for 1 h at room temperature on a shaker. Besides Figure 1A, the only concentration of DIBO-AF555 used was 71.4 μM. Labeling of collagen Lys with Cy5 was performed as previously described (321). In double labeling experiments, the reaction of AHA with DIBO-AF555 was followed by the reaction of Lys with Cy5 in the same buffer.

Fluorescently labeled samples were mixed with lithium dodecyl sulfate sample buffer (Invitrogen), denatured for 10 min at 55-65 °C, and separated on

precast 3-8% Tris-acetate mini gels (Invitrogen). The dye front was run off the gel to reduce fluorescence background. Gel images were captured in an FLA5000 fluorescence scanner (Fuji Medical Systems, Stamford, CT) and analyzed with Multigauge 3.0 software supplied with the scanner. The total amount of secreted and intracellular collagen was determined from the known concentration of the internal standard and measured ratio of Cy5 fluorescence intensities in the collagen and internal standard bands as previously described (244).

Procollagen Folding Experiments

MEFs, pOBs, or human fibroblasts were plated in 22-cm^2 dishes, grown to confluence in the appropriate growth medium, stimulated with fresh 250 μM (human fibroblasts) or 100 μM (MEFs or pOBs) ascorbic acid 2-phosphate for 1 day (human fibroblasts) or 16 hours (MEFs or pOBs), depleted of methionine for 30 min, pulse labeled with 500 μM AHA for 10 min in the labeling medium, and chased with 10 mM methionine in the chase medium for different time intervals from 0 to 120 min. All media were pre-warmed to 37°C and cell culture dishes were maintained on a heat block set to 38°C to ensure that the cells were at 37°C during all media changes. After the chase, a dish was incubated at 22°C for 10 s, cell lysis buffer concentrate was added directly to the media for a final concentration of 1% NP40, 200 μg/mL chymotrypsin, 80 μg/mL trypsin, 2 mM EGTA (all from Sigma). The dish was shaken for 10 s, incubated for 50 s, and shaken again for 10 s. At 75 s after the lysis buffer addition, the dish was tilted slightly to allow lysate to pool. At 90 s, the lysate was collected into a clean 2.0 mL microcentrifuge tube. At 120 s, protease inhibitors (5 mM EDTA, 1 mM phenylmethylsulfonyl fluoride, 5 mM benzamidine, 10 mM NEM) were added to stop the enzymatic digestion. The lysate was vortexed, placed on ice, and mixed

with internal collagen standard (0.15-0.78 μg/mL final concentration) and Tris-HCl (100 mM final concentration, pH 7.4). Collagen was precipitated, labeled, and analyzed as described above.

Pulse Chase Analysis of Procollagen Residence Time

Collagen pulse chase measurements were performed on pOBs and MEFs using azidohomoalanine (Aha) labeling as described previously (322). MEFs, pOBs, or human fibroblasts were plated in ~10 cm^2 dishes, grown to confluence in the appropriate growth medium, stimulated with fresh 250 μM (human fibroblasts) or 100 μM (MEFs or pOBs) ascorbic acid 2-phosphate for 1 day (human fibroblasts) or 16 hours (MEFs or pOBs), depleted of methionine for 30 min, pulse labeled with 500 μM AHA for 2 hours in the labeling medium, and chased with 10 mM methionine in the chase medium for different time intervals from 0 to 120 min. For experiments utilizing inhibitors, inhibitors were added to both pulse and chase media. Procollagen isolation, purification, labeling, and gel electrophorese was done as described above.

BMSC Differentiation

Freshly isolated BMSCs were plated at 20,000 nucleated cells/25 cm^2 flask for CFU-F and CFU-ALP and 100,000 nucleated cells/~10 cm^2 dish for CFU-OB in sextuplicate and incubated for 14 days without removal from the incubator. On day 14, cells were stained first for alkaline phosphatase activity (Leukocyte Alkaline Phosphatase Kit based on napthol AS-BI and fast red violet LB and fast red violet LB, Sigma). Images were taken, then the same cultures were stained with Crystal Violet (Sigma) for nucleated cells, and images were

taken again. CFU-F represents the number of colonies with >20 cells stained with Crystal Violet. CFU-ALP represents the number of colonies with >15 cells positive for alkaline phosphatase activity.

After 14 days, media in plates for CFU-OB was replaced with osteogenic media (Normal BMSC growth media + 5 nM Dexamethasone (Sigma) + 5mM β-glycerol phosphate (Sigma)) for two weeks with regular media changes, then fixed and stained with Alizarin red (Sigma) according to manufacturers protocol. As CFU-OB was measured after 2 additional weeks of growth compared to CFU-F and CFU-ALP, it represents the number of colonies with >50 cells that deposited mineral stained with alizarin red in BMSCs isolated from either control mice or low protein diet mice.

DIFFERENTIAL SCANNING CALORIMETRY (DSC)

Human procollagen precipitated with ammonium sulfate was either resuspended and dialyzed in PBS at 4°C or treated with 0.1 mg/mL pepsin in 0.5 M acetic acid overnight at 4°C, followed by 0.7 M NaCl precipitation, resuspension and dialysis in 2 mM HCl, pH 2.3.

For secreted collagen, G610C/+ pOBs were stimulated with 100 uM ascorbic acid-2-phosphate in αMem with 0.5% FBS and media was collected either after 1 hour or 16 hours, then precipitated with ammonium sulfate, treated with 0.1 mg/mL pepsin in 0.5 M acetic acid overnight at 4°C, followed by 0.7 M NaCl precipitation two times, resuspension and dialysis in 2 mM HCl, pH 2.3 or 0.5M glycerol buffer, pH 7.4 overnight. Matrix was grown in normal culturing conditions for 3 weeks, then scraped off the cell culture dish, incubated for 4 days in 0.5M Acetic acid and 0.1 mg/mL pepsin at 4° C, salt precipitated twice in 0.7 M NaCl, resuspended and dialyzed in 0.5M glycerol buffer, pH 7.4.

For collagen extracted from skin of E18.5 G610C/+ animals, skin was dissected, cleaned, and treated with 0.1 mg/mL pepsin in 0.5 M acetic acid for 5 days at 4°C, followed by 0.7 M NaCl precipitation two times, resuspension and dialysis in 2 mM HCl, pH 2.3.

The resulting ~0.1 mg/ml solutions of procollagen and collagen were scanned at 0.125 °C/min or 0.25 °C/min heating rate in a Nano III DSC instrument (Calorimetry Sciences Corporation).

ELECTRON MICROSCOPY

Osteoblasts were cultured on an Aclar film (Electron Microscopy Sciences) for 3 weeks in 6-well plates with normal growth medium. The resulting matrix/pOB samples were fixed with fresh 2.5% glutaraldehyde (Sigma) in 0.13M Sodium Cacodylate (Sigma) buffer for 1 hour at room temperature and stored at 4 °C in 0.13M Sodium Cacodylate buffer until analysis. Fixed samples were processed into Spurr's epoxy via increasing concentrations of ethanol followed by propylene oxide. Semi-thin, 1 μm sections were cut from plastic blocks, stained with Toluidine Blue O stain and examined in a microscope. Thin, 70-90 nm sections were prepared from selected samples, stained with uranyl acetate and lead citrate, and examined in a JEOL 1400 electron microscope operating at 80 kV. Sample embedding, staining, sectioning and EM imaging were performed at Electron Microscopy Unit of NICHD Microscopy and Imaging Core under the supervision of Dr. Luis (Chip) Dye.

IMMUNOFLUORESCENCE

For immunofluorescence, p2 BMSCs from 1 WT and 2 G610C/+ animals were fixed with 4% formaldehyde and permeabilized with 0.3% Triton X100. Primary antibody for p65 was incubated overnight at 4° C. AlexaFluor 555 labeled secondary antibodies to rabbit (Invitrogen) were used, DAPI stained (Life sciences), and cells were visualized on an Evos FL Auto microscope (Life Sciences). Cells from ~10 fields of vision at 20x magnification were counted (~300 WT cells and ~600 G610C/+ cells), and the fractions of p65 nucleus positive cells were calculated.

INHIBITORS, CYTOKINES, AND ANTIBODIES

Inhibitors

100 nM Bafilomycin A1 (Sigma), 25 uM Chloroquine (Sigma), 10 mM 3-MA (Sigma), or 10 μM Leupeptin (Boehringer Ingelheim)/10 mM NH_4Cl were utilized to inhibit autophagy/lysosomal degradation. 100 nM Rapamycin (Cell Signaling) or nutrient deprivation in MEM (CellGro), 100 μM ascorbic acid, and 1% Pen-Strep was used to activate autophagy. 2.6 nM Bortezomib, 8 μM Eeyarestatin 1 (Sigma), 5μM Lactacystin (EMD Millipore), or 4 μM MG132 (EMD Millipore) were used to inhibit ERAD/proteasome, All chemicals were added to standard growth medium for experiments, unless explicitly described otherwise.

Cytokines

Cytokines were added to normal growth media for time indicated. Final cytokine concentrations were 10 ng/mL TGFβ2 (Peprotech), and 100 ng/mL Wnt3a (Peprotech).

Antibodies

Antibodies used were procollagen α1 C-propeptide (LF42, Larry Fisher), p62 (Cell Signaling), LC3A/B (Cell Signaling), β-actin (Abcam), eIF2α (Cell Signaling), phospho-eIF2α (Cell Signaling), Atf6 (Abcam), Calnexin (Abcam), Calreticulin (Abcam), Bip (Cell Signaling), HSP47 (Enzo Lifesciences), phospho-Smad2 (Cell Signaling), p65 (Cell Signaling), phospho-p65 (Cell Signaling). AlexaFluor 488, 555, or 632 secondary antibodies to rabbit, mouse, or rat (Life Sciences) were used for visualization.

OSTEOBLAST MINERALIZATION

WT and G610C/+ pOBs were plated in triplicate at four different dilutions: 40,000 cells/well, 20,000 cells/well, 10,000 cells/well, and 5,000 cells/well in a 24 well plate. Osteogenic media (Normal pOB growth media + 5 mM β-glycerol phosphate) was added the next day and media was replaced regularly. To detect mineral in live, unfixed cells, on Day 5 and 13 we added a final concentration of 20 μM Xylenol Orange (Sigma) in osteogenic media and incubated overnight in the normal cell culture environment as described previously (323). The next day

excess xylenol orange was removed with multiple PBS washes, and the cells were scanned with a 532 nm laser (FUJI FLA5000 scanner). Analysis was done using MultiGauge 3.0 software.

QUANTITATIVE REAL TIME POLYMERASE CHAIN REACTION (QPCR)

Human Fibroblasts

RNA was isolated from fibroblasts with an RNeasy kit (Qiagen), reverse transcribed with SuperScript III First Strand Synthesis Supermix and random hexamers as primers (Invitrogen), and analyzed in a 7500 Fast Real Time PCR system (Applied Biosystems) with Taqman gene expression assays (DDIT3 (CHOP), Hs00358796_g1; HSPA5 (BIP), Hs00607129_gH; BCL2 (BCL2), Hs00608023_m1; CRYAB (αB crystalline), Hs00157107_m1; COL1A1 (procollagen α1(I)), Hs00164004_m1; Applied Biosystems). The same CT threshold value was used for all samples. Relative mRNA quantity was calculated from ΔΔCT values by utilizing HPRT1 (Hypoxanthine Phosphoribosyltransferase 1), Hs99999909_m1 and B2M (B2M), Hs99999907_m1 (Applied Biosystems) as endogenous controls and assuming 100% PCR efficiency (324).

Mouse MEFs, pOBs, and Calvaria

For *in cellulo* RNA extraction, cell culture media was aspirated, and RNA was collected with TRIzol reagent (Invitrogen). For *in vivo* RNA extraction, calvaria was flash frozen in RNAlater (Invitrogen), pulverized at liquid nitrogen temperature, and isolated with TRIzol. RNA was purified using DirectZol RNA MiniPrep kit (Zymo Research), reverse transcribed with SuperScript III First Strand Synthesis Supermix and random hexamers as primers (Invitrogen), and

analyzed in a 7500 Fast Real Time PCR system (Applied Biosystems) with Taqman gene expression assays. The same CT threshold value was used for all samples. Relative mRNA quantity was calculated from ΔΔCT values assuming 100% PCR efficiency (324) on a 7500 Fast Real Time PCR system (Applied Biosystems) with Taqman gene expression assays (Table 3).

Gene	Protein	Taqman Assay ID
Col1a1	collagen α1 chain	Mm00801666_g1
Col1a2	collagen α2 chain	Mm00483888_m1
Gapdh	glyceraldehyde-3-phosphate dehydrogenase	Mm99999915_g1
B2m	β-2-microglubulin	Mm00437762_m1
HPRT1	Hypoxanthine Phosphoribosyltransferase 1	Mm01545399_m1
Spp1	osteopontin	Mm00436767_m1
Ibsp	bone sialoprotein	Mm00492555_m1
Sp7	osterix	Mm00504574_m1
Runx2	runt –related transcription factor 2	Mm00501584_m1
Dmp1	dentin morphogenetic protein 1	Mm01208363_m1
Bglap	bone γ-carboxyglutamate protein	Mm03413826_mH
Ifitm5	Bril	Mm00804741_g1
Serpinh1	HSP47	Mm00438058_g1
Hspa5	BIP	Mm00517690_g1
Ddit3	Chop	Mm01135937_g1
Nfkbia	nuclear factor of kappa light polypeptide gene enhancer in B-cells inhibitor, α	Mm00477800_g1
Cryab	αB crystalline	Mm00515567_m1
Cdkn1a	Cyclin dependent kinase inhibitor 1a	Mm04205640_g1
SerpinE1	Serpin peptidase inhibiter, clade E	Mm00435860_m1

Table 3. Taqman gene expression assays

Xbp1 Splicing in pOBs and Calvaria

Xbp1 splicing was analyzed using 1 μg total RNA collected from each sample, reverse transcribed as described above. Standard PCR was performed using primers ACACGCTTGGGAATGGACAC (XPB1-F) and CCATGGGAAGATGTTCTGGG (XBP1-R) and Phusion High Fidelity DNA polymerase (Thermo Scientific). PCR was run using standard cycling conditions on a PeqStar 2x gradient thermal cycler (Peqlab). PCR products were run on a 2% agarose gel with Ethidum bromide.

RAMAN SPECTROSCOPY

Raman microscopy was done as described previously (74). Briefly, cells were cultured for 3 (pOBs) or 8 (MEFs) weeks in standard culturing conditions, with media changes every 2-3 days. At collection, the resulting matrix was rinsed with PBS then fixed in 0.7% formaldehyde in 0.7x PBS at 37°C for 4 hours followed by room temperature overnight. Matrix samples were mounted on quartz slides, and auto-fluorescence was observed and calculated to represent cell cytoplasm. Within at least 10 different regions of the matrix, Raman scattered light was collected from lasers pointed either to the cell cytoplasm or to the cell periphery at a 7μm high focal volume to capture cells and matrix, and corrected for contributions of water and quartz. Using purified collagen as a reference, matrix collagen to cell organic ratios were calculated by analyzing Raman spectra within spectral regions where collagen and cell cytoplasm have different spectra. Intracellular collagen levels were too small to contribute to the measurements.

NON AHA LABELED TOTAL INTRACELLULAR PROCOLLAGEN AND SECRETION RATE

Collagen secretion rate experiments were performed on pOBs and MEFs in triplicate 10 cm^2 wells of a 6-well plate. Briefly, 16 hours prior to each experiment, confluent cells were given growth medium containing fresh ascorbic acid. Fresh ascorbic acid containing medium (0.5% FBS; DMEM- MEFs, αMEM-pOBs) was added at time zero. Secreted collagen was collected hourly in the culture medium, to which 1 mM phenylmethylsulfonyl fluoride, 5 mM benzamidine, 10 mM N-ethylmaleimide, internal standard and 1x TE buffer was added. For each time point, the number of cells in one well was counted and used to normalize total secreted and intracellular collagen per cell. Intracellular procollagen from the other two wells was extracted by washing the cells with PBS for 10 minutes at 4 °C on a rocker, followed by gentle lysis with cell extraction buffer (1% NP40, 50 mM Tris-HCl, 150 mM NaCl, 5 mM EDTA, 1 mM phenylmethylsulfonyl fluoride, 5 mM benzamidine, 10 mM N-ethylmaleimide, and internal collagen standard, pH 8.0). Collagen was precipitated with 176 mg/mL ammonium sulfate, treated with 0.1 mg/mL pepsin in 0.5 M acetic acid, reprecipitated with 0.7 M NaCl, resuspended in stain buffer (0.1M Sodium Carbonate, 0.5M NaCl, pH 9.3), fluorescently labeled with Cy5 as described previously (321), and analyzed by gel electrophoresis as described above.

SKELETAL STAINING AND X-RAYS

Pups from G610C/+ male and G610/+ female breeding pairs were collected within several hours of birth. Live pups were euthanized by decapitation. For skeletal staining without x-ray radiography, dead/euthanized pups were skinned, eviscerated, fixed in 95% ethanol overnight and stained overnight in 0.02% Alcian Blue 8 GX, 0.005% Alizarin Red, 5% acetic acid, 70%

ethanol. After a brief wash in water, soft tissues were cleared in 2% KOH followed by 1% KOH. The remaining skeletons were gradually transferred into 0.25% KOH, 50% glycerol for final clearing, storage and imaging. For x-ray radiography, dead/euthanized pups were eviscerated and fixed overnight in 70% ethanol; their heads were carefully cut with a scalpel at mid-sagittal plane prior to x-ray imaging, and x-rays were performed on a Faxitron. After the imaging, the heads and bodies were skinned and processed for skeletal staining as described above.

TOTAL PROTEOGLYCAN AND COLLAGEN MEASUREMENTS *IN VIVO*

Skin was dissected from E18 fetuses and frozen until ready for use. Skin was then divided, and one half was used for DSC experiments. For DSC experiments, collagen was extracted by 5 day digestion in 0.1 mg/mL pepsin followed by selective salt precipitation and dialysis in 2 mM HCl, as described above. For Sircol (Biocolor) and Blyscan (Biocolor) assays, skin was flash frozen, pulverized, and put into preweighed 1.7 mL microcentrifuge tubes. Samples were spun to remove excess liquid, and weighed. Assays were continued as detailed by manufacturer's instructions, absorbance spectra of each sample was measured on a NanoDrop 2000 (Thermo Scientific), and normalized to the standard curve of controls then to initial sample weight.

WESTERN BLOTTING

For western blot analysis, at time of collection cells were washed once with PBS, lysed in 2% SDS, 4x LDS, 50 mM DTT, 1x PhosphoStop (Roche), 1 mM phenylmethylsulfonyl fluoride, 5 mM benzamidine, 10 mM N-ethylmaleimide,

50 mM Tris, 150 mM NaCl, and 5 mM EDTA, vortexed vigorously, and frozen at -80 °C until ready for analysis. From freezer, samples were heated at 95°C for 10 minutes. Samples were loaded onto a gel, and transferred onto a 0.45 μm nitrocellulose membrane. Different gels were used to best resolve proteins of different molecular weights, including 3-8% Tris Acetate, 4-12% Bis-Tris, and 12% Bis-Tris. After transfer, the membrane was blocked with 5% BSA in TBS, then primary antibodies were added and rocked at 4°C overnight. Secondary antibodies conjugated to AlexaFluor dyes (Life Sciences) were used and images were captured in an FLA5000 fluorescence scanner (Fuji Medical Systems, Stamford, CT) and analyzed with Multigauge 3.0 software supplied with the scanner, normalizing the protein of interest to β-actin amount on the same gel lane.

SECTION 5: BIBLIOGRAPHY AND VITAE

Bibliography

1. Seeman, E. (2008) Chapter 1- Modeling and Remodeling. in *Principles of Bone Biology (Third Edition)* (Bilezikian, J. P., Raisz, L.G., Martin, T.J. ed.), Academic Press, San Diego. pp 3-28

2. Boskey, A. L., Robey, P.G. (2013) The Composition of Bone. in *Primer on the metabolic bone diseases and disorders of mineral metabolism* (Rosen, C. J., and American Society for Bone and Mineral Research. eds.), 8th Ed., Wiley-Blackwell, Ames, Iowa. pp 49-58

3. Goldberg, M., and Boskey, A. L. (1996) Lipids and biomineralizations. *Progress in histochemistry and cytochemistry* **31**, 1-187

4. Mackie, E. J., Ahmed, Y. A., Tatarczuch, L., Chen, K. S., and Mirams, M. (2008) Endochondral ossification: how cartilage is converted into bone in the developing skeleton. *The international journal of biochemistry & cell biology* **40**, 46-62

5. Karaplis, A. C. (2008) Chapter 3- Embyronic Development of Bone and Regulation of Intramembranous and Endochondral Bone Formation. in *Principles of Bone Biology (Third Edition)* (Bilezikian, J. P., Raisz, L.G., Martin, T.J. ed.), Academic Press, San Diego. pp 53-84

6. Rossert, J., Terraz, C., and Dupont, S. (2000) Regulation of type I collagen genes expression. *Nephrology, dialysis, transplantation : official publication of the European Dialysis and Transplant Association - European Renal Association* **15 Suppl 6**, 66-68

7. Bou-Gharios, G., Crombrugghe, B. (2008) Chapter 15- Type I Collagen Structure, Synthesis, and Regulation. in *Principles of Bone Biology (Third Edition)* (Bilezikian, J. P., Raisz, L.G., Martin, T.J. ed.), Academic Press, San Diego. pp 285-318

8. Krupsky, M., Kuang, P. P., and Goldstein, R. H. (1997) Regulation of type I collagen mRNA by amino acid deprivation in human lung fibroblasts. *The Journal of biological chemistry* **272**, 13864-13868

9. Ricupero, D. A., Poliks, C. F., Rishikof, D. C., Cuttle, K. A., Kuang, P. P., and Goldstein, R. H. (2001) Phosphatidylinositol 3-kinase-dependent stabilization of alpha1(I) collagen mRNA in human lung fibroblasts. *American journal of physiology. Cell physiology* **281**, C99-C105

10. Shegogue, D., and Trojanowska, M. (2004) Mammalian target of rapamycin positively regulates collagen type I production via a phosphatidylinositol 3-kinase-independent pathway. *The Journal of biological chemistry* **279**, 23166-23175

11. Lindquist, J. N., Parsons, C. J., Stefanovic, B., and Brenner, D. A. (2004) Regulation of alpha1(I) collagen messenger RNA decay by interactions with alphaCP at the 3'-untranslated region. *The Journal of biological chemistry* **279**, 23822-23829

12. Ueno, T., Kaneko, K., Sata, T., Hattori, S., and Ogawa-Goto, K. (2012) Regulation of polysome assembly on the endoplasmic reticulum by a coiled-coil protein, p180. *Nucleic Acids Res* **40**, 3006-3017

13. Stefanovic, B. (2013) RNA protein interactions governing expression of the most abundant protein in human body, type I collagen. *Wiley interdisciplinary reviews. RNA* **4**, 535-545

14. Vuust, J., and Piez, K. A. (1972) A kinetic study of collagen biosynthesis. *The Journal of biological chemistry* **247**, 856-862

15. Bachinger, H. P., Fessler, L. I., Timpl, R., and Fessler, J. H. (1981) Chain assembly intermediate in the biosynthesis of type III procollagen in chick embryo blood vessels. *The Journal of biological chemistry* **256**, 13193-13199

16. Koivu, J. (1987) Identification of disulfide bonds in carboxy-terminal propeptides of human type I procollagen. *FEBS letters* **212**, 229-232

17. McLaughlin, S. H., and Bulleid, N. J. (1998) Molecular recognition in procollagen chain assembly. *Matrix biology : journal of the International Society for Matrix Biology* **16**, 369-377

18. Olsen, B. R. (1982) The carboxyl propeptides of procollagen: structure and functional considerations. in *New trends in basement membrane research* (Kuhn K. Schoene, H., Timpl, R. ed.), Raven Press, New York. pp 225-236

19. Lees, J. F., Tasab, M., and Bulleid, N. J. (1997) Identification of the molecular recognition sequence which determines the type-specific assembly of procollagen. *The EMBO journal* **16**, 908-916

20. Boudko, S. P., Engel, J., and Bachinger, H. P. (2012) The crucial role of trimerization domains in collagen folding. *The international journal of biochemistry & cell biology* **44**, 21-32

21. Bachinger, H. P. (1987) The influence of peptidyl-prolyl cis-trans isomerase on the in vitro folding of type III collagen. *The Journal of biological chemistry* **262**, 17144-17148

22. Brodsky, B., Persikov, A. (2014) Structural Consequences of Glycine Missense Mutations in Osteogenesis Imperfecta. in *Osteogenesis Imperfecta* (Shapiro, J. R., Byers, P.H., Glorieux, F.H., Sponseller, P.D. ed.), Academic Press, Sand Diego. pp 115-124

23. Makareeva, E., Aviles, N. A., and Leikin, S. (2011) Chaperoning osteogenesis: new protein-folding disease paradigms. *Trends in cell biology* **21**, 168-176

24. Anfinsen, C. B. (1973) Principles that govern the folding of protein chains. *Science* **181**, 223-230

25. Anfinsen, C. B. (1972) Studies on the Princples that Govern the Folding of Protein Chains. in *Nobel Lectures, Chemistry*, Nobel Media AB 2014, Nobelprize.org

26. Leikina, E., Mertts, M. V., Kuznetsova, N., and Leikin, S. (2002) Type I collagen is thermally unstable at body temperature. *Proceedings of the*

National Academy of Sciences of the United States of America **99**, 1314-1318

27. Miles, C. A., and Ghelashvili, M. (1999) Polymer-in-a-box mechanism for the thermal stabilization of collagen molecules in fibers. *Biophys J* **76**, 3243-3252

28. Bruckner, P., and Prockop, D. J. (1981) Proteolytic-Enzymes as Probes for the Triple-Helical Conformation of Procollagen. *Analytical biochemistry* **110**, 360-368

29. Nagase, H., Visse, R., and Murphy, G. (2006) Structure and function of matrix metalloproteinases and TIMPs. *Cardiovascular research* **69**, 562-573

30. Makareeva, E., and Leikin, S. (2007) Procollagen triple helix assembly: an unconventional chaperone-assisted folding paradigm. *PloS one* **2**, e1029

31. Myllyharju, J. (2003) Prolyl 4-hydroxylases, the key enzymes of collagen biosynthesis. *Matrix biology : journal of the International Society for Matrix Biology* **22**, 15-24

32. Vranka, J. A., Sakai, L. Y., and Bachinger, H. P. (2004) Prolyl 3-hydroxylase 1, enzyme characterization and identification of a novel family of enzymes. *The Journal of biological chemistry* **279**, 23615-23621

33. Murad, S., Grove, D., Lindberg, K. A., Reynolds, G., Sivarajah, A., and Pinnell, S. R. (1981) Regulation of collagen synthesis by ascorbic acid. *Proceedings of the National Academy of Sciences of the United States of America* **78**, 2879-2882

34. Makareeva, E., Mertz, E. L., Kuznetsova, N. V., Sutter, M. B., DeRidder, A. M., Cabral, W. A., Barnes, A. M., McBride, D. J., Marini, J. C., and Leikin, S. (2008) Structural heterogeneity of type I collagen triple helix and its role in osteogenesis imperfecta. *The Journal of biological chemistry* **283**, 4787-4798

35. Shoulders, M. D., and Raines, R. T. (2009) Collagen structure and stability. *Annu Rev Biochem* **78**, 929-958

36. Hudson, D. M., Kim, L. S., Weis, M., Cohn, D. H., and Eyre, D. R. (2012) Peptidyl 3-hydroxyproline binding properties of type I collagen suggest a function in fibril supramolecular assembly. *Biochemistry* **51**, 2417-2424

37. Myllyharju, J., and Kivirikko, K. I. (2004) Collagens, modifying enzymes and their mutations in humans, flies and worms. *Trends in genetics : TIG* **20**, 33-43

38. Malhotra, V., and Erlmann, P. (2011) Protein export at the ER: loading big collagens into COPII carriers. *The EMBO journal* **30**, 3475-3480

39. Saito, K., Chen, M., Bard, F., Chen, S., Zhou, H., Woodley, D., Polischuk, R., Schekman, R., and Malhotra, V. (2009) TANGO1 facilitates cargo loading at endoplasmic reticulum exit sites. *Cell* **136**, 891-902

40. Smith, T., Ferreira, L. R., Hebert, C., Norris, K., and Sauk, J. J. (1995) Hsp47 and cyclophilin B traverse the endoplasmic reticulum with procollagen into pre-Golgi intermediate vesicles. A role for Hsp47 and cyclophilin B in the export of procollagen from the endoplasmic reticulum. *The Journal of biological chemistry* **270**, 18323-18328

41. Trelstad, R. L., and Hayashi, K. (1979) Tendon collagen fibrillogenesis: intracellular subassemblies and cell surface changes associated with fibril growth. *Developmental biology* **71**, 228-242

42. Canty-Laird, E. G., Lu, Y., and Kadler, K. E. (2012) Stepwise proteolytic activation of type I procollagen to collagen within the secretory pathway of tendon fibroblasts in situ. *The Biochemical journal* **441**, 707-717

43. Canty, E. G., and Kadler, K. E. (2005) Procollagen trafficking, processing and fibrillogenesis. *Journal of cell science* **118**, 1341-1353

44. Hojima, Y., van der Rest, M., and Prockop, D. J. (1985) Type I procollagen carboxyl-terminal proteinase from chick embryo tendons. Purification and characterization. *The Journal of biological chemistry* **260**, 15996-16003

45. Tuderman, L., Kivirikko, K. I., and Prockop, D. J. (1978) Partial purification and characterization of a neutral protease which cleaves the N-terminal propeptides from procollagen. *Biochemistry* **17**, 2948-2954

46. Fedarko, N. (2014) Osteoblast/Osteoclast Development and Function in Osteogenesis Imperfecta. in *Osteogenesis Imperfecta* (Shapiro, J. R., Byers, P.H., Glorieux, F.H., Sponseller, P.D. ed.), Academic Press, Sand Diego. pp 45-56

47. Birk, D. E., Nurminskaya, M. V., and Zycband, E. I. (1995) Collagen fibrillogenesis in situ: fibril segments undergo post-depositional modifications resulting in linear and lateral growth during matrix development. *Developmental dynamics : an official publication of the American Association of Anatomists* **202**, 229-243

48. Privalov, P. L. (1982) Stability of proteins. Proteins which do not present a single cooperative system. *Adv Protein Chem* **35**, 1-104

49. Kadler, K. E., Hill, A., and Canty-Laird, E. G. (2008) Collagen fibrillogenesis: fibronectin, integrins, and minor collagens as organizers and nucleators. *Curr Opin Cell Biol* **20**, 495-501

50. Appenzeller-Herzog, C. (2012) Updates on "endoplasmic reticulum redox". *Antioxidants & redox signaling* **16**, 760-762

51. Bulleid, N. J. (2012) Disulfide bond formation in the mammalian endoplasmic reticulum. *Cold Spring Harbor perspectives in biology* **4**

52. Koivu, J., Myllyla, R., Helaakoski, T., Pihlajaniemi, T., Tasanen, K., and Kivirikko, K. I. (1987) A single polypeptide acts both as the beta subunit of prolyl 4-hydroxylase and as a protein disulfide-isomerase. *The Journal of biological chemistry* **262**, 6447-6449

53. Pihlajaniemi, T., Helaakoski, T., Tasanen, K., Myllyla, R., Huhtala, M. L., Koivu, J., and Kivirikko, K. I. (1987) Molecular cloning of the beta-subunit of human prolyl 4-hydroxylase. This subunit and protein disulphide isomerase are products of the same gene. *The EMBO journal* **6**, 643-649

54. Lamande, S. R., and Bateman, J. F. (1995) The type I collagen pro alpha 1(I) COOH-terminal propeptide N-linked oligosaccharide. Functional analysis by site-directed mutagenesis. *The Journal of biological chemistry* **270**, 17858-17865

55. Ellgaard, L., and Helenius, A. (2001) ER quality control: towards an understanding at the molecular level. *Curr Opin Cell Biol* **13**, 431-437

56. Beck, K., Boswell, B. A., Ridgway, C. C., and Bachinger, H. P. (1996) Triple helix formation of procollagen type I can occur at the rough endoplasmic reticulum membrane. *The Journal of biological chemistry* **271**, 21566-21573

57. Williams, D. B. (2006) Beyond lectins: the calnexin/calreticulin chaperone system of the endoplasmic reticulum. *Journal of cell science* **119**, 615-623

58. John, L. M., Lechleiter, J. D., and Camacho, P. (1998) Differential modulation of SERCA2 isoforms by calreticulin. *The Journal of cell biology* **142**, 963-973

59. Hartl, F. U., and Hayer-Hartl, M. (2002) Molecular chaperones in the cytosol: from nascent chain to folded protein. *Science* **295**, 1852-1858

60. Chessler, S. D., and Byers, P. H. (1993) BiP binds type I procollagen pro alpha chains with mutations in the carboxyl-terminal propeptide synthesized by cells from patients with osteogenesis imperfecta. *The Journal of biological chemistry* **268**, 18226-18233

61. Flynn, G. C., Pohl, J., Flocco, M. T., and Rothman, J. E. (1991) Peptide-binding specificity of the molecular chaperone BiP. *Nature* **353**, 726-730

62. Ishida, Y., and Nagata, K. (2011) Hsp47 as a collagen-specific molecular chaperone. *Methods Enzymol* **499**, 167-182

63. Koide, T., Asada, S., Takahara, Y., Nishikawa, Y., Nagata, K., and Kitagawa, K. (2006) Specific recognition of the collagen triple helix by chaperone HSP47: minimal structural requirement and spatial molecular orientation. *The Journal of biological chemistry* **281**, 3432-3438

64. Koide, T., Nishikawa, Y., Asada, S., Yamazaki, C. M., Takahara, Y., Homma, D. L., Otaka, A., Ohtani, K., Wakamiya, N., Nagata, K., and Kitagawa, K. (2006) Specific recognition of the collagen triple helix by chaperone HSP47. II. The HSP47-binding structural motif in collagens and related proteins. *The Journal of biological chemistry* **281**, 11177-11185

65. Koide, T., Takahara, Y., Asada, S., and Nagata, K. (2002) Xaa-Arg-Gly triplets in the collagen triple helix are dominant binding sites for the molecular chaperone HSP47. *The Journal of biological chemistry* **277**, 6178-6182

66. Yagi-Utsumi, M., Yoshikawa, S., Yamaguchi, Y., Nishi, Y., Kurimoto, E., Ishida, Y., Homma, T., Hoseki, J., Nishikawa, Y., Koide, T., Nagata, K., and Kato, K. (2012) NMR and mutational identification of the collagen-binding site of the chaperone Hsp47. *PloS one* **7**, e45930

67. Makareeva, E., Leikin, S. (2014) Collagen Structure, Folding and Function. in *Osteogenesis Imperfecta* (Shapiro, J. R., Byers, P.H., Glorieux, F.H., Sponseller, P.D. ed.), Academic Press, Sand Diego. pp 71-84

68. Bonfanti, L., Mironov, A. A., Jr., Martinez-Menarguez, J. A., Martella, O., Fusella, A., Baldassarre, M., Buccione, R., Geuze, H. J., Mironov, A. A., and Luini, A. (1998) Procollagen traverses the Golgi stack without leaving the lumen of cisternae: evidence for cisternal maturation. *Cell* **95**, 993-1003

69. Christiansen, H. E., Schwarze, U., Pyott, S. M., AlSwaid, A., Al Balwi, M., Alrasheed, S., Pepin, M. G., Weis, M. A., Eyre, D. R., and Byers, P. H. (2010) Homozygosity for a missense mutation in SERPINH1, which encodes the collagen chaperone protein HSP47, results in severe recessive osteogenesis imperfecta. *American journal of human genetics* **86**, 389-398

70. Ishida, Y., Kubota, H., Yamamoto, A., Kitamura, A., Bachinger, H. P., and Nagata, K. (2006) Type I collagen in Hsp47-null cells is aggregated in endoplasmic reticulum and deficient in N-propeptide processing and fibrillogenesis. *Molecular biology of the cell* **17**, 2346-2355

71. Ishikawa, Y., Vranka, J., Wirz, J., Nagata, K., and Bachinger, H. P. (2008) The rough endoplasmic reticulum-resident FK506-binding protein FKBP65

is a molecular chaperone that interacts with collagens. *The Journal of biological chemistry* **283**, 31584-31590

72. Alanay, Y., Avaygan, H., Camacho, N., Utine, G. E., Boduroglu, K., Aktas, D., Alikasifoglu, M., Tuncbilek, E., Orhan, D., Bakar, F. T., Zabel, B., Superti-Furga, A., Bruckner-Tuderman, L., Curry, C. J., Pyott, S., Byers, P. H., Eyre, D. R., Baldridge, D., Lee, B., Merrill, A. E., Davis, E. C., Cohn, D. H., Akarsu, N., and Krakow, D. (2010) Mutations in the gene encoding the RER protein FKBP65 cause autosomal-recessive osteogenesis imperfecta. *American journal of human genetics* **86**, 551-559

73. Zeng, B., MacDonald, J. R., Bann, J. G., Beck, K., Gambee, J. E., Boswell, B. A., and Bachinger, H. P. (1998) Chicken FK506-binding protein, FKBP65, a member of the FKBP family of peptidylprolyl cis-trans isomerases, is only partially inhibited by FK506. *The Biochemical journal* **330 (Pt 1)**, 109-114

74. Barnes, A. M., Cabral, W. A., Weis, M., Makareeva, E., Mertz, E. L., Leikin, S., Eyre, D., Trujillo, C., and Marini, J. C. (2012) Absence of FKBP10 in recessive type XI osteogenesis imperfecta leads to diminished collagen cross-linking and reduced collagen deposition in extracellular matrix. *Human mutation* **33**, 1589-1598

75. Murphy, L. A., Ramirez, E. A., Trinh, V. T., Herman, A. M., Anderson, V. C., and Brewster, J. L. (2011) Endoplasmic reticulum stress or mutation of an EF-hand Ca(2+)-binding domain directs the FKBP65 rotamase to an ERAD-based proteolysis. *Cell stress & chaperones* **16**, 607-619

76. Cabral, W. A., Perdivara, I., Weis, M., Terajima, M., Blissett, A. R., Chang, W., Perosky, J. E., Makareeva, E. N., Mertz, E. L., Leikin, S., Tomer, K. B., Kozloff, K. M., Eyre, D. R., Yamauchi, M., and Marini, J. C. (2014) Abnormal type I collagen post-translational modification and crosslinking in a cyclophilin B KO mouse model of recessive osteogenesis imperfecta. *PLoS genetics* **10**, e1004465

77. Ishikawa, Y., Vranka, J. A., Boudko, S. P., Pokidysheva, E., Mizuno, K., Zientek, K., Keene, D. R., Rashmir-Raven, A. M., Nagata, K., Winand, N. J., and Bachinger, H. P. (2012) Mutation in cyclophilin B that causes hyperelastosis cutis in American Quarter Horse does not affect peptidylprolyl cis-trans isomerase activity but shows altered cyclophilin B-

protein interactions and affects collagen folding. *The Journal of biological chemistry* **287**, 22253-22265

78. Ishikawa, Y., Wirz, J., Vranka, J. A., Nagata, K., and Bachinger, H. P. (2009) Biochemical characterization of the prolyl 3-hydroxylase 1.cartilage-associated protein.cyclophilin B complex. *The Journal of biological chemistry* **284**, 17641-17647

79. Ishikawa, Y., and Bachinger, H. P. (2013) A molecular ensemble in the rER for procollagen maturation. *Biochimica et biophysica acta* **1833**, 2479-2491

80. Choi, J. W., Sutor, S. L., Lindquist, L., Evans, G. L., Madden, B. J., Bergen, H. R., 3rd, Hefferan, T. E., Yaszemski, M. J., and Bram, R. J. (2009) Severe osteogenesis imperfecta in cyclophilin B-deficient mice. *PLoS genetics* **5**, e1000750

81. Morello, R., Bertin, T. K., Chen, Y., Hicks, J., Tonachini, L., Monticone, M., Castagnola, P., Rauch, F., Glorieux, F. H., Vranka, J., Bachinger, H. P., Pace, J. M., Schwarze, U., Byers, P. H., Weis, M., Fernandes, R. J., Eyre, D. R., Yao, Z., Boyce, B. F., and Lee, B. (2006) CRTAP is required for prolyl 3- hydroxylation and mutations cause recessive osteogenesis imperfecta. *Cell* **127**, 291-304

82. Vranka, J. A., Pokidysheva, E., Hayashi, L., Zientek, K., Mizuno, K., Ishikawa, Y., Maddox, K., Tufa, S., Keene, D. R., Klein, R., and Bachinger, H. P. (2010) Prolyl 3-hydroxylase 1 null mice display abnormalities in fibrillar collagen-rich tissues such as tendons, skin, and bones. *The Journal of biological chemistry* **285**, 17253-17262

83. Chang, W., Barnes, A. M., Cabral, W. A., Bodurtha, J. N., and Marini, J. C. (2010) Prolyl 3-hydroxylase 1 and CRTAP are mutually stabilizing in the endoplasmic reticulum collagen prolyl 3-hydroxylation complex. *Human molecular genetics* **19**, 223-234

84. Barnes, A. M., Carter, E. M., Cabral, W. A., Weis, M., Chang, W., Makareeva, E., Leikin, S., Rotimi, C. N., Eyre, D. R., Raggio, C. L., and Marini, J. C. (2010) Lack of cyclophilin B in osteogenesis imperfecta with normal collagen folding. *The New England journal of medicine* **362**, 521-528

85. Cabral, W. A., Chang, W., Barnes, A. M., Weis, M., Scott, M. A., Leikin, S., Makareeva, E., Kuznetsova, N. V., Rosenbaum, K. N., Tifft, C. J., Bulas, D. I., Kozma, C., Smith, P. A., Eyre, D. R., and Marini, J. C. (2007) Prolyl 3-hydroxylase 1 deficiency causes a recessive metabolic bone disorder resembling lethal/severe osteogenesis imperfecta. *Nature genetics* **39**, 359-365

86. Cabral, W. A., Makareeva, E., Ishikawa, M., Barnes, A., Weis, M.A., Lacbawan, F., Eyre, D., Yamada, Y., Leikin, S., Marini, J. (2014) Absence of ER cation channel TMEM38B/TRIC-B causes recessive osteogenesis imperfecta by dysregulation of collagen post-translational modification. Presented at the European Calcified Tissue Society Congress ECTS 2014. Czech Republic, Prague. *Bone Abstracts* **3**

87. Yazawa, M., Ferrante, C., Feng, J., Mio, K., Ogura, T., Zhang, M., Lin, P. H., Pan, Z., Komazaki, S., Kato, K., Nishi, M., Zhao, X., Weisleder, N., Sato, C., Ma, J., and Takeshima, H. (2007) TRIC channels are essential for Ca2+ handling in intracellular stores. *Nature* **448**, 78-82

88. Yamazaki, D., Komazaki, S., Nakanishi, H., Mishima, A., Nishi, M., Yazawa, M., Yamazaki, T., Taguchi, R., and Takeshima, H. (2009) Essential role of the TRIC-B channel in Ca2+ handling of alveolar epithelial cells and in perinatal lung maturation. *Development* **136**, 2355-2361

89. Lisse, T. S., Thiele, F., Fuchs, H., Hans, W., Przemeck, G. K., Abe, K., Rathkolb, B., Quintanilla-Martinez, L., Hoelzlwimmer, G., Helfrich, M., Wolf, E., Ralston, S. H., and Hrabe de Angelis, M. (2008) ER stress-mediated apoptosis in a new mouse model of osteogenesis imperfecta. *PLoS genetics* **4**, e7

90. Poliard, A., Nifuji, A., Lamblin, D., Plee, E., Forest, C., and Kellermann, O. (1995) Controlled conversion of an immortalized mesodermal progenitor cell towards osteogenic, chondrogenic, or adipogenic pathways. *The Journal of cell biology* **130**, 1461-1472

91. Aubin, J. E. (2008) Chapter 4- Mesenchymal Stem Cells and Osteoblast Differentiation. in *Principles of Bone Biology (Third Edition)* (Bilezikian, J. P., Raisz, L.G., Martin, T.J. ed.), Academic Press, San Diego. pp 85-107

92. Aubin, J. E. (1998) Bone stem cells. *Journal of cellular biochemistry. Supplement* **30-31**, 73-82

93. Liu, F., Malaval, L., and Aubin, J. E. (2003) Global amplification polymerase chain reaction reveals novel transitional stages during osteoprogenitor differentiation. *Journal of cell science* **116**, 1787-1796

94. Kalajzic, I., Staal, A., Yang, W. P., Wu, Y., Johnson, S. E., Feyen, J. H., Krueger, W., Maye, P., Yu, F., Zhao, Y., Kuo, L., Gupta, R. R., Achenie, L. E., Wang, H. W., Shin, D. G., and Rowe, D. W. (2005) Expression profile of osteoblast lineage at defined stages of differentiation. *The Journal of biological chemistry* **280**, 24618-24626

95. Komori, T., Yagi, H., Nomura, S., Yamaguchi, A., Sasaki, K., Deguchi, K., Shimizu, Y., Bronson, R. T., Gao, Y. H., Inada, M., Sato, M., Okamoto, R., Kitamura, Y., Yoshiki, S., and Kishimoto, T. (1997) Targeted disruption of Cbfa1 results in a complete lack of bone formation owing to maturational arrest of osteoblasts. *Cell* **89**, 755-764

96. Yoshida, C. A., and Komori, T. (2005) Role of Runx proteins in chondrogenesis. *Critical reviews in eukaryotic gene expression* **15**, 243-254

97. Malaval, L., Liu, F., Roche, P., and Aubin, J. E. (1999) Kinetics of osteoprogenitor proliferation and osteoblast differentiation in vitro. *Journal of cellular biochemistry* **74**, 616-627

98. Candeliere, G. A., Liu, F., and Aubin, J. E. (2001) Individual osteoblasts in the developing calvaria express different gene repertoires. *Bone* **28**, 351-361

99. Roman-Roman, S., Garcia, T., Jackson, A., Theilhaber, J., Rawadi, G., Connolly, T., Spinella-Jaegle, S., Kawai, S., Courtois, B., Bushnell, S., Auberval, M., Call, K., and Baron, R. (2003) Identification of genes regulated during osteoblastic differentiation by genome-wide expression analysis of mouse calvaria primary osteoblasts in vitro. *Bone* **32**, 474-482

100. Vanleene, M., Saldanha, Z., Cloyd, K. L., Jell, G., Bou-Gharios, G., Bassett, J. H., Williams, G. R., Fisk, N. M., Oyen, M. L., Stevens, M. M.,

Guillot, P. V., and Shefelbine, S. J. (2011) Transplantation of human fetal blood stem cells in the osteogenesis imperfecta mouse leads to improvement in multiscale tissue properties. *Blood* **117**, 1053-1060

101. Parfitt, A. M. (1977) The cellular basis of bone turnover and bone loss: a rebuttal of the osteocytic resorption--bone flow theory. *Clinical orthopaedics and related research*, 236-247

102. Dallas, S. L., Veno, P. A., Rosser, J. L., Barragan-Adjemian, C., Rowe, D. W., Kalajzic, I., and Bonewald, L. F. (2009) Time lapse imaging techniques for comparison of mineralization dynamics in primary murine osteoblasts and the late osteoblast/early osteocyte-like cell line MLO-A5. *Cells, tissues, organs* **189**, 6-11

103. Franz-Odendaal, T. A., Hall, B. K., and Witten, P. E. (2006) Buried alive: how osteoblasts become osteocytes. *Developmental dynamics : an official publication of the American Association of Anatomists* **235**, 176-190

104. Dallas, S. L., and Bonewald, L. F. (2010) Dynamics of the transition from osteoblast to osteocyte. *Annals of the New York Academy of Sciences* **1192**, 437-443

105. Klein-Nulend J., B., L.F. (2008) Chapter 8- The Osteocyte. in *Principles of Bone Biology (Third Edition)* (Bilezikian, J. P., Raisz, L.G., Martin, T.J. ed.), Academic Press, San Diego. pp 85-107

106. Miller, S. C., and Jee, W. S. (1987) The bone lining cell: a distinct phenotype? *Calcified tissue international* **41**, 1-5

107. Manolagas, S. C. (2000) Birth and death of bone cells: basic regulatory mechanisms and implications for the pathogenesis and treatment of osteoporosis. *Endocrine reviews* **21**, 115-137

108. Jilka, R. L., Bellido, T., Almeida, M., Plotkin, L.I., O'Brien, C.A., Weinstein, R.S., Manolagas, S.C. (2008) Chapter 13- Apoptosis of Bone Cells in *Principles of Bone Biology (Third Edition)* (Bilezikian, J. P., Raisz, L.G., Martin, T.J. ed.), Academic Press, San Diego. pp 237-261

109. Kerr, J. F., Wyllie, A. H., and Currie, A. R. (1972) Apoptosis: a basic biological phenomenon with wide-ranging implications in tissue kinetics. *British journal of cancer* **26**, 239-257

110. Lee, N. K., Sowa, H., Hinoi, E., Ferron, M., Ahn, J. D., Confavreux, C., Dacquin, R., Mee, P. J., McKee, M. D., Jung, D. Y., Zhang, Z., Kim, J. K., Mauvais-Jarvis, F., Ducy, P., and Karsenty, G. (2007) Endocrine regulation of energy metabolism by the skeleton. *Cell* **130**, 456-469

111. Karsenty, G. (2006) Convergence between bone and energy homeostases: leptin regulation of bone mass. *Cell metabolism* **4**, 341-348

112. Derynck, R., and Akhurst, R. J. (2007) Differentiation plasticity regulated by TGF-beta family proteins in development and disease. *Nature cell biology* **9**, 1000-1004

113. Dallas, S. L., Alliston, T., Bonewald, L. (2008) Transforming Growth Factor B. in *Principles of Bone Biology (Third Edition)* (Bilezikian, J. P., Raisz, L.G., Martin, T.J. ed.), Academic Press, San Diego. pp 1145-1166

114. Pfeilschifter, J., and Mundy, G. R. (1987) Modulation of type beta transforming growth factor activity in bone cultures by osteotropic hormones. *Proceedings of the National Academy of Sciences of the United States of America* **84**, 2024-2028

115. Pelton, R. W., Saxena, B., Jones, M., Moses, H. L., and Gold, L. I. (1991) Immunohistochemical localization of TGF beta 1, TGF beta 2, and TGF beta 3 in the mouse embryo: expression patterns suggest multiple roles during embryonic development. *The Journal of cell biology* **115**, 1091-1105

116. Tang, Y., Wu, X., Lei, W., Pang, L., Wan, C., Shi, Z., Zhao, L., Nagy, T. R., Peng, X., Hu, J., Feng, X., Van Hul, W., Wan, M., and Cao, X. (2009) TGF-beta1-induced migration of bone mesenchymal stem cells couples bone resorption with formation. *Nature medicine* **15**, 757-765

117. Chen, G., Deng, C., and Li, Y. P. (2012) TGF-beta and BMP signaling in osteoblast differentiation and bone formation. *International journal of biological sciences* **8**, 272-288

118. Yang, T., Grafe, I., Bae, Y., Chen, S., Chen, Y., Bertin, T. K., Jiang, M. M., Ambrose, C. G., and Lee, B. (2013) E-selectin ligand 1 regulates bone remodeling by limiting bioactive TGF-beta in the bone microenvironment. *Proceedings of the National Academy of Sciences of the United States of America* **110**, 7336-7341

119. Maeda, S., Hayashi, M., Komiya, S., Imamura, T., and Miyazono, K. (2004) Endogenous TGF-beta signaling suppresses maturation of osteoblastic mesenchymal cells. *The EMBO journal* **23**, 552-563

120. Kim, S. I., Na, H. J., Ding, Y., Wang, Z., Lee, S. J., and Choi, M. E. (2012) Autophagy promotes intracellular degradation of type I collagen induced by transforming growth factor (TGF)-beta1. *The Journal of biological chemistry* **287**, 11677-11688

121. Zimmerman, K. A., Graham, L. V., Pallero, M. A., and Murphy-Ullrich, J. E. (2013) Calreticulin regulates transforming growth factor-beta-stimulated extracellular matrix production. *The Journal of biological chemistry* **288**, 14584-14598

122. Nesti, L. J., Caterson, E. J., Li, W. J., Chang, R., McCann, T. D., Hoek, J. B., and Tuan, R. S. (2007) TGF-beta1 calcium signaling in osteoblasts. *Journal of cellular biochemistry* **101**, 348-359

123. Janssens, K., ten Dijke, P., Janssens, S., and Van Hul, W. (2005) Transforming growth factor-beta1 to the bone. *Endocrine reviews* **26**, 743-774

124. Rosen, V., Gamer, L.W., Lyons, K.M. . (2008) Chapter 54- Bone Morphogenetic Proteins and the Skeleton. in *Principles of Bone Biology (Third Edition)* (Bilezikian, J. P., Raisz, L.G., Martin, T.J. ed.), Academic Press, San Diego. pp 1167-1175

125. Abe, E., Yamamoto, M., Taguchi, Y., Lecka-Czernik, B., O'Brien, C. A., Economides, A. N., Stahl, N., Jilka, R. L., and Manolagas, S. C. (2000) Essential requirement of BMPs-2/4 for both osteoblast and osteoclast formation in murine bone marrow cultures from adult mice: antagonism by noggin. *Journal of bone and mineral research : the official journal of the American Society for Bone and Mineral Research* **15**, 663-673

126. Tanaka, K., Kaji, H., Yamaguchi, T., Kanazawa, I., Canaff, L., Hendy, G. N., and Sugimoto, T. (2014) Involvement of the osteoinductive factors, Tmem119 and BMP-2, and the ER stress response PERK-eIF2alpha-ATF4 pathway in the commitment of myoblastic into osteoblastic cells. *Calcified tissue international* **94**, 454-464

127. Saito, A., Ochiai, K., Kondo, S., Tsumagari, K., Murakami, T., Cavener, D. R., and Imaizumi, K. (2011) Endoplasmic reticulum stress response mediated by the PERK-eIF2(alpha)-ATF4 pathway is involved in osteoblast differentiation induced by BMP2. *The Journal of biological chemistry* **286**, 4809-4818

128. Guo, F. J., Jiang, R., Xiong, Z., Xia, F., Li, M., Chen, L., and Liu, C. J. (2014) IRE1a constitutes a negative feedback loop with BMP2 and acts as a novel mediator in modulating osteogenic differentiation. *Cell death & disease* **5**, e1239

129. Jang, W. G., Kim, E. J., Kim, D. K., Ryoo, H. M., Lee, K. B., Kim, S. H., Choi, H. S., and Koh, J. T. (2012) BMP2 protein regulates osteocalcin expression via Runx2-mediated Atf6 gene transcription. *The Journal of biological chemistry* **287**, 905-915

130. Krishnan, V., Bryant, H. U., and Macdougald, O. A. (2006) Regulation of bone mass by Wnt signaling. *The Journal of clinical investigation* **116**, 1202-1209

131. Nuttall, M. E., and Gimble, J. M. (2000) Is there a therapeutic opportunity to either prevent or treat osteopenic disorders by inhibiting marrow adipogenesis? *Bone* **27**, 177-184

132. Ross, S. E., Hemati, N., Longo, K. A., Bennett, C. N., Lucas, P. C., Erickson, R. L., and MacDougald, O. A. (2000) Inhibition of adipogenesis by Wnt signaling. *Science* **289**, 950-953

133. Almeida, M., Han, L., Bellido, T., Manolagas, S. C., and Kousteni, S. (2005) Wnt proteins prevent apoptosis of both uncommitted osteoblast progenitors and differentiated osteoblasts by beta-catenin-dependent and -independent signaling cascades involving Src/ERK and phosphatidylinositol 3-kinase/AKT. *The Journal of biological chemistry* **280**, 41342-41351

134. Glass, D. A., 2nd, Bialek, P., Ahn, J. D., Starbuck, M., Patel, M. S., Clevers, H., Taketo, M. M., Long, F., McMahon, A. P., Lang, R. A., and Karsenty, G. (2005) Canonical Wnt signaling in differentiated osteoblasts controls osteoclast differentiation. *Developmental cell* **8**, 751-764

135. Clevers, H. (2006) Wnt/beta-catenin signaling in development and disease. *Cell* **127**, 469-480

136. Johnson, M. L. (2008) Chapter 6- Wnt Signaling and Bone. in *Principles of Bone Biology (Third Edition)* (Bilezikian, J. P., Raisz, L.G., Martin, T.J. ed.), Academic Press, San Diego. pp 121-137

137. Gong, Y., Slee, R. B., Fukai, N., Rawadi, G., Roman-Roman, S., Reginato, A. M., Wang, H., Cundy, T., Glorieux, F. H., Lev, D., Zacharin, M., Oexle, K., Marcelino, J., Suwairi, W., Heeger, S., Sabatakos, G., Apte, S., Adkins, W. N., Allgrove, J., Arslan-Kirchner, M., Batch, J. A., Beighton, P., Black, G. C., Boles, R. G., Boon, L. M., Borrone, C., Brunner, H. G., Carle, G. F., Dallapiccola, B., De Paepe, A., Floege, B., Halfhide, M. L., Hall, B., Hennekam, R. C., Hirose, T., Jans, A., Juppner, H., Kim, C. A., Keppler-Noreuil, K., Kohlschuetter, A., LaCombe, D., Lambert, M., Lemyre, E., Letteboer, T., Peltonen, L., Ramesar, R. S., Romanengo, M., Somer, H., Steichen-Gersdorf, E., Steinmann, B., Sullivan, B., Superti-Furga, A., Swoboda, W., van den Boogaard, M. J., Van Hul, W., Vikkula, M., Votruba, M., Zabel, B., Garcia, T., Baron, R., Olsen, B. R., Warman, M. L., and Osteoporosis-Pseudoglioma Syndrome Collaborative, G. (2001) LDL receptor-related protein 5 (LRP5) affects bone accrual and eye development. *Cell* **107**, 513-523

138. Kato, M., Patel, M. S., Levasseur, R., Lobov, I., Chang, B. H., Glass, D. A., 2nd, Hartmann, C., Li, L., Hwang, T. H., Brayton, C. F., Lang, R. A., Karsenty, G., and Chan, L. (2002) Cbfa1-independent decrease in osteoblast proliferation, osteopenia, and persistent embryonic eye vascularization in mice deficient in Lrp5, a Wnt coreceptor. *The Journal of cell biology* **157**, 303-314

139. Ai, M., Holmen, S. L., Van Hul, W., Williams, B. O., and Warman, M. L. (2005) Reduced affinity to and inhibition by DKK1 form a common mechanism by which high bone mass-associated missense mutations in LRP5 affect canonical Wnt signaling. *Molecular and cellular biology* **25**, 4946-4955

140. Boyden, L. M., Mao, J., Belsky, J., Mitzner, L., Farhi, A., Mitnick, M. A., Wu, D., Insogna, K., and Lifton, R. P. (2002) High bone density due to a mutation in LDL-receptor-related protein 5. *The New England journal of medicine* **346**, 1513-1521

141. Byers, P. H. (1993) *Osteogenesis Imperfecta*, Wiley-Liss, New York

142. Shapiro, J. (2014) Clinical and Genetic Classification of Osteogenesis Imperfecta and Epidemiology. in *Osteogenesis Imperfecta* (Shapiro, J. R., Byers, P.H., Glorieux, F.H., Sponseller, P.D. ed.), Academic Press, Sand Diego. pp 15-22

143. Forlino, A., Cabral, W. A., Barnes, A. M., and Marini, J. C. (2011) New perspectives on osteogenesis imperfecta. *Nature reviews. Endocrinology* **7**, 540-557

144. Malfait, F., Symoens, S., Coucke, P., Nunes, L., De Almeida, S., and De Paepe, A. (2006) Total absence of the alpha2(I) chain of collagen type I causes a rare form of Ehlers-Danlos syndrome with hypermobility and propensity to cardiac valvular problems. *Journal of medical genetics* **43**, e36

145. Nicholls, A. C., Osse, G., Schloon, H. G., Lenard, H. G., Deak, S., Myers, J. C., Prockop, D. J., Weigel, W. R., Fryer, P., and Pope, F. M. (1984) The clinical features of homozygous alpha 2(I) collagen deficient osteogenesis imperfecta. *Journal of medical genetics* **21**, 257-262

146. Drogemuller, C., Becker, D., Brunner, A., Haase, B., Kircher, P., Seeliger, F., Fehr, M., Baumann, U., Lindblad-Toh, K., and Leeb, T. (2009) A missense mutation in the SERPINH1 gene in Dachshunds with osteogenesis imperfecta. *PLoS genetics* **5**, e1000579

147. Barnes, A. M., Duncan, G., Weis, M., Paton, W., Cabral, W. A., Mertz, E. L., Makareeva, E., Gambello, M. J., Lacbawan, F. L., Leikin, S., Fertala, A., Eyre, D. R., Bale, S. J., and Marini, J. C. (2013) Kuskokwim syndrome, a recessive congenital contracture disorder, extends the phenotype of FKBP10 mutations. *Human mutation* **34**, 1279-1288

148. Puig-Hervas, M. T., Temtamy, S., Aglan, M., Valencia, M., Martinez-Glez, V., Ballesta-Martinez, M. J., Lopez-Gonzalez, V., Ashour, A. M., Amr, K., Pulido, V., Guillen-Navarro, E., Lapunzina, P., Caparros-Martin, J. A., and Ruiz-Perez, V. L. (2012) Mutations in PLOD2 cause autosomal-recessive connective tissue disorders within the Bruck syndrome--osteogenesis imperfecta phenotypic spectrum. *Human mutation* **33**, 1444-1449

149. Barnes, A. M., Chang, W., Morello, R., Cabral, W. A., Weis, M., Eyre, D. R., Leikin, S., Makareeva, E., Kuznetsova, N., Uveges, T. E., Ashok, A., Flor, A. W., Mulvihill, J. J., Wilson, P. L., Sundaram, U. T., Lee, B., and Marini, J. C. (2006) Deficiency of cartilage-associated protein in recessive lethal osteogenesis imperfecta. *The New England journal of medicine* **355**, 2757-2764

150. van Dijk, F. S., Nesbitt, I. M., Zwikstra, E. H., Nikkels, P. G., Piersma, S. R., Fratantoni, S. A., Jimenez, C. R., Huizer, M., Morsman, A. C., Cobben, J. M., van Roij, M. H., Elting, M. W., Verbeke, J. I., Wijnaendts, L. C., Shaw, N. J., Hogler, W., McKeown, C., Sistermans, E. A., Dalton, A., Meijers-Heijboer, H., and Pals, G. (2009) PPIB mutations cause severe osteogenesis imperfecta. *American journal of human genetics* **85**, 521-527

151. Rubinato, E., Morgan, A., D'Eustacchio, A., Pecile, V., Gortani, G., Gasparini, P., and Faletra, F. (2014) A novel deletion mutation involving TMEM38B in a patient with autosomal recessive osteogenesis imperfecta. *Gene* **545**, 290-292

152. Volodarsky, M., Markus, B., Cohen, I., Staretz-Chacham, O., Flusser, H., Landau, D., Shelef, I., Langer, Y., and Birk, O. S. (2013) A deletion mutation in TMEM38B associated with autosomal recessive osteogenesis imperfecta. *Human mutation* **34**, 582-586

153. Akiyama, T., Dass, C. R., Shinoda, Y., Kawano, H., Tanaka, S., and Choong, P. F. (2010) PEDF regulates osteoclasts via osteoprotegerin and RANKL. *Biochemical and biophysical research communications* **391**, 789-794

154. Becker, J., Semler, O., Gilissen, C., Li, Y., Bolz, H. J., Giunta, C., Bergmann, C., Rohrbach, M., Koerber, F., Zimmermann, K., de Vries, P., Wirth, B., Schoenau, E., Wollnik, B., Veltman, J. A., Hoischen, A., and Netzer, C. (2011) Exome sequencing identifies truncating mutations in

human SERPINF1 in autosomal-recessive osteogenesis imperfecta. *American journal of human genetics* **88**, 362-371

155. Homan, E. P., Rauch, F., Grafe, I., Lietman, C., Doll, J. A., Dawson, B., Bertin, T., Napierala, D., Morello, R., Gibbs, R., White, L., Miki, R., Cohn, D. H., Crawford, S., Travers, R., Glorieux, F. H., and Lee, B. (2011) Mutations in SERPINF1 cause osteogenesis imperfecta type VI. *Journal of bone and mineral research : the official journal of the American Society for Bone and Mineral Research* **26**, 2798-2803

156. Moffatt, P., Gaumond, M. H., Salois, P., Sellin, K., Bessette, M. C., Godin, E., de Oliveira, P. T., Atkins, G. J., Nanci, A., and Thomas, G. (2008) Bril: a novel bone-specific modulator of mineralization. *Journal of bone and mineral research : the official journal of the American Society for Bone and Mineral Research* **23**, 1497-1508

157. Semler, O., Garbes, L., Keupp, K., Swan, D., Zimmermann, K., Becker, J., Iden, S., Wirth, B., Eysel, P., Koerber, F., Schoenau, E., Bohlander, S. K., Wollnik, B., and Netzer, C. (2012) A mutation in the 5'-UTR of IFITM5 creates an in-frame start codon and causes autosomal-dominant osteogenesis imperfecta type V with hyperplastic callus. *American journal of human genetics* **91**, 349-357

158. Cho, T. J., Lee, K. E., Lee, S. K., Song, S. J., Kim, K. J., Jeon, D., Lee, G., Kim, H. N., Lee, H. R., Eom, H. H., Lee, Z. H., Kim, O. H., Park, W. Y., Park, S. S., Ikegawa, S., Yoo, W. J., Choi, I. H., and Kim, J. W. (2012) A single recurrent mutation in the 5'-UTR of IFITM5 causes osteogenesis imperfecta type V. *American journal of human genetics* **91**, 343-348

159. Bragdon, B., Moseychuk, O., Saldanha, S., King, D., Julian, J., and Nohe, A. (2011) Bone morphogenetic proteins: a critical review. *Cellular signalling* **23**, 609-620

160. Martinez-Glez, V., Valencia, M., Caparros-Martin, J. A., Aglan, M., Temtamy, S., Tenorio, J., Pulido, V., Lindert, U., Rohrbach, M., Eyre, D., Giunta, C., Lapunzina, P., and Ruiz-Perez, V. L. (2012) Identification of a mutation causing deficient BMP1/mTLD proteolytic activity in autosomal recessive osteogenesis imperfecta. *Human mutation* **33**, 343-350

161. Lapunzina, P., Aglan, M., Temtamy, S., Caparros-Martin, J. A., Valencia, M., Leton, R., Martinez-Glez, V., Elhossini, R., Amr, K., Vilaboa, N., and Ruiz-Perez, V. L. (2010) Identification of a frameshift mutation in Osterix in a patient with recessive osteogenesis imperfecta. *American journal of human genetics* **87**, 110-114

162. Fahiminiya, S., Majewski, J., Mort, J., Moffatt, P., Glorieux, F. H., and Rauch, F. (2013) Mutations in WNT1 are a cause of osteogenesis imperfecta. *Journal of medical genetics* **50**, 345-348

163. Keupp, K., Beleggia, F., Kayserili, H., Barnes, A. M., Steiner, M., Semler, O., Fischer, B., Yigit, G., Janda, C. Y., Becker, J., Breer, S., Altunoglu, U., Grunhagen, J., Krawitz, P., Hecht, J., Schinke, T., Makareeva, E., Lausch, E., Cankaya, T., Caparros-Martin, J. A., Lapunzina, P., Temtamy, S., Aglan, M., Zabel, B., Eysel, P., Koerber, F., Leikin, S., Garcia, K. C., Netzer, C., Schonau, E., Ruiz-Perez, V. L., Mundlos, S., Amling, M., Kornak, U., Marini, J., and Wollnik, B. (2013) Mutations in WNT1 cause different forms of bone fragility. *American journal of human genetics* **92**, 565-574

164. Laine, C. M., Joeng, K. S., Campeau, P. M., Kiviranta, R., Tarkkonen, K., Grover, M., Lu, J. T., Pekkinen, M., Wessman, M., Heino, T. J., Nieminen-Pihala, V., Aronen, M., Laine, T., Kroger, H., Cole, W. G., Lehesjoki, A. E., Nevarez, L., Krakow, D., Curry, C. J., Cohn, D. H., Gibbs, R. A., Lee, B. H., and Makitie, O. (2013) WNT1 mutations in early-onset osteoporosis and osteogenesis imperfecta. *The New England journal of medicine* **368**, 1809-1816

165. Pyott, S. M., Tran, T. T., Leistritz, D. F., Pepin, M. G., Mendelsohn, N. J., Temme, R. T., Fernandez, B. A., Elsayed, S. M., Elsobky, E., Verma, I., Nair, S., Turner, E. H., Smith, J. D., Jarvik, G. P., and Byers, P. H. (2013) WNT1 mutations in families affected by moderately severe and progressive recessive osteogenesis imperfecta. *American journal of human genetics* **92**, 590-597

166. Murakami, T., Saito, A., Hino, S., Kondo, S., Kanemoto, S., Chihara, K., Sekiya, H., Tsumagari, K., Ochiai, K., Yoshinaga, K., Saitoh, M., Nishimura, R., Yoneda, T., Kou, I., Furuichi, T., Ikegawa, S., Ikawa, M., Okabe, M., Wanaka, A., and Imaizumi, K. (2009) Signalling mediated by the endoplasmic reticulum stress transducer OASIS is involved in bone formation. *Nature cell biology* **11**, 1205-1211

167. Marini, J. C., Forlino, A., Cabral, W. A., Barnes, A. M., San Antonio, J. D., Milgrom, S., Hyland, J. C., Korkko, J., Prockop, D. J., De Paepe, A., Coucke, P., Symoens, S., Glorieux, F. H., Roughley, P. J., Lund, A. M., Kuurila-Svahn, K., Hartikka, H., Cohn, D. H., Krakow, D., Mottes, M., Schwarze, U., Chen, D., Yang, K., Kuslich, C., Troendle, J., Dalgleish, R., and Byers, P. H. (2007) Consortium for osteogenesis imperfecta mutations in the helical domain of type I collagen: regions rich in lethal mutations align with collagen binding sites for integrins and proteoglycans. *Human mutation* **28**, 209-221

168. Willing, M. C., Cohn, D. H., and Byers, P. H. (1990) Frameshift mutation near the 3' end of the COL1A1 gene of type I collagen predicts an elongated Pro alpha 1(I) chain and results in osteogenesis imperfecta type I. *The Journal of clinical investigation* **85**, 282-290

169. Daley, E., Streeten, E. A., Sorkin, J. D., Kuznetsova, N., Shapses, S. A., Carleton, S. M., Shuldiner, A. R., Marini, J. C., Phillips, C. L., Goldstein, S. A., Leikin, S., and McBride, D. J., Jr. (2010) Variable bone fragility associated with an Amish COL1A2 variant and a knock-in mouse model. *Journal of bone and mineral research : the official journal of the American Society for Bone and Mineral Research* **25**, 247-261

170. Ponnapakkam, T. P., Sledge, D. Gensure, R. (2006) A novel COL1A2 mutation leading to osteogenesis imperfecta type 1 in identical twins. . in *57th Annual Meeting of The American Society of Human Genetics*, New Orleans, LA

171. Sameshima, K., Kodama, A., Tshiani, K., Matsuda, Y., Miyata, K., and Naritomi, K. (1988) Osteogenesis imperfecta in twins: case report and review of literature. *Acta paediatrica Japonica; Overseas edition* **30**, 621-626

172. Fajolu, I., Ezeaka, V., Elumelu, O., Ananti, C., Iroha, E., Egri-Okwaji, M. (2012) Osteogenesis Imperfecta In A Set of Nigerian Twins- A Case Report. *The Internet Journal of Pediatrics and Neonatology* **14**

173. Rowe, D. W., Shapiro, J. R., Poirier, M., and Schlesinger, S. (1985) Diminished type I collagen synthesis and reduced alpha 1(I) collagen messenger RNA in cultured fibroblasts from patients with dominantly

inherited (type I) osteogenesis imperfecta. *The Journal of clinical investigation* **76**, 604-611

174. Ishida, Y., Yamamoto, A., Kitamura, A., Lamande, S. R., Yoshimori, T., Bateman, J. F., Kubota, H., and Nagata, K. (2009) Autophagic elimination of misfolded procollagen aggregates in the endoplasmic reticulum as a means of cell protection. *Molecular biology of the cell* **20**, 2744-2754

175. Lightfoot, S. J., Holmes, D. F., Brass, A., Grant, M. E., Byers, P. H., and Kadler, K. E. (1992) Type I procollagens containing substitutions of aspartate, arginine, and cysteine for glycine in the pro alpha 1 (I) chain are cleaved slowly by N-proteinase, but only the cysteine substitution introduces a kink in the molecule. *The Journal of biological chemistry* **267**, 25521-25528

176. Vogel, B. E., Doelz, R., Kadler, K. E., Hojima, Y., Engel, J., and Prockop, D. J. (1988) A substitution of cysteine for glycine 748 of the alpha 1 chain produces a kink at this site in the procollagen I molecule and an altered N-proteinase cleavage site over 225 nm away. *The Journal of biological chemistry* **263**, 19249-19255

177. Forlino, A., Kuznetsova, N. V., Marini, J. C., and Leikin, S. (2007) Selective retention and degradation of molecules with a single mutant alpha1(I) chain in the Brtl IV mouse model of OI. *Matrix biology : journal of the International Society for Matrix Biology* **26**, 604-614

178. Hetz, C. (2012) The unfolded protein response: controlling cell fate decisions under ER stress and beyond. *Nat Rev Mol Cell Biol* **13**, 89-102

179. Pahl, H. L., and Baeuerle, P. A. (1996) Activation of NF-kappa B by ER stress requires both Ca2+ and reactive oxygen intermediates as messengers. *FEBS letters* **392**, 129-136

180. Pahl, H. L., Sester, M., Burgert, H. G., and Baeuerle, P. A. (1996) Activation of transcription factor NF-kappaB by the adenovirus E3/19K protein requires its ER retention. *The Journal of cell biology* **132**, 511-522

181. Ekeowa, U. I., Gooptu, B., Belorgey, D., Hagglof, P., Karlsson-Li, S., Miranda, E., Perez, J., MacLeod, I., Kroger, H., Marciniak, S. J., Crowther,

D. C., and Lomas, D. A. (2009) alpha1-Antitrypsin deficiency, chronic obstructive pulmonary disease and the serpinopathies. *Clinical science* **116**, 837-850

182. Hidvegi, T., Schmidt, B. Z., Hale, P., and Perlmutter, D. H. (2005) Accumulation of mutant alpha1-antitrypsin Z in the endoplasmic reticulum activates caspases-4 and -12, NFkappaB, and BAP31 but not the unfolded protein response. *The Journal of biological chemistry* **280**, 39002-39015

183. Teckman, J. H., and Perlmutter, D. H. (2000) Retention of mutant alpha(1)-antitrypsin Z in endoplasmic reticulum is associated with an autophagic response. *American journal of physiology. Gastrointestinal and liver physiology* **279**, G961-974

184. Lawless, M. W., Greene, C. M., Mulgrew, A., Taggart, C. C., O'Neill, S. J., and McElvaney, N. G. (2004) Activation of endoplasmic reticulum-specific stress responses associated with the conformational disease Z alpha 1-antitrypsin deficiency. *Journal of immunology* **172**, 5722-5726

185. Kamimoto, T., Shoji, S., Hidvegi, T., Mizushima, N., Umebayashi, K., Perlmutter, D. H., and Yoshimori, T. (2006) Intracellular inclusions containing mutant alpha1-antitrypsin Z are propagated in the absence of autophagic activity. *The Journal of biological chemistry* **281**, 4467-4476

186. Perlmutter, D. H. (2002) Liver injury in alpha1-antitrypsin deficiency: an aggregated protein induces mitochondrial injury. *The Journal of clinical investigation* **110**, 1579-1583

187. Jiang, H. Y., Wek, S. A., McGrath, B. C., Scheuner, D., Kaufman, R. J., Cavener, D. R., and Wek, R. C. (2003) Phosphorylation of the alpha subunit of eukaryotic initiation factor 2 is required for activation of NF-kappaB in response to diverse cellular stresses. *Molecular and cellular biology* **23**, 5651-5663

188. Raghunath, M., Bruckner, P., and Steinmann, B. (1994) Delayed triple helix formation of mutant collagen from patients with osteogenesis imperfecta. *Journal of molecular biology* **236**, 940-949

189. Steinmann, B., Nicholls, A., and Pope, F. M. (1986) Clinical variability of osteogenesis imperfecta reflecting molecular heterogeneity: cysteine substitutions in the alpha 1(I) collagen chain producing lethal and mild forms. *The Journal of biological chemistry* **261**, 8958-8964

190. Fitzgerald, J., Lamande, S. R., and Bateman, J. F. (1999) Proteasomal degradation of unassembled mutant type I collagen pro-alpha1(I) chains. *The Journal of biological chemistry* **274**, 27392-27398

191. Lamande, S. R., Chessler, S. D., Golub, S. B., Byers, P. H., Chan, D., Cole, W. G., Sillence, D. O., and Bateman, J. F. (1995) Endoplasmic reticulum-mediated quality control of type I collagen production by cells from osteogenesis imperfecta patients with mutations in the pro alpha 1 (I) chain carboxyl-terminal propeptide which impair subunit assembly. *The Journal of biological chemistry* **270**, 8642-8649

192. Cole, W. G., Patterson, E., Bonadio, J., Campbell, P. E., and Fortune, D. W. (1992) The clinicopathological features of three babies with osteogenesis imperfecta resulting from the substitution of glycine by valine in the pro alpha 1 (I) chain of type I procollagen. *Journal of medical genetics* **29**, 112-118

193. Cole, W. G., Chow, C. W., Rogers, J. G., and Bateman, J. F. (1990) The clinical features of three babies with osteogenesis imperfecta resulting from the substitution of glycine by arginine in the pro alpha 1(I) chain of type I procollagen. *Journal of medical genetics* **27**, 228-235

194. Lamande, S. R., Dahl, H. H., Cole, W. G., and Bateman, J. F. (1989) Characterization of point mutations in the collagen COL1A1 and COL1A2 genes causing lethal perinatal osteogenesis imperfecta. *The Journal of biological chemistry* **264**, 15809-15812

195. Forlino, A., Tani, C., Rossi, A., Lupi, A., Campari, E., Gualeni, B., Bianchi, L., Armini, A., Cetta, G., Bini, L., and Marini, J. C. (2007) Differential expression of both extracellular and intracellular proteins is involved in the lethal or nonlethal phenotypic variation of BrtIIV, a murine model for osteogenesis imperfecta. *Proteomics* **7**, 1877-1891

196. Gioia, R., Panaroni, C., Besio, R., Palladini, G., Merlini, G., Giansanti, V., Scovassi, I. A., Villani, S., Villa, I., Villa, A., Vezzoni, P., Tenni, R., Rossi,

A., Marini, J. C., and Forlino, A. (2012) Impaired osteoblastogenesis in a murine model of dominant osteogenesis imperfecta: a new target for osteogenesis imperfecta pharmacological therapy. *Stem cells* **30**, 1465-1476

197. Fedarko, N. S., Robey, P. G., and Vetter, U. K. (1995) Extracellular matrix stoichiometry in osteoblasts from patients with osteogenesis imperfecta. *Journal of bone and mineral research : the official journal of the American Society for Bone and Mineral Research* **10**, 1122-1129

198. Fedarko, N. S., Moerike, M., Brenner, R., Robey, P. G., and Vetter, U. (1992) Extracellular matrix formation by osteoblasts from patients with osteogenesis imperfecta. *Journal of bone and mineral research : the official journal of the American Society for Bone and Mineral Research* **7**, 921-930

199. Gebken, J., Brenner, R., Feydt, A., Notbohm, H., Brinckmann, J., Muller, P. K., and Batge, B. (2000) Increased cell surface expression of receptors for transforming growth factor-beta on osteoblasts from patients with Osteogenesis imperfecta. *Pathobiology : journal of immunopathology, molecular and cellular biology* **68**, 106-112

200. Morike, M., Windsheimer, E., Brenner, R., Nerlich, A., Bushart, G., Teller, W., and Vetter, U. (1993) Effects of transforming growth factor beta on cells derived from bone and callus of patients with osteogenesis imperfecta. *Journal of orthopaedic research : official publication of the Orthopaedic Research Society* **11**, 564-572

201. Grafe, I., Yang, T., Alexander, S., Homan, E. P., Lietman, C., Jiang, M. M., Bertin, T., Munivez, E., Chen, Y., Dawson, B., Ishikawa, Y., Weis, M. A., Sampath, T. K., Ambrose, C., Eyre, D., Bachinger, H. P., and Lee, B. (2014) Excessive transforming growth factor-beta signaling is a common mechanism in osteogenesis imperfecta. *Nature medicine* **20**, 670-675

202. Fedarko, N. S., Sponseller, P. D., and Shapiro, J. R. (1996) Long-term extracellular matrix metabolism by cultured human osteogenesis imperfecta osteoblasts. *Journal of bone and mineral research : the official journal of the American Society for Bone and Mineral Research* **11**, 800-805

203. Rauch, F., Travers, R., Parfitt, A. M., and Glorieux, F. H. (2000) Static and dynamic bone histomorphometry in children with osteogenesis imperfecta. *Bone* **26**, 581-589

204. Fedarko, N. S., Vetter, U. K., Weinstein, S., and Robey, P. G. (1992) Age-related changes in hyaluronan, proteoglycan, collagen, and osteonectin synthesis by human bone cells. *Journal of cellular physiology* **151**, 215-227

205. Carden, A., Rajachar, R. M., Morris, M. D., and Kohn, D. H. (2003) Ultrastructural changes accompanying the mechanical deformation of bone tissue: a Raman imaging study. *Calcified tissue international* **72**, 166-175

206. Imbert, L., Auregan, J. C., Pernelle, K., and Hoc, T. (2014) Mechanical and mineral properties of osteogenesis imperfecta human bones at the tissue level. *Bone* **65**, 18-24

207. Eyre, D. R., and Weis, M. A. (2013) Bone collagen: new clues to its mineralization mechanism from recessive osteogenesis imperfecta. *Calcified tissue international* **93**, 338-347

208. Fratzl-Zelman, N., Schmidt, I., Roschger, P., Glorieux, F. H., Klaushofer, K., Fratzl, P., Rauch, F., and Wagermaier, W. (2014) Mineral particle size in children with osteogenesis imperfecta type I is not increased independently of specific collagen mutations. *Bone* **60**, 122-128

209. Bonadio, J., Saunders, T. L., Tsai, E., Goldstein, S. A., Morris-Wiman, J., Brinkley, L., Dolan, D. F., Altschuler, R. A., Hawkins, J. E., Jr., Bateman, J. F., and et al. (1990) Transgenic mouse model of the mild dominant form of osteogenesis imperfecta. *Proceedings of the National Academy of Sciences of the United States of America* **87**, 7145-7149

210. Harbers, K., Kuehn, M., Delius, H., and Jaenisch, R. (1984) Insertion of retrovirus into the first intron of alpha 1(I) collagen gene to embryonic lethal mutation in mice. *Proceedings of the National Academy of Sciences of the United States of America* **81**, 1504-1508

211. Hartung, S., Jaenisch, R., and Breindl, M. (1986) Retrovirus insertion inactivates mouse alpha 1(I) collagen gene by blocking initiation of transcription. *Nature* **320**, 365-367

212. Phillips, C. L., Carleton, S.M., Gentry, B.A. (2014) Animal Models of Osteogenesis Imperfecta. in *Osteogenesis Imperfecta* (Shapiro, J. R., Byers, P.H., Glorieux, F.H., Sponseller, P.D. ed.), Academic Press, Sand Diego. pp 197-207

213. Sokolov, B. P., Mays, P. K., Khillan, J. S., and Prockop, D. J. (1993) Tissue- and development-specific expression in transgenic mice of a type I procollagen (COL1A1) minigene construct with 2.3 kb of the promoter region and 2 kb of the 3'-flanking region. Specificity is independent of the putative regulatory sequences in the first intron. *Biochemistry* **32**, 9242-9249

214. Stacey, A., Bateman, J., Choi, T., Mascara, T., Cole, W., and Jaenisch, R. (1988) Perinatal lethal osteogenesis imperfecta in transgenic mice bearing an engineered mutant pro-alpha 1(I) collagen gene. *Nature* **332**, 131-136

215. Chipman, S. D., Sweet, H. O., McBride, D. J., Jr., Davisson, M. T., Marks, S. C., Jr., Shuldiner, A. R., Wenstrup, R. J., Rowe, D. W., and Shapiro, J. R. (1993) Defective pro alpha 2(I) collagen synthesis in a recessive mutation in mice: a model of human osteogenesis imperfecta. *Proceedings of the National Academy of Sciences of the United States of America* **90**, 1701-1705

216. Pihlajaniemi, T., Dickson, L. A., Pope, F. M., Korhonen, V. R., Nicholls, A., Prockop, D. J., and Myers, J. C. (1984) Osteogenesis imperfecta: cloning of a pro-alpha 2(I) collagen gene with a frameshift mutation. *The Journal of biological chemistry* **259**, 12941-12944

217. Chen, F., Guo, R., Itoh, S., Moreno, L., Rosenthal, E., Zappitelli, T., Zirngibl, R. A., Flenniken, A., Cole, W., Grynpas, M., Osborne, L. R., Vogel, W., Adamson, L., Rossant, J., and Aubin, J. E. (2014) First mouse model for combined osteogenesis imperfecta and Ehlers-Danlos syndrome. *Journal of bone and mineral research : the official journal of the American Society for Bone and Mineral Research* **29**, 1412-1423

218. Forlino, A., Porter, F. D., Lee, E. J., Westphal, H., and Marini, J. C. (1999) Use of the Cre/lox recombination system to develop a non-lethal knock-in murine model for osteogenesis imperfecta with an alpha1(I) G349C substitution. Variability in phenotype in BrtlIV mice. *The Journal of biological chemistry* **274**, 37923-37931

219. Uveges, T. E., Collin-Osdoby, P., Cabral, W. A., Ledgard, F., Goldberg, L., Bergwitz, C., Forlino, A., Osdoby, P., Gronowicz, G. A., and Marini, J. C. (2008) Cellular mechanism of decreased bone in Brtl mouse model of OI: imbalance of decreased osteoblast function and increased osteoclasts and their precursors. *Journal of bone and mineral research : the official journal of the American Society for Bone and Mineral Research* **23**, 1983-1994

220. Jansens, A., and Braakman, I. (2003) Pulse-chase labeling techniques for the analysis of protein maturation and degradation. *Methods in molecular biology* **232**, 133-145

221. Pollard, J. (1996) Radioisotopic Labeling of Proteins for Polyacrylamide Gel Electrophoresis. in *The Protein Protocols Handbook* (Walker, J. ed.), Humana Press. pp 121-126

222. Bonifacino, J. S. (2001) Metabolic labeling with amino acids. *Current Protocols in Molecular Biology* **44:VI**, 10.18.11-10.18.10

223. Coligan, J. E., Gates, F. T., Kimball, E. S., and Maloy, W. L. (1983) Radiochemical Sequence-Analysis of Biosynthetically Labeled Proteins. *Method Enzymol* **91**, 413-434

224. Barsh, G. S., and Byers, P. H. (1981) Reduced secretion of structurally abnormal type I procollagen in a form of osteogenesis imperfecta. *Proceedings of the National Academy of Sciences of the United States of America* **78**, 5142-5146

225. Bateman, J. F., Mascara, T., Chan, D., and Cole, W. G. (1984) Abnormal type I collagen metabolism by cultured fibroblasts in lethal perinatal osteogenesis imperfecta. *The Biochemical journal* **217**, 103-115

226. Ong, S. E., and Mann, M. (2006) A practical recipe for stable isotope labeling by amino acids in cell culture (SILAC). *Nat Protoc* **1**, 2650-2660

227. Van Hoof, D., Pinkse, M. W. H., Oostwaard, D. W. V., Mummery, C. L., Heck, A. J. R., and Krijgsveld, J. (2007) An experimental correction for arginine-to-proline conversion artifacts in SILAC-based quantitative proteomics. *Nat Methods* **4**, 677-678

228. Boersema, P. J., Raijmakers, R., Lemeer, S., Mohammed, S., and Heck, A. J. R. (2009) Multiplex peptide stable isotope dimethyl labeling for quantitative proteomics. *Nat Protoc* **4**, 484-494

229. Mann, M. (2006) Functional and quantitative proteomics using SILAC. *Nat Rev Mol Cell Bio* **7**, 952-958

230. Johnson, J. A., Lu, Y. Y., Van Deventer, J. A., and Tirrell, D. A. (2010) Residue-specific incorporation of non-canonical amino acids into proteins: recent developments and applications. *Current opinion in chemical biology* **14**, 774-780

231. Dieterich, D. C., Link, A. J., Graumann, J., Tirrell, D. A., and Schuman, E. M. (2006) Selective identification of newly synthesized proteins in mammalian cells using bioorthogonal noncanonical amino acid tagging (BONCAT). *Proceedings of the National Academy of Sciences of the United States of America* **103**, 9482-9487

232. Prescher, J., and Bertozzi, C. (2005) Chemistry in living systems. *Nat Chem Biol* **1**, 13-21

233. Baskin, J. M., Prescher, J. A., Laughlin, S. T., Agard, N. J., Chang, P. V., Miller, I. A., Lo, A., Codelli, J. A., and Bertozzi, C. R. (2007) Copper-free click chemistry for dynamic in vivo imaging. *Proceedings of the National Academy of Sciences of the United States of America* **104**, 16793-16797

234. Griffin, R. J. (1994) The medicinal chemistry of the azido group. *Prog Med Chem* **31**, 121-232

235. Dieterich, D., Hodas, J., Gouzer, G., Shadrin, I., Ngo, J., Triller, A., Tirrell, D., and Schuman, E. (2010) In situ visualization and dynamics of newly synthesized proteins in rat hippocampal neurons. *Nat Neurosci* **13**, 897-U149

236. Taskent-Sezgin, H., Chung, J., Banerjee, P., Nagarajan, S., Dyer, R., Carrico, I., and Raleigh, D. (2010) Azidohomoalanine: A Conformationally Sensitive IR Probe of Protein Folding, Protein Structure, and Electrostatics. *Angew Chem* **49**, 7473-7475

237. Yeargin, J., and Haas, M. (1995) Elevated Levels of Wild-Type P53 Induced by Radiolabeling of Cells Leads to Apoptosis or Sustained Growth Arrest. *Curr Biol* **5**, 423-431

238. Hu, V. W., and Heikka, D. S. (2000) Radiolabeling revisited: metabolic labeling with (35)S-methionine inhibits cell cycle progression, proliferation, and survival. *FASEB J* **14**, 448-454

239. Hu, V. W., Heikka, D. S., Dieffenbach, P. B., and Ha, L. (2001) Metabolic radiolabeling: experimental tool or Trojan horse? (35)S-Methionine induces DNA fragmentation and p53-dependent ROS production. *FASEB J* **15**, 1562-1568

240. Marko, N. F., Dieffenbach, P. B., Yan, G., Ceryak, S., Howell, R. W., Mccaffrey, T. A., and Hu, V. W. (2003) Does metabolic radiolabeling stimulate the stress response? Gene expression profiling reveals differential cellular responses to internal beta vs. external gamma radiation. *FASEB J* **17**, 1470-1486

241. Solary, E., Bertrand, R., Jenkins, J., and Pommier, Y. (1992) Radiolabeling of DNA Can Induce Its Fragmentation in Hl-60 Human Promyelocytic Leukemic-Cells. *Exp Cell Res* **203**, 495-498

242. Yanokura, M., Takase, K., Yamamoto, K., and Teraoka, H. (2000) Cell death and cell-cycle arrest induced by incorporation of [H-3]thymidine into human haemopoietic cell lines. *Int J Radiat Biol* **76**, 295-303

243. Dover, R., Jayaram, Y., Patel, K., and Chinery, R. (1994) P53 Expression in Cultured-Cells Following Radioisotope Labeling. *Journal of cell science* **107**, 1181-1184

244. Makareeva, E., Han, S. J., Vera, J. C., Sackett, D. L., Holmbeck, K., Phillips, C. L., Visse, R., Nagase, H., and Leikin, S. (2010) Carcinomas

Contain a Matrix Metalloproteinase-Resistant Isoform of Type I Collagen Exerting Selective Support to Invasion. *Cancer research* **70**, 4366-4374

245. Lander, H. (1997) An essential role for free radicals and derived species in signal transduction. *FASEB J* **11**, 118-124

246. Chau, J. F., Jia, D., Wang, Z., Liu, Z., Hu, Y., Zhang, X., Jia, H., Lai, K. P., Leong, W. F., Au, B. J., Mishina, Y., Chen, Y. G., Biondi, C., Robertson, E., Xie, D., Liu, H., He, L., Wang, X., Yu, Q., and Li, B. (2012) A crucial role for bone morphogenetic protein-Smad1 signalling in the DNA damage response. *Nat Commun* **3**, 836

247. Ong, S. E., Blagoev, B., Kratchmarova, I., Kristensen, D. B., Steen, H., Pandey, A., and Mann, M. (2002) Stable isotope labeling by amino acids in cell culture, SILAC, as a simple and accurate approach to expression proteomics. *Mol Cell Proteomics* **1**, 376-386

248. Dieterich, D., Lee, J., Link, A., Graumann, J., Tirrell, D., and Schuman, E. (2007) Labeling, detection and identification of newly synthesized proteomes with bioorthogonal non-canonical amino-acid tagging. *Nat Protoc* **2**, 532-540

249. Kiick, K., Saxon, E., Tirrell, D., and Bertozzi, C. (2002) Incorporation of azides into recombinant proteins for chemoselective modification by the Staudinger ligation. *Proc Natl Acad Sci U S A* **99**, 19-24

250. Bateman, J. F., Chan, D., Mascara, T., Rogers, J. G., and Cole, W. G. (1986) Collagen defects in lethal perinatal osteogenesis imperfecta. *The Biochemical journal* **240**, 699-708

251. Vogel, B. E., Minor, R. R., Freund, M., and Prockop, D. J. (1987) A point mutation in a type I procollagen gene converts glycine 748 of the alpha 1 chain to cysteine and destabilizes the triple helix in a lethal variant of osteogenesis imperfecta. *J Biol Chem* **262**, 14737-14744

252. Jiang, X., Iseki, S., Maxson, R. E., Sucov, H. M., and Morriss-Kay, G. M. (2002) Tissue origins and interactions in the mammalian skull vault. *Developmental biology* **241**, 106-116

253. Morriss-Kay, G. M. (2001) Derivation of the mammalian skull vault. *Journal of anatomy* **199**, 143-151

254. Bateman, J. F., Chan, D., Walker, I. D., Rogers, J. G., and Cole, W. G. (1987) Lethal perinatal osteogenesis imperfecta due to the substitution of arginine for glycine at residue 391 of the alpha 1(I) chain of type I collagen. *The Journal of biological chemistry* **262**, 7021-7027

255. Bonadio, J., and Byers, P. H. (1985) Subtle structural alterations in the chains of type I procollagen produce osteogenesis imperfecta type II. *Nature* **316**, 363-366

256. Forlino, A., Keene, D. R., Schmidt, K., and Marini, J. C. (1998) An alpha2(I) glycine to aspartate substitution is responsible for the presence of a kink in type I collagen in a lethal case of osteogenesis imperfecta. *Matrix biology : journal of the International Society for Matrix Biology* **17**, 575-584

257. Tsuneyoshi, T., Westerhausen, A., Constantinou, C. D., and Prockop, D. J. (1991) Substitutions for glycine alpha 1-637 and glycine alpha 2-694 of type I procollagen in lethal osteogenesis imperfecta. The conformational strain on the triple helix introduced by a glycine substitution can be transmitted along the helix. *The Journal of biological chemistry* **266**, 15608-15613

258. Wallis, G. A., Starman, B. J., Schwartz, M. F., and Byers, P. H. (1990) Substitution of arginine for glycine at position 847 in the triple-helical domain of the alpha 1 (I) chain of type I collagen produces lethal osteogenesis imperfecta. Molecules that contain one or two abnormal chains differ in stability and secretion. *The Journal of biological chemistry* **265**, 18628-18633

259. Bateman, J. F., Boot-Handford, R. P., and Lamande, S. R. (2009) Genetic diseases of connective tissues: cellular and extracellular effects of ECM mutations. *Nature Reviews Genetics* **10**, 173-183

260. Zoncu, R., Bar-Peled, L., Efeyan, A., Wang, S., Sancak, Y., and Sabatini, D. M. (2011) mTORC1 senses lysosomal amino acids through an inside-out mechanism that requires the vacuolar H(+)-ATPase. *Science* **334**, 678-683

261. Lamb, C. A., Yoshimori, T., and Tooze, S. A. (2013) The autophagosome: origins unknown, biogenesis complex. *Nat Rev Mol Cell Biol* **14**, 759-774

262. Kroemer, G., Marino, G., and Levine, B. (2010) Autophagy and the integrated stress response. *Mol Cell* **40**, 280-293

263. Bernales, S., McDonald, K. L., and Walter, P. (2006) Autophagy counterbalances endoplasmic reticulum expansion during the unfolded protein response. *PLoS Biol* **4**, e423

264. Hoyer-Hansen, M., Bastholm, L., Szyniarowski, P., Campanella, M., Szabadkai, G., Farkas, T., Bianchi, K., Fehrenbacher, N., Elling, F., Rizzuto, R., Mathiasen, I. S., and Jaattela, M. (2007) Control of macroautophagy by calcium, calmodulin-dependent kinase kinase-beta, and Bcl-2. *Mol Cell* **25**, 193-205

265. Gao, W., Ding, W. X., Stolz, D. B., and Yin, X. M. (2008) Induction of macroautophagy by exogenously introduced calcium. *Autophagy* **4**, 754-761

266. Hetz, C., Thielen, P., Matus, S., Nassif, M., Court, F., Kiffin, R., Martinez, G., Cuervo, A. M., Brown, R. H., and Glimcher, L. H. (2009) XBP-1 deficiency in the nervous system protects against amyotrophic lateral sclerosis by increasing autophagy. *Genes & development* **23**, 2294-2306

267. Gulow, K., Bienert, D., and Haas, I. G. (2002) BiP is feed-back regulated by control of protein translation efficiency. *Journal of cell science* **115**, 2443-2452

268. Kozutsumi, Y., Segal, M., Normington, K., Gething, M. J., and Sambrook, J. (1988) The presence of malfolded proteins in the endoplasmic reticulum signals the induction of glucose-regulated proteins. *Nature* **332**, 462-464

269. Wu, Y. T., Tan, H. L., Shui, G., Bauvy, C., Huang, Q., Wenk, M. R., Ong, C. N., Codogno, P., and Shen, H. M. (2010) Dual role of 3-methyladenine in modulation of autophagy via different temporal patterns of inhibition on class I and III phosphoinositide 3-kinase. *The Journal of biological chemistry* **285**, 10850-10861

270. Lee, D. H., and Goldberg, A. L. (1998) Proteasome inhibitors: valuable new tools for cell biologists. *Trends in cell biology* **8**, 397-403

271. Fineschi, S., Reith, W., Guerne, P. A., Dayer, J. M., and Chizzolini, C. (2006) Proteasome blockade exerts an antifibrotic activity by coordinately down-regulating type I collagen and tissue inhibitor of metalloproteinase-1 and up-regulating metalloproteinase-1 production in human dermal fibroblasts. *FASEB journal : official publication of the Federation of American Societies for Experimental Biology* **20**, 562-564

272. Shen, J., Chen, X., Hendershot, L., and Prywes, R. (2002) ER stress regulation of ATF6 localization by dissociation of BiP/GRP78 binding and unmasking of Golgi localization signals. *Developmental cell* **3**, 99-111

273. Bertolotti, A., Zhang, Y., Hendershot, L. M., Harding, H. P., and Ron, D. (2000) Dynamic interaction of BiP and ER stress transducers in the unfolded-protein response. *Nature cell biology* **2**, 326-332

274. Burdakov, D., Petersen, O. H., and Verkhratsky, A. (2005) Intraluminal calcium as a primary regulator of endoplasmic reticulum function. *Cell calcium* **38**, 303-310

275. Donnelly, N., Gorman, A. M., Gupta, S., and Samali, A. (2013) The eIF2alpha kinases: their structures and functions. *Cellular and molecular life sciences : CMLS* **70**, 3493-3511

276. He, C., and Klionsky, D. J. (2009) Regulation mechanisms and signaling pathways of autophagy. *Annual review of genetics* **43**, 67-93

277. Nakamura, T., Furuhashi, M., Li, P., Cao, H., Tuncman, G., Sonenberg, N., Gorgun, C. Z., and Hotamisligil, G. S. (2010) Double-stranded RNA-dependent protein kinase links pathogen sensing with stress and metabolic homeostasis. *Cell* **140**, 338-348

278. O'Dea, E., and Hoffmann, A. (2009) NF-kappaB signaling. *Wiley interdisciplinary reviews. Systems biology and medicine* **1**, 107-115

279. Kojima, T., Miyaishi, O., Saga, S., Ishiguro, N., Tsutsui, Y., and Iwata, H. (1998) The retention of abnormal type I procollagen and correlated expression of HSP 47 in fibroblasts from a patient with lethal osteogenesis imperfecta. *The Journal of pathology* **184**, 212-218

280. Alles, N., Soysa, N. S., Hayashi, J., Khan, M., Shimoda, A., Shimokawa, H., Ritzeler, O., Akiyoshi, K., Aoki, K., and Ohya, K. (2010) Suppression of NF-kappaB increases bone formation and ameliorates osteopenia in ovariectomized mice. *Endocrinology* **151**, 4626-4634

281. Chang, J., Wang, Z., Tang, E., Fan, Z., McCauley, L., Franceschi, R., Guan, K., Krebsbach, P. H., and Wang, C. Y. (2009) Inhibition of osteoblastic bone formation by nuclear factor-kappaB. *Nature medicine* **15**, 682-689

282. Cho, H. H., Shin, K. K., Kim, Y. J., Song, J. S., Kim, J. M., Bae, Y. C., Kim, C. D., and Jung, J. S. (2010) NF-kappaB activation stimulates osteogenic differentiation of mesenchymal stem cells derived from human adipose tissue by increasing TAZ expression. *Journal of cellular physiology* **223**, 168-177

283. Gilbert, L., He, X., Farmer, P., Rubin, J., Drissi, H., van Wijnen, A. J., Lian, J. B., Stein, G. S., and Nanes, M. S. (2002) Expression of the osteoblast differentiation factor RUNX2 (Cbfa1/AML3/Pebp2alpha A) is inhibited by tumor necrosis factor-alpha. *The Journal of biological chemistry* **277**, 2695-2701

284. Gilbert, L. C., Rubin, J., and Nanes, M. S. (2005) The p55 TNF receptor mediates TNF inhibition of osteoblast differentiation independently of apoptosis. *American journal of physiology. Endocrinology and metabolism* **288**, E1011-1018

285. Hess, K., Ushmorov, A., Fiedler, J., Brenner, R. E., and Wirth, T. (2009) TNFalpha promotes osteogenic differentiation of human mesenchymal stem cells by triggering the NF-kappaB signaling pathway. *Bone* **45**, 367-376

286. Lencel, P., Delplace, S., Hardouin, P., and Magne, D. (2011) TNF-alpha stimulates alkaline phosphatase and mineralization through PPARgamma inhibition in human osteoblasts. *Bone* **48**, 242-249

287. Li, Y., Li, A., Strait, K., Zhang, H., Nanes, M. S., and Weitzmann, M. N. (2007) Endogenous TNFalpha lowers maximum peak bone mass and inhibits osteoblastic Smad activation through NF-kappaB. *Journal of bone and mineral research : the official journal of the American Society for Bone and Mineral Research* **22**, 646-655

288. Seo, Y., Fukushima, H., Maruyama, T., Kuroishi, K. N., Osawa, K., Nagano, K., Aoki, K., Weih, F., Doi, T., Zhang, M., Ohya, K., Katagiri, T., Hosokawa, R., and Jimi, E. (2012) Accumulation of p100, a precursor of NF-kappaB2, enhances osteoblastic differentiation in vitro and bone formation in vivo in aly/aly mice. *Molecular endocrinology* **26**, 414-422

289. Yamazaki, M., Fukushima, H., Shin, M., Katagiri, T., Doi, T., Takahashi, T., and Jimi, E. (2009) Tumor necrosis factor alpha represses bone morphogenetic protein (BMP) signaling by interfering with the DNA binding of Smads through the activation of NF-kappaB. *The Journal of biological chemistry* **284**, 35987-35995

290. Giuliani, N., Morandi, F., Tagliaferri, S., Lazzaretti, M., Bonomini, S., Crugnola, M., Mancini, C., Martella, E., Ferrari, L., Tabilio, A., and Rizzoli, V. (2007) The proteasome inhibitor bortezomib affects osteoblast differentiation in vitro and in vivo in multiple myeloma patients. *Blood* **110**, 334-338

291. Ding, W. X., Ni, H. M., Gao, W., Yoshimori, T., Stolz, D. B., Ron, D., and Yin, X. M. (2007) Linking of autophagy to ubiquitin-proteasome system is important for the regulation of endoplasmic reticulum stress and cell viability. *The American journal of pathology* **171**, 513-524

292. Hidvegi, T., Mirnics, K., Hale, P., Ewing, M., Beckett, C., and Perlmutter, D. H. (2007) Regulator of G Signaling 16 is a marker for the distinct endoplasmic reticulum stress state associated with aggregated mutant alpha1-antitrypsin Z in the classical form of alpha1-antitrypsin deficiency. *The Journal of biological chemistry* **282**, 27769-27780

293. St-Arnaud, R., Prud'homme, J., Leung-Hagesteijn, C., and Dedhar, S. (1995) Constitutive expression of calreticulin in osteoblasts inhibits mineralization. *The Journal of cell biology* **131**, 1351-1359

294. Michalak, M., Burns, K., Andrin, C., Mesaeli, N., Jass, G. H., Busaan, J. L., and Opas, M. (1996) Endoplasmic reticulum form of calreticulin modulates glucocorticoid-sensitive gene expression. *The Journal of biological chemistry* **271**, 29436-29445

295. Olkku, A., and Mahonen, A. (2009) Calreticulin mediated glucocorticoid receptor export is involved in beta-catenin translocation and Wnt signalling inhibition in human osteoblastic cells. *Bone* **44**, 555-565

296. Nollet, M., Santucci-Darmanin, S., Breuil, V., Al-Sahlanee, R., Cros, C., Topi, M., Momier, D., Samson, M., Pagnotta, S., Cailleteau, L., Battaglia, S., Farlay, D., Dacquin, R., Barois, N., Jurdic, P., Boivin, G., Heymann, D., Lafont, F., Lu, S. S., Dempster, D. W., Carle, G. F., and Pierrefite-Carle, V. (2014) Autophagy in osteoblasts is involved in mineralization and bone homeostasis. *Autophagy* **10**, 1965-1977

297. Liu, F., Fang, F., Yuan, H., Yang, D., Chen, Y., Williams, L., Goldstein, S. A., Krebsbach, P. H., and Guan, J. L. (2013) Suppression of autophagy by FIP200 deletion leads to osteopenia in mice through the inhibition of osteoblast terminal differentiation. *Journal of bone and mineral research : the official journal of the American Society for Bone and Mineral Research* **28**, 2414-2430

298. Fujita, E., Kouroku, Y., Isoai, A., Kumagai, H., Misutani, A., Matsuda, C., Hayashi, Y. K., and Momoi, T. (2007) Two endoplasmic reticulum-associated degradation (ERAD) systems for the novel variant of the mutant dysferlin: ubiquitin/proteasome ERAD(I) and autophagy/lysosome ERAD(II). *Human molecular genetics* **16**, 618-629

299. Grumati, P., Coletto, L., Sabatelli, P., Cescon, M., Angelin, A., Bertaggia, E., Blaauw, B., Urciuolo, A., Tiepolo, T., Merlini, L., Maraldi, N. M., Bernardi, P., Sandri, M., and Bonaldo, P. (2010) Autophagy is defective in collagen VI muscular dystrophies, and its reactivation rescues myofiber degeneration. *Nature medicine* **16**, 1313-1320

300. Makareeva, E., Aviles, N. A., and Leikin, S. (2011) Chaperoning osteogenesis: new protein-folding disease paradigms. *Trends Cell Biol* **21**, 168-176

301. Van Goor, F., Hadida, S., Grootenhuis, P. D., Burton, B., Cao, D., Neuberger, T., Turnbull, A., Singh, A., Joubran, J., Hazlewood, A., Zhou, J., McCartney, J., Arumugam, V., Decker, C., Yang, J., Young, C., Olson, E. R., Wine, J. J., Frizzell, R. A., Ashlock, M., and Negulescu, P. (2009) Rescue of CF airway epithelial cell function in vitro by a CFTR potentiator, VX-770. *Proceedings of the National Academy of Sciences of the United States of America* **106**, 18825-18830

302. Ravikumar, B., Vacher, C., Berger, Z., Davies, J. E., Luo, S., Oroz, L. G., Scaravilli, F., Easton, D. F., Duden, R., O'Kane, C. J., and Rubinsztein, D. C. (2004) Inhibition of mTOR induces autophagy and reduces toxicity of polyglutamine expansions in fly and mouse models of Huntington disease. *Nature genetics* **36**, 585-595

303. Sletten, E. M., and Bertozzi, C. R. (2011) From mechanism to mouse: a tale of two bioorthogonal reactions. *Acc Chem Res* **44**, 666-676

304. Kilberg, M. S., Shan, J., and Su, N. (2009) ATF4-dependent transcription mediates signaling of amino acid limitation. *Trends in endocrinology and metabolism: TEM* **20**, 436-443

305. Qu, D., Teckman, J. H., Omura, S., and Perlmutter, D. H. (1996) Degradation of a mutant secretory protein, alpha1-antitrypsin Z, in the endoplasmic reticulum requires proteasome activity. *The Journal of biological chemistry* **271**, 22791-22795

306. Hara, T., Nakamura, K., Matsui, M., Yamamoto, A., Nakahara, Y., Suzuki-Migishima, R., Yokoyama, M., Mishima, K., Saito, I., Okano, H., and Mizushima, N. (2006) Suppression of basal autophagy in neural cells causes neurodegenerative disease in mice. *Nature* **441**, 885-889

307. Zhang, M., Xuan, S., Bouxsein, M. L., von Stechow, D., Akeno, N., Faugere, M. C., Malluche, H., Zhao, G., Rosen, C. J., Efstratiadis, A., and Clemens, T. L. (2002) Osteoblast-specific knockout of the insulin-like growth factor (IGF) receptor gene reveals an essential role of IGF signaling in bone matrix mineralization. *The Journal of biological chemistry* **277**, 44005-44012

308. Mizushima, N. (2004) Methods for monitoring autophagy. *The international journal of biochemistry & cell biology* **36**, 2491-2502

309. Mizushima, N., Yamamoto, A., Matsui, M., Yoshimori, T., and Ohsumi, Y. (2004) In vivo analysis of autophagy in response to nutrient starvation using transgenic mice expressing a fluorescent autophagosome marker. *Molecular biology of the cell* **15**, 1101-1111

310. Pyo, J. O., Yoo, S. M., Ahn, H. H., Nah, J., Hong, S. H., Kam, T. I., Jung, S., and Jung, Y. K. (2013) Overexpression of Atg5 in mice activates autophagy and extends lifespan. *Nature communications* **4**, 2300

311. Romero, D. F., Buchinsky, F. J., Rucinski, B., Cvetkovic, M., Bryer, H. P., Liang, X. G., Ma, Y. F., Jee, W. S., and Epstein, S. (1995) Rapamycin: a bone sparing immunosuppressant? *Journal of bone and mineral research : the official journal of the American Society for Bone and Mineral Research* **10**, 760-768

312. Sanchez, C. P., and He, Y. Z. (2009) Bone growth during rapamycin therapy in young rats. *BMC Pediatr* **9**, 3

313. Shui, C., Riggs, B. L., and Khosla, S. (2002) The immunosuppressant rapamycin, alone or with transforming growth factor-beta, enhances osteoclast differentiation of RAW264.7 monocyte-macrophage cells in the presence of RANK-ligand. *Calcified tissue international* **71**, 437-446

314. Singha, U. K., Jiang, Y., Yu, S., Luo, M., Lu, Y., Zhang, J., and Xiao, G. (2008) Rapamycin inhibits osteoblast proliferation and differentiation in MC3T3-E1 cells and primary mouse bone marrow stromal cells. *Journal of cellular biochemistry* **103**, 434-446

315. Isales, C., Hamrick, M., Ding, K., Zhong, Q., Bollag, W., Shi, X.-M., Hill, W., Rowse, J., Elsalanty, M., Chutkin, N., and Insogna, K. (2011) The impact of dietary protein on bone mass and strength in the aging animal. in *Forum on Aging and Skeletal Health*, ASBMR, Bethesda, MD

316. Cuervo, A. M. (2008) Autophagy and aging: keeping that old broom working. *Trends in genetics : TIG* **24**, 604-612

317. Choi, B. H., and Kim, J. S. (2004) Age-related decline in expression of calnexin. *Experimental & molecular medicine* **36**, 499-503

318. Garfield, A. S. (2010) Derivation of primary mouse embryonic fibroblast (PMEF) cultures. *Methods in molecular biology* **633**, 19-27

319. Bakker, A. D., and Klein-Nulend, J. (2012) Osteoblast isolation from murine calvaria and long bones. *Methods in molecular biology* **816**, 19-29

320. Suire, C., Brouard, N., Hirschi, K., and Simmons, P. J. (2012) Isolation of the stromal-vascular fraction of mouse bone marrow markedly enhances the yield of clonogenic stromal progenitors. *Blood* **119**, e86-95

321. Makareeva, E., Cabral, W. A., Marini, J. C., and Leikin, S. (2006) Molecular mechanism of alpha 1(I)-osteogenesis imperfecta/Ehlers-Danlos syndrome: unfolding of an N-anchor domain at the N-terminal end of the type I collagen triple helix. *The Journal of biological chemistry* **281**, 6463-6470

322. Mirigian, L. S., Makareeva, E., and Leikin, S. (2014) Pulse-chase analysis of procollagen biosynthesis by azidohomoalanine labeling. *Connective tissue research* **55**, 403-410

323. Wang, Y. H., Liu, Y., Maye, P., and Rowe, D. W. (2006) Examination of mineralized nodule formation in living osteoblastic cultures using fluorescent dyes. *Biotechnology progress* **22**, 1697-1701

324. Schmittgen, T. D., and Livak, K. J. (2008) Analyzing real-time PCR data by the comparative C-T method. *Nat Protoc* **3**, 1101-1108

Vitae

LYNN MIRIGIAN
4601 N Park Ave Apt 1810, Chevy Chase, MD, 20815
Phone: (260) 571-8220 Email: lynn.mirigian@gmail.com

CORE EXPERTISE/SUMMARY

* Over six years of research experience in academic, government, and industry environments
* Extensive knowledge of biophysical, biochemical, molecular and cell biology techniques
* Specialist in bone, connective tissue, and matrix biology
* Proven success in coordinating multidisciplinary teams to complete projects on time
* Leadership minded with an excitement for analytical thinking and problem solving
* Strong written and verbal communicator with expertise in Adobe Creative Suite and MS Office Suite
* Experienced in teaching technical information to non-experts

PROFESSIONAL EXPERIENCE

Doctoral Research Scientist *2009 – present*
National Institutes of Health and University of Texas Medical Branch

Completed PhD dissertation research project in the laboratory of Dr. Sergey Leikin at the National Institutes of Health (NIH) with mentorship from Dr. José Barral at the University of Texas Medical Branch (UTMB).

First student from UTMB to be accepted into the graduate partnership program at NIH.

Designed experimental plans, executed them, and analyzed data. Results were presented at conferences, invited presentations, and in peer-reviewed publications.

Developed an assay to replace radioisostopes with a safe alternative, resulting in quicker turnaround time from experiment to result, improved ability to simultaneously measure cell stress, and a safer laboratory environment.

First to describe a unique cell stress response to genetic osteoporosis resulting in new translational approaches to treating the disease.

Managed multiple successful student projects through the summer intern program.

Assisted in lab management responsibilities by managing inventory, setting up maintenance contracts for scientific devices, budgeting for each fiscal year, and finding ways to cut costs on laboratory supplies.

Crop Protection Research and Development Intern- Formulations 2009
Dow Agrosciences

Evaluated polymers to enhance formulations of existing pesticides to reduce solvent usage and improve environmental impact.

Devised a screening test that determined ideal pesticide/polymer/solvent ratio compositions of pesticides and herbicides.

Successful projects resulted in multiple enhanced formulations progressing into the next phase of development.

Research and Teacher Assistant 2007-2009
Butler University

Taught and evaluated students in general biology class through individual mentorship and encouraging critical analysis of experimental results.

Managed administrative tasks pertaining to the class including grading and organizing supplies necessary for laboratory experiments.

Created a sortable database to efficiently catalog records for the remaining years of a long-term population ecology study.

EDUCATION

Doctor of Philosophy in Biomedical Sciences 2009 - present
National Institutes of Health and University of Texas Medical Branch

Relevant coursework: Advanced Cell Biology, Biological Importance of Modifications in DNA and Chromatin, Introduction to HIV/AIDs Research, Biostatistics, Immunology, Biochemistry, Ethics of Science, Biological Transport, Sensory Motor Integration

Thesis: Procollagen misfolding and osteoblast malfunction in Osteogenesis Imperfecta.

Completion date: March 2015

Bachelor of Science in Biology 2009
Butler University

Graduated with honors in Biology and a Chemistry minor

Relevant coursework: Organic Chemistry, Molecular and Vertebrate Biology, Genetics, Physics

CERTIFICATES, TRAINING, AND AWARDS

Project Management Training Course, LearnSmart Systems, 2014

NIH Translational Sciences Training Program, 2013

NIH Teaching Workshop, 2012

NIH Graduate Student Fellowship, 2010-2015

UTMB Deans Academic Scholarship, 2010-2015

UTMB Toxicology Scholar Award, 2009-2010

Morton Finney Leadership Program Scholarship, 2005-2009

Academic Merit Scholarship, 2005-2009

PUBLICATIONS

Mirigian, L., et al. (2014). Pulse chase analysis of procollagen biosynthesis by azidohomoalanine labeling. Connective Tissue Research 55:5-6, 403-410

Mirigian, L., et al. (2013). Collagen degradation by tumor-associated trypsins. Archives of Biochemistry and Biophysics 535:111-114.

INVITED PRESENTATIONS

NIDCR/NIH Craniofacial and Skeletal Diseases Branch Seminar Series, 2014. Procollagen misfolding and degradation through autophagy in the G610C mouse model of osteogenesis imperfecta

NIH Extracellular Matrix and Skeletal Biology Data Club, 2013 and 2014. Osteoblast malfunction in the G610C mouse model of osteogenesis imperfecta

Gordon Research Seminar on Collagen, 2013. ER stress response to procollagen misfolding leads to osteoblast malfunction in the Amish mouse model of OI.

NICHD/NIH Graduate Research Forum, 2012. Using Azidohomoalanine as a replacement for radioisotopes in pulse/chase kinetic assays.